BOSTON UNIVERSITY

GRADUATE SCHOOL OF ARTS AND SCIENCES

MEASURING NEURON/GLIAL CELLULAR ARRANGEMENT IN THE MAMMALIAN CORTEX

Final Oral Examination

ANDREW INGLIS
PhD candidate

H. EUGENE STANLEY
University Professor and Professor of Physics

BU Physics Department

- H.E. Stanley
- William Morrison

BU Neuroanatomy Department

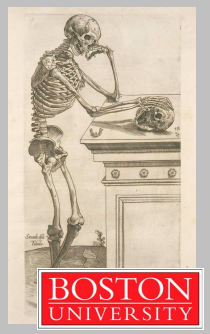

- Douglas Rosene
- Lela Giannaris
- Larissa Estrada
- Christopher Tonn

Drexel University

Physics Department

- Brigita Urbanc
- Luis Cruz

University of Arizona

Evelyn F. McKnight Brain Institute

- Carol Barnes
- James Lister

Main Questions

Why are neurons and other cells in the brain spatially arranged the way they are? Why is this an important question?

How can we quantify spatial arrangement properties of cells in the brain? What are the experimental tools and what are the measurements?

What do cell arrangements tell us about how the brain develops, becomes diseased, and age?

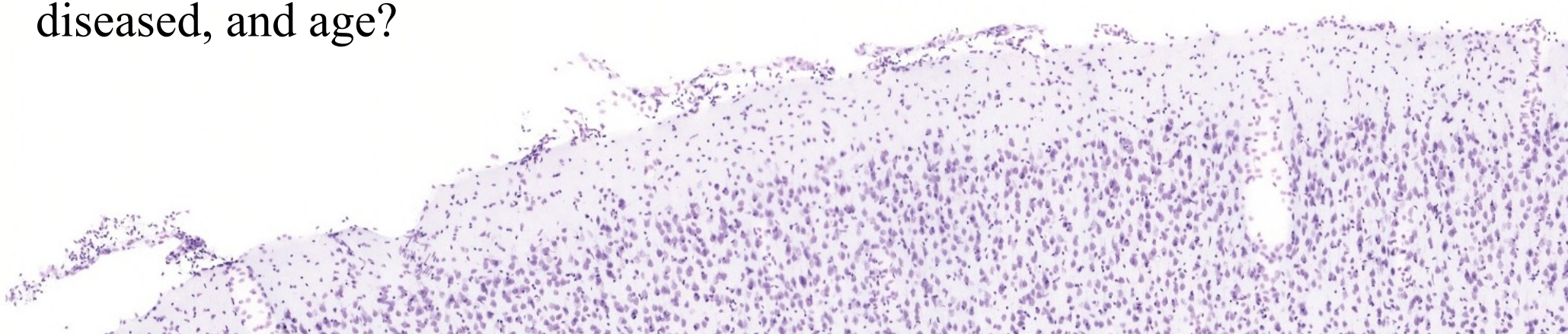

Outline

1. Motivation
2. Theory
3. Method
4. Results
5. Future Work
6. Conclusion

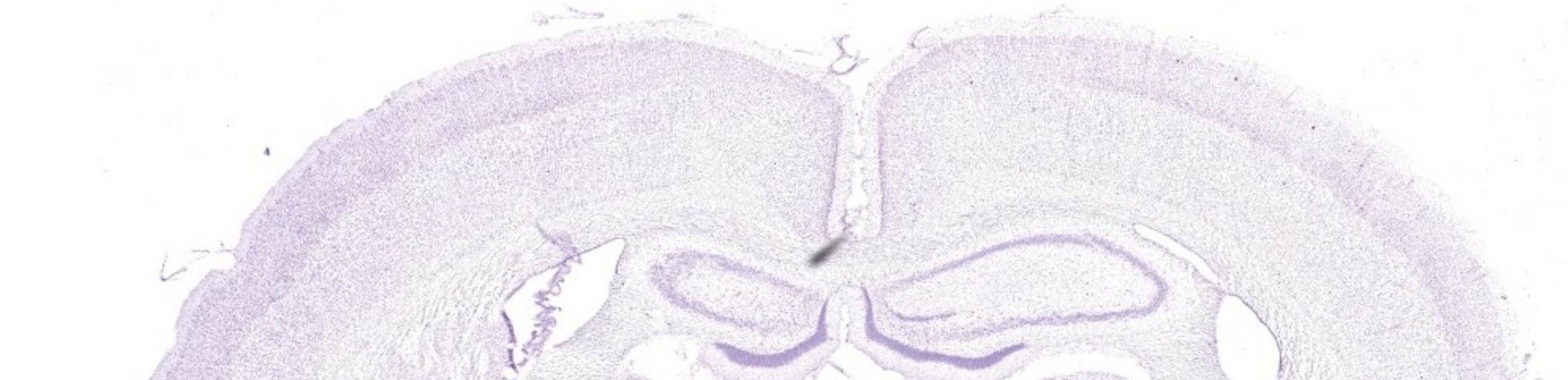

Motivation

Michelle Hildebrandt · Tom Pieper · Peter Winkler
Dieter Kolodziejczyk · Hans Holthausen
Ingmar Blümcke

Neuropathological spectrum of cortical dysplasia in children with severe focal epilepsies

Received: 15 November 2004 / Revised: 16 February 2005 / Accepted: 16 February 2005 / Published online: 17 June 2005

Abstract Cortical dysplasias comprise a variable spectrum of clinical, neuroradiological and histopathological findings. We report about a cohort of 25 pediatric patients (mean age 8.1 ± 4.8 years) with severe drug-resistant early onset focal epilepsies (mean duration 2.1 ± 0.4 years), mental/psychomotor retardation, and multilobar epileptogenesis. Compared to age-matched biopsy controls, microscopical inspection of neurosurgically resected specimens revealed dysplastic neurons histological abnormalities occurring during postnatal maturation of the brain challenge any neuropathological classification in this group of young patients, we propose that these findings are classified according to FCD type I. Our observations support a concept compatible with regional loss of high-order brain organization.

Keywords Brain · Development · Epilepsy · Focal cortical dysplasia · Neuropathology

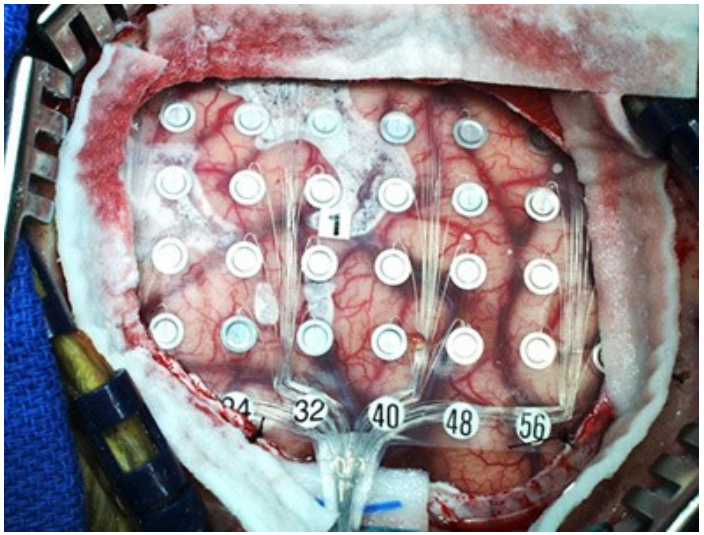

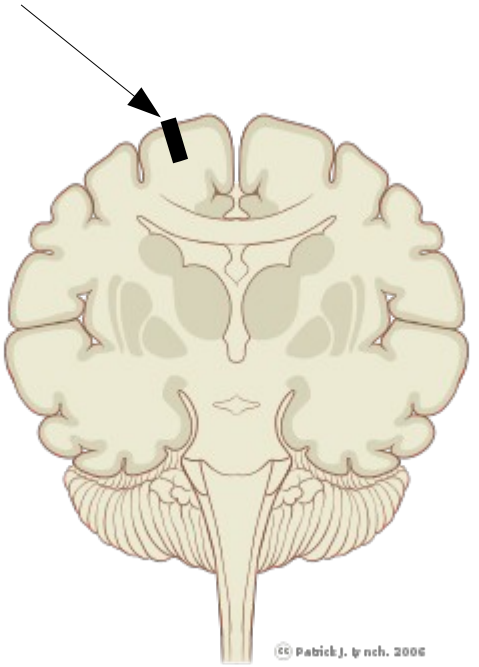

Michelle Hildebrandt · Tom Pieper · Peter Winkler
Dieter Kolodziejczyk · Hans Holthausen
Ingmar Blümcke

Neuropathological spectrum of cortical dysplasia in children with severe focal epilepsies

Received: 15 November 2004 / Revised: 16 February 2005 / Accepted: 16 February 2005 /

Abstract Cortical dysplasias comprise a variable spectrum of clinical, neuroradiological and histopathological findings. We report about a cohort of 25 pediatric patients (mean age 8.1 ± 4.8 years) with severe drug-resistant early onset focal epilepsies (mean duration 2.1 ± 0.4 years), mental/psychomotor retardation, and multilobar epileptogenesis. Compared to age-matched biopsy controls, microscopical inspection of neurosur-

histological abno
maturation of the
classification in th
that these finding
I. Our observatio
regional loss of h

Keywords Brain
cortical dysplasia

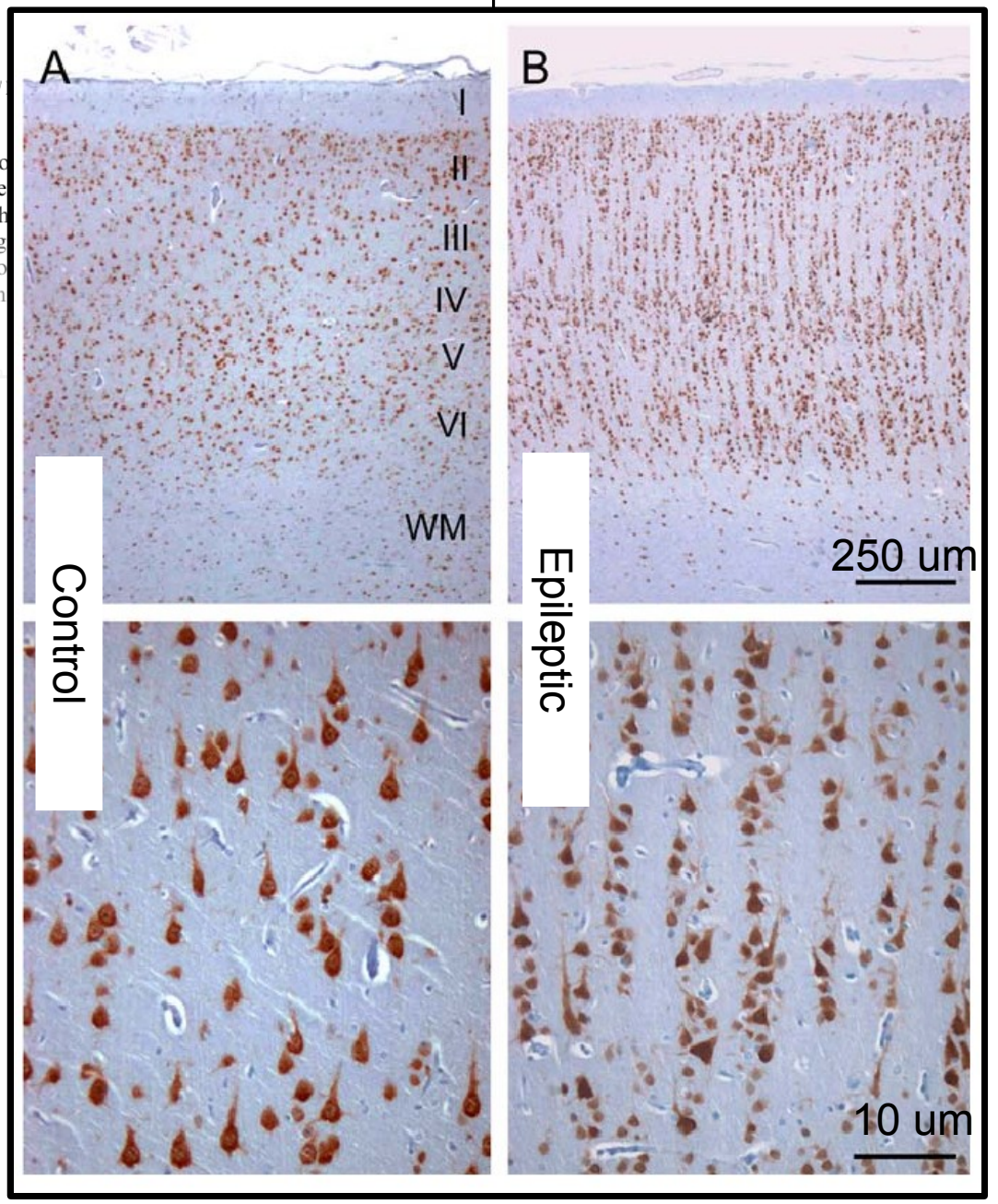

Michelle Hildebrandt · Tom Pieper · Peter Winkler
Dieter Kolodziejczyk · Hans Holthausen
Ingmar Blümcke

Neuropathological spectrum of cortical dysplasia in children with severe focal epilepsies

Received: 15 November 2004 / Revised: 16 February 2005 / Accepted: 16 February 2005 /

Abstract Cortical dysplasias comprise a variable spectrum of clinical, neuroradiological and histopathological findings. We report about a cohort of 25 pediatric patients (mean age 8.1 ± 4.8 years) with severe drug-resistant early onset focal epilepsies (mean duration 2.1 ± 0.4 years), mental/psychomotor retardation, and multilobar epileptogenesis. Compared to age-matched biopsy controls, microscopical inspection of neurosur-

histological abno
maturation of the
classification in th
that these finding
I. Our observatio
regional loss of h

Keywords Brain
cortical dysplasia

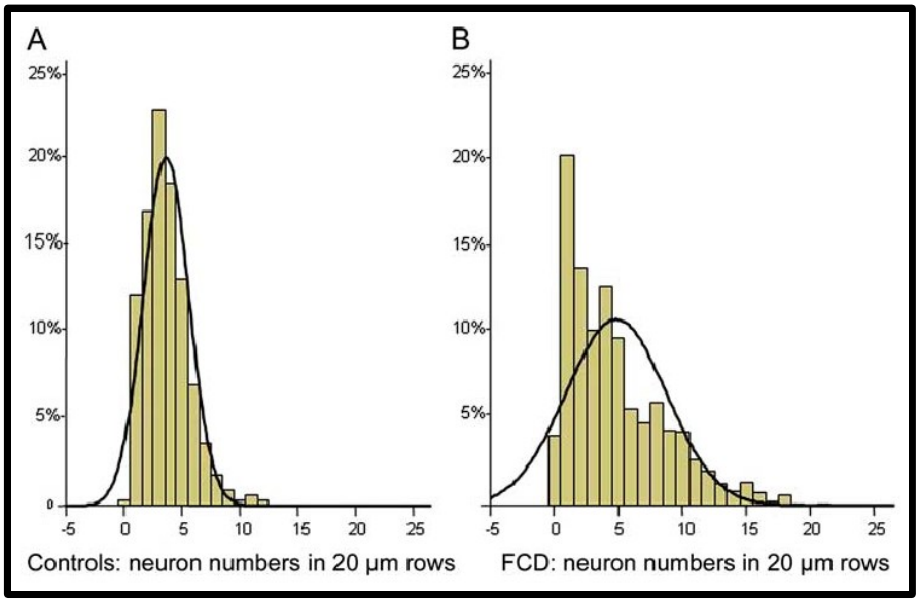

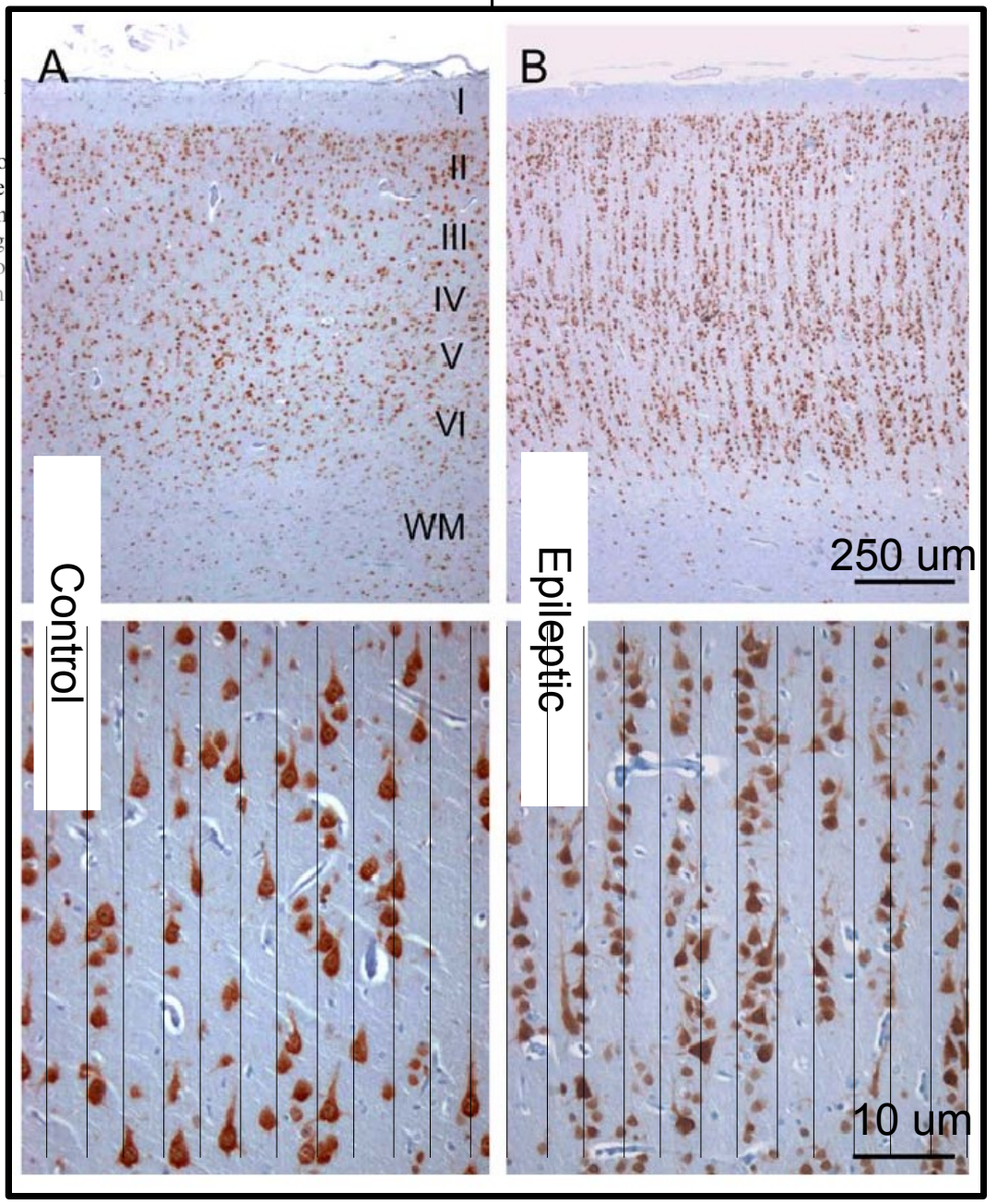

- “Focal cortical dysplasias (FDC) represent patterns of aberrant architectural organization of the neocortex and adjacent white matter.”
- “All other patients presented with rather subtle but statistically significant neuro-anatomical abnormalities.”

Received: 15 November 2004 / Revised: 16 February 2005 / Accepted: 16 February 2005 /

Abstract Cortical dysplasias comprise a variable spectrum of clinical, neuroradiological and histopathological findings. We report about a cohort of 25 pediatric patients (mean age 8.1 ± 4.8 years) with severe drug-resistant early onset focal epilepsies (mean duration 2.1 ± 0.4 years), mental/psychomotor retardation, and multilobar epileptogenesis. Compared to age-matched biopsy controls, microscopical inspection of neurosur-

histological abno
maturation of the
classification in th
that these finding
I. Our observatio
regional loss of h

Keywords Brain
cortical dysplasia

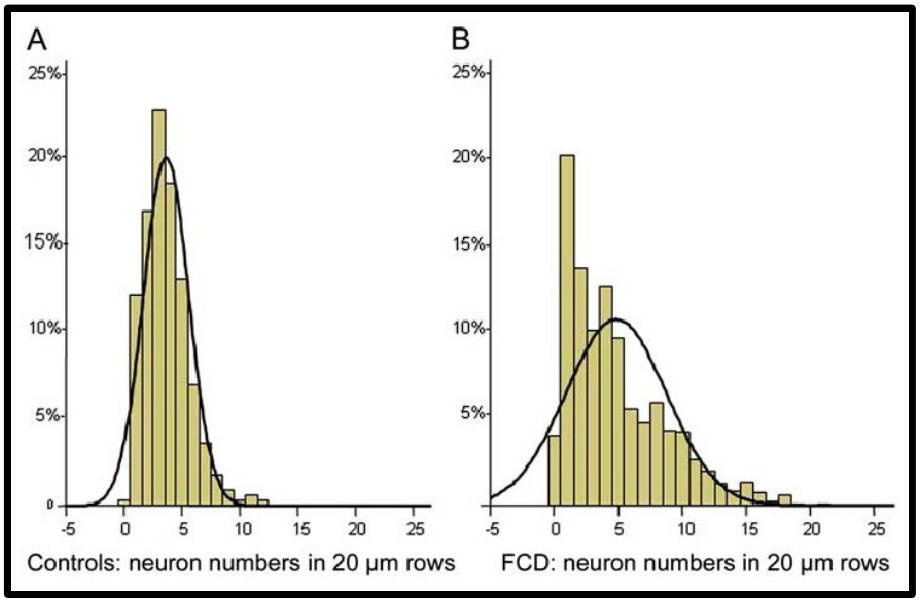

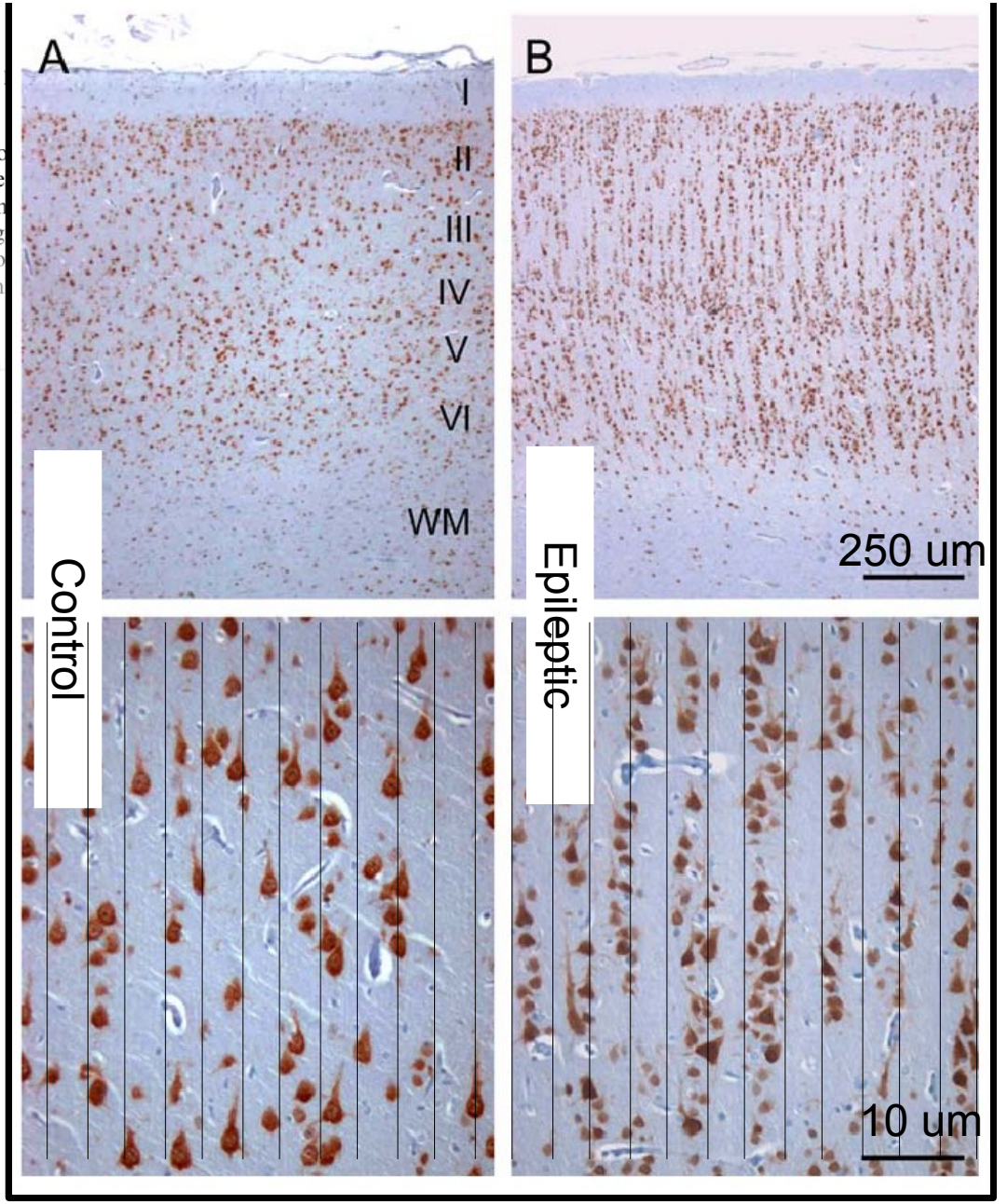

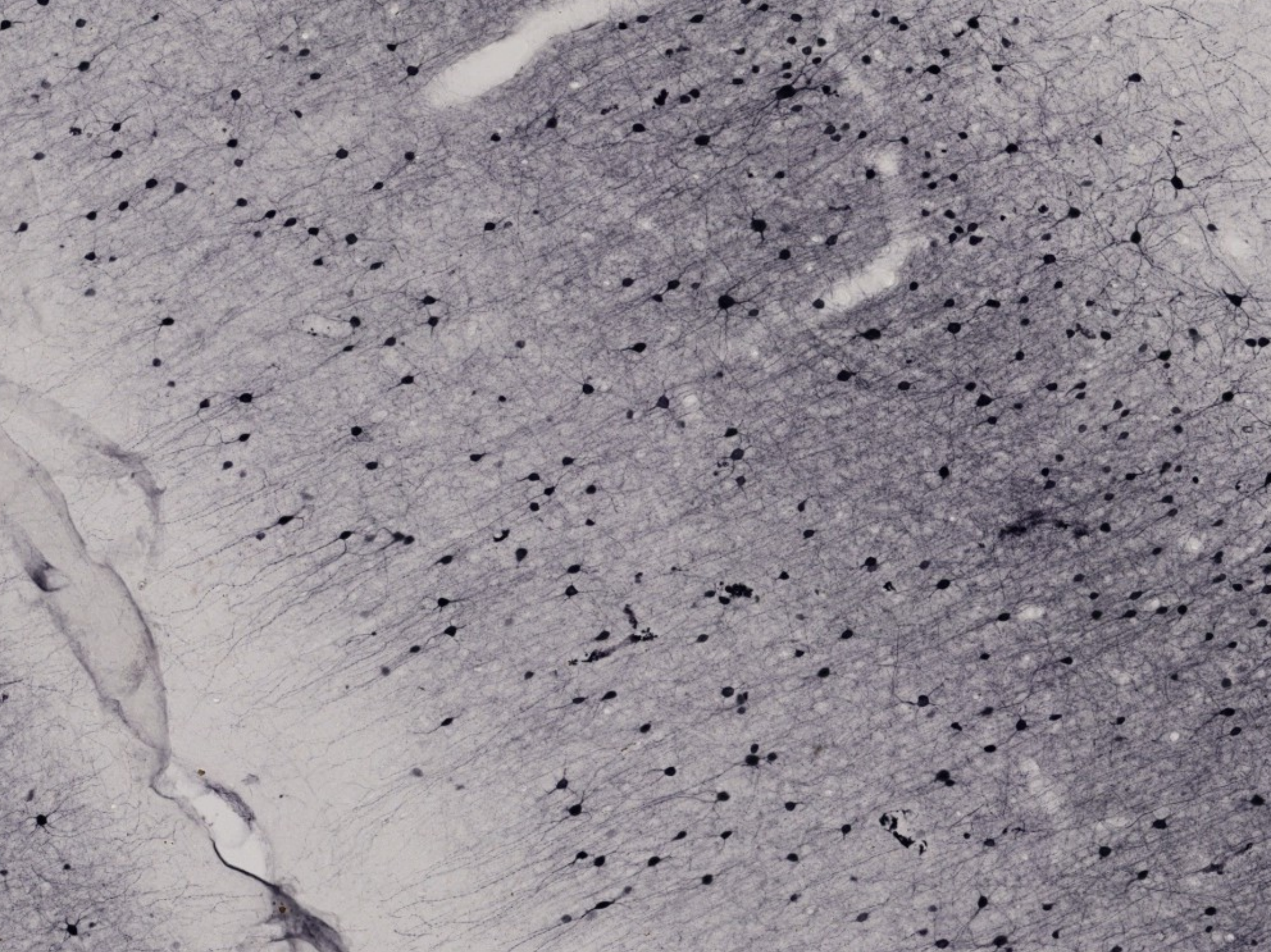

Brain Review

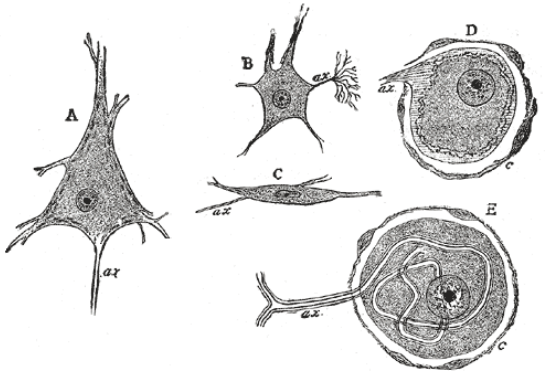

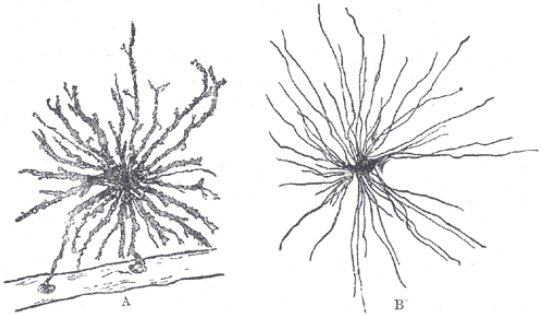

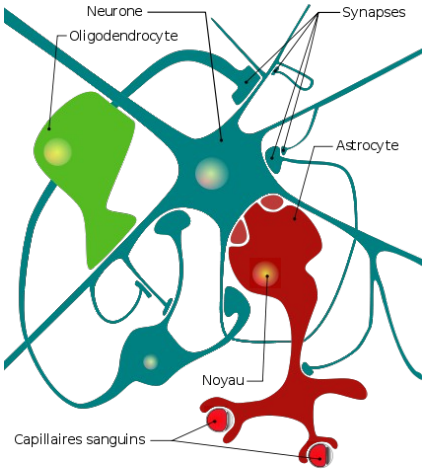

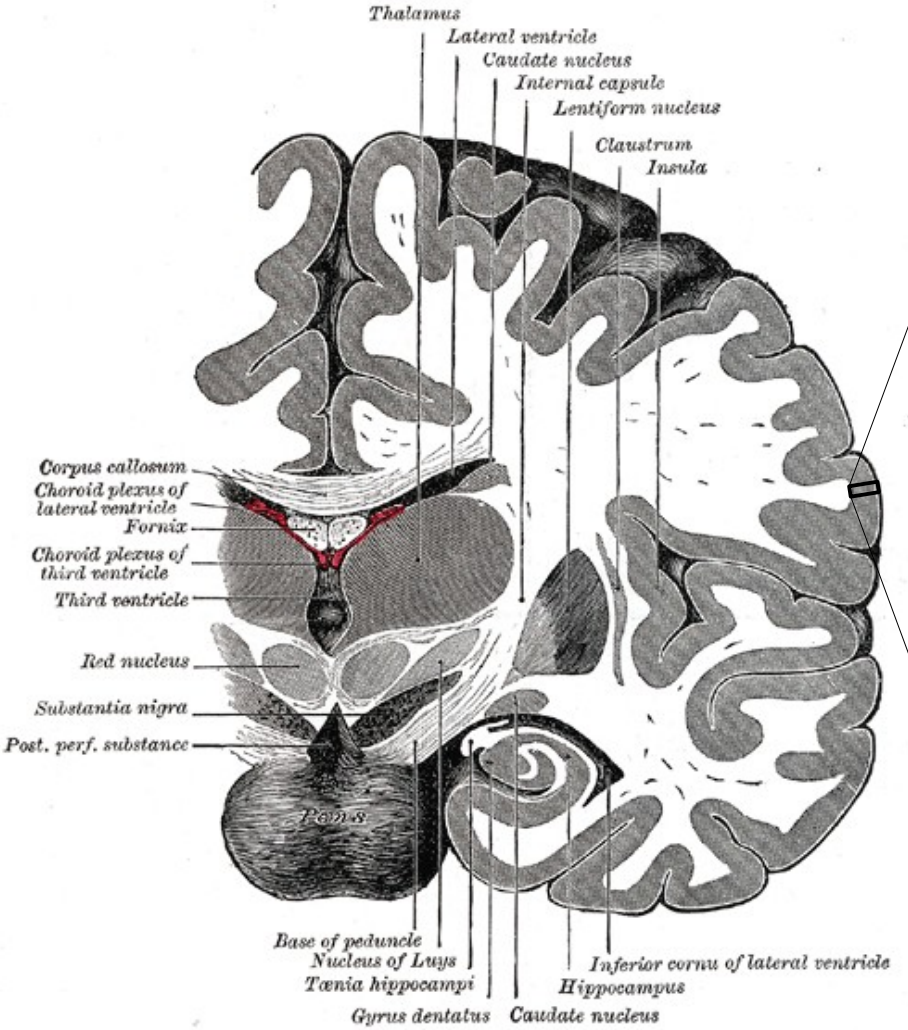

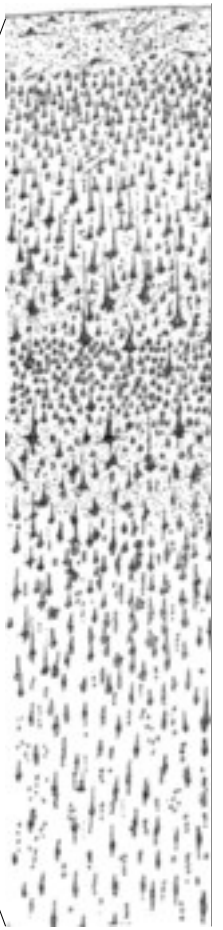

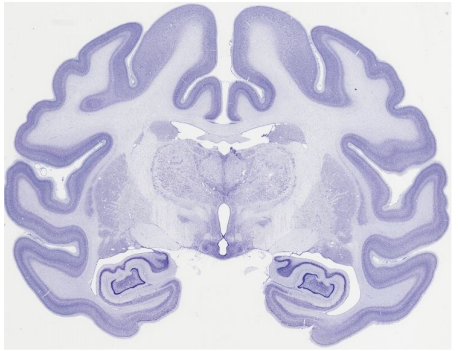

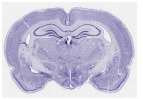

Why Neuroanatomy?

Magnetic Resonance Imaging **(MRI)**

Functional MRI **(fMRI)**

Diffusion Tensor Imaging **(DTI)**

Two-photon Imaging **(2PI)**

Positron emission tomography **(PET)**

Electroencephalography **(EEG)**

MagnetoEncephaloGraphy **(MEG/SQUID)**

Computed Tomography **(CT)**

Needle Electrodes **(NE)**

Case Studies **(CS)**

Neuroanatomy **(NA)**

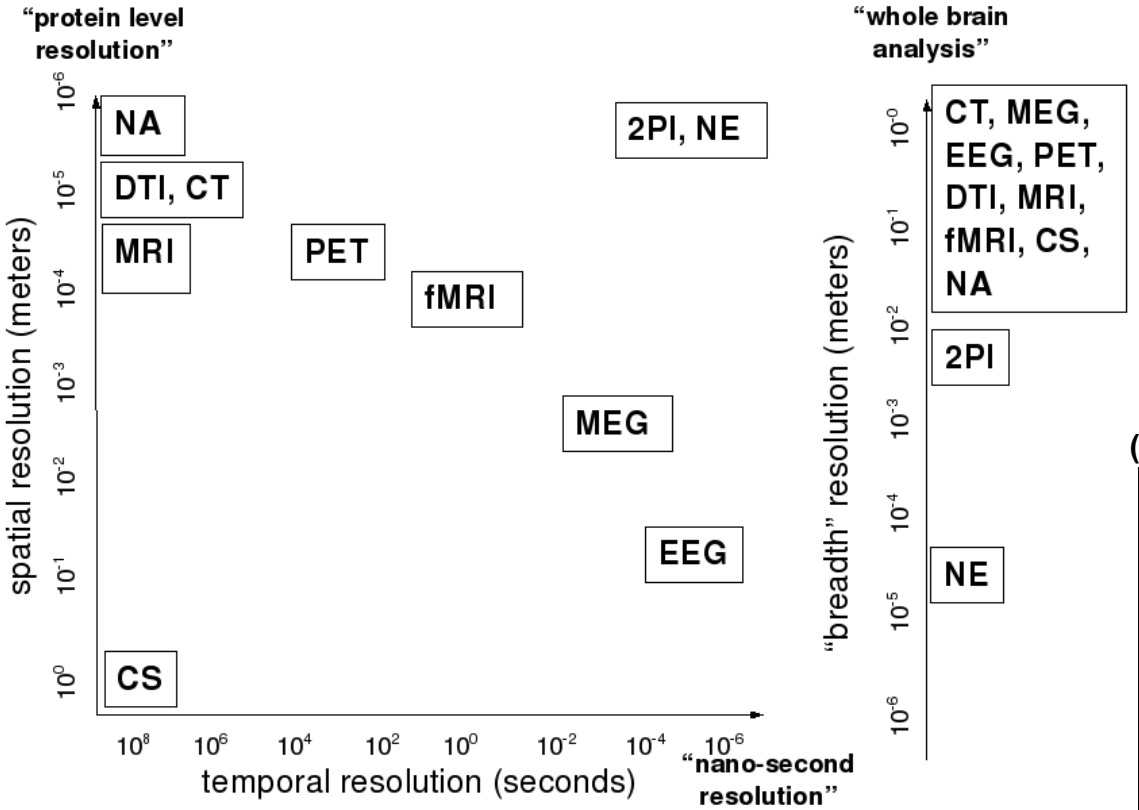

(Functional Magnetic Resonance Imaging)

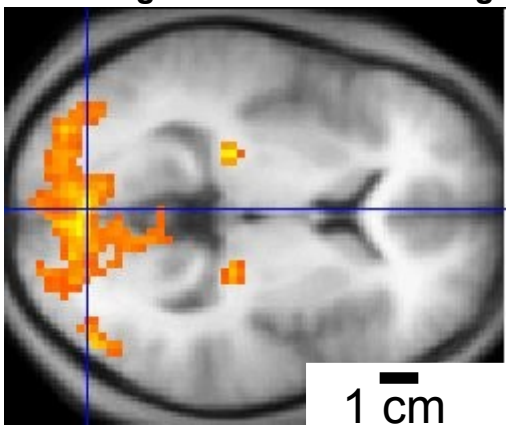

(Needle electrodes)

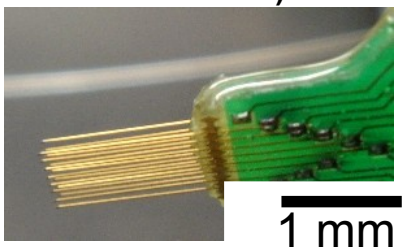

(Neuroanatomy)

Why Neuroanatomy?

Magnetic Resonance Imaging **(MRI)**

Functional MRI **(fMRI)**

Diffusion Tensor Imaging **(DTI)**

Two-photon Imaging **(2PI)**

Positron emission tomography **(PET)**

Electroencephalography **(EEG)**

MagnetoEncephalo Graphy **(MEG/SQUID)**

Computed Tomography **(CT)**

Needle Electrodes **(NE)**

Case Studies **(CS)**

Neuroanatomy **(NA)**

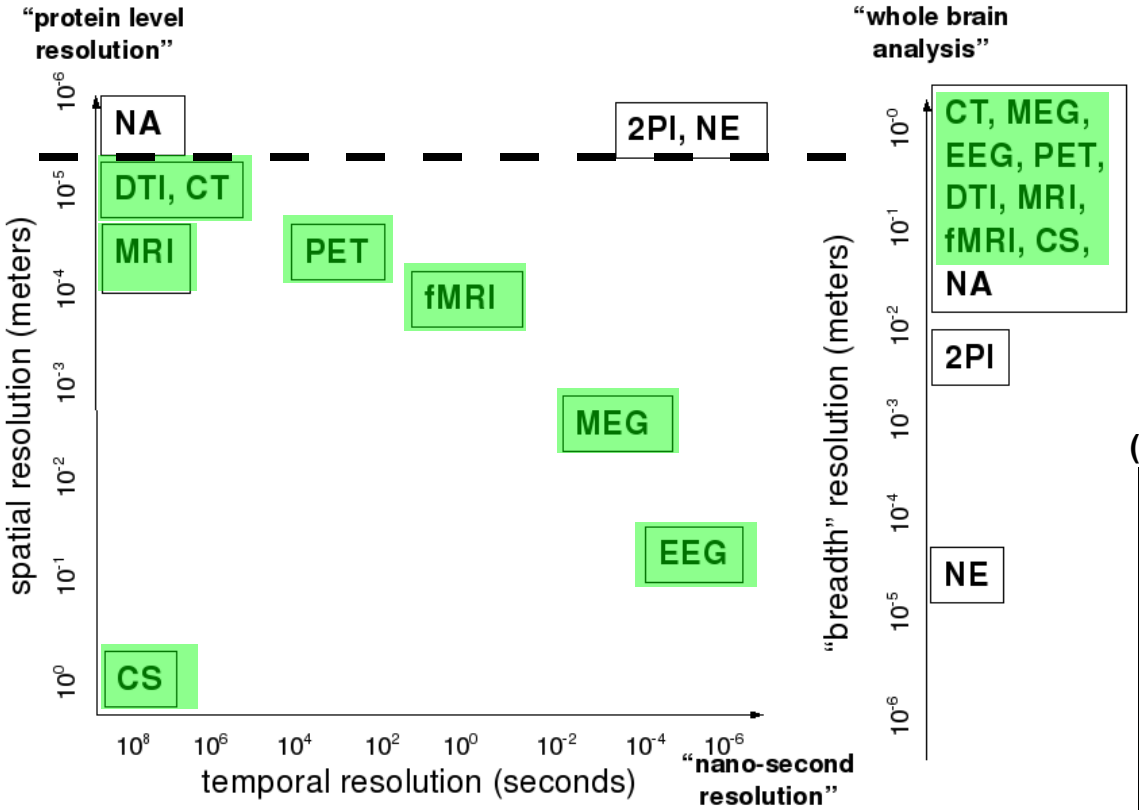

(Functional Magnetic Resonance Imaging)

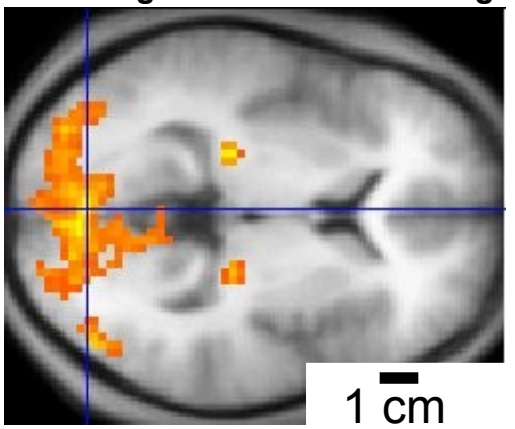

(Needle electrodes)

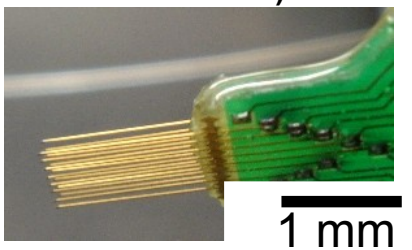

(Neuroanatomy)

Overall Method

Rattus norvegicus

Macaca mulatta

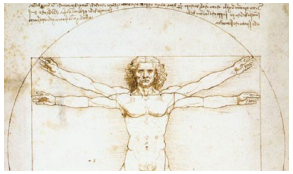

Homo sapiens

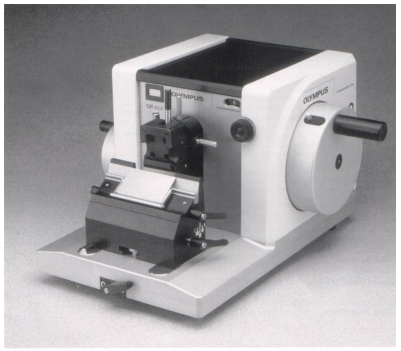

Microtome

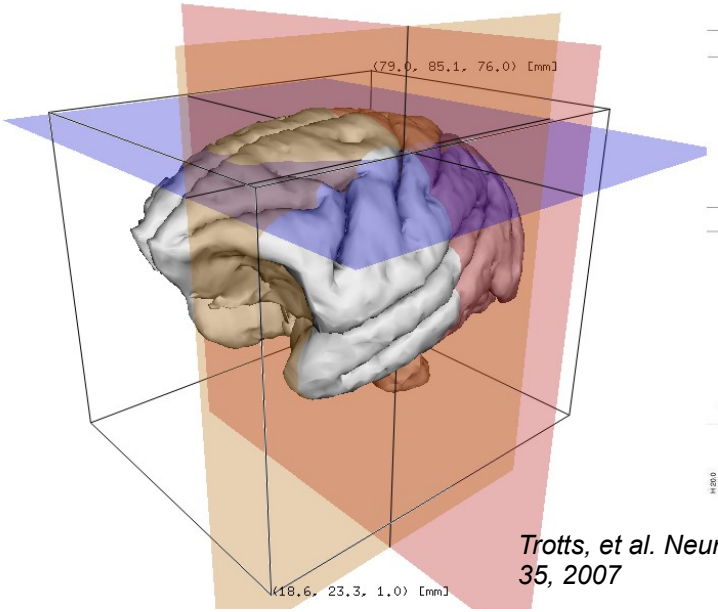

Trotts, et al. NeuroImage, 35, 2007

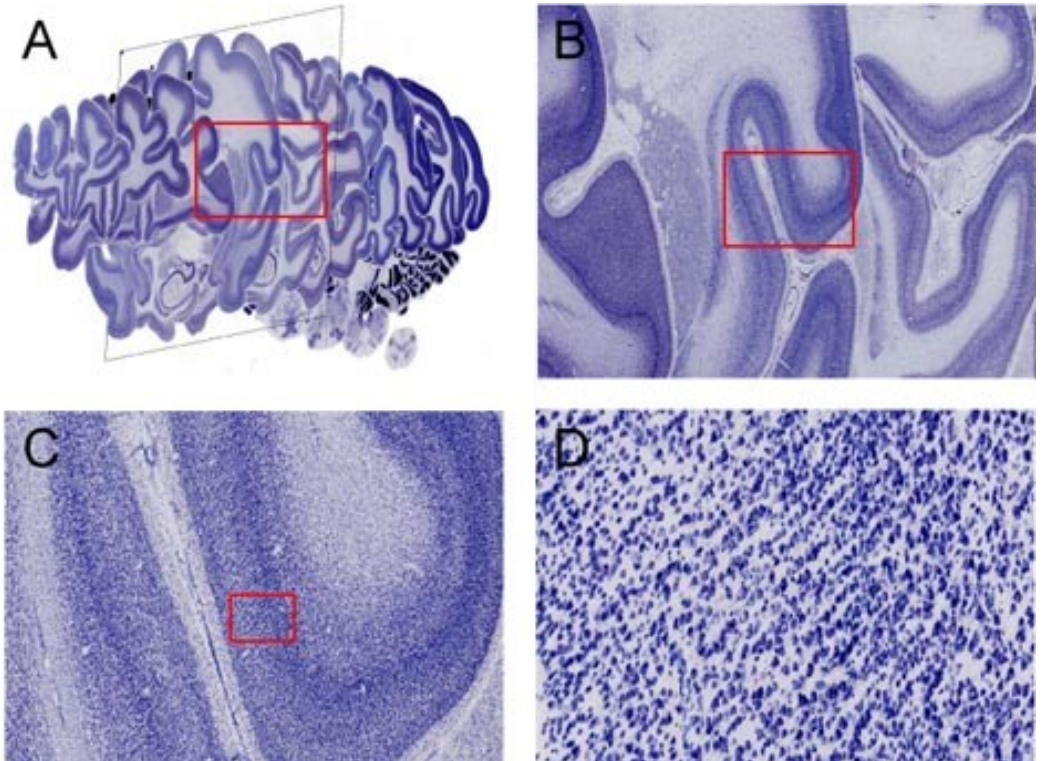

Mikula, et al. NeuroImage, 35, 2007

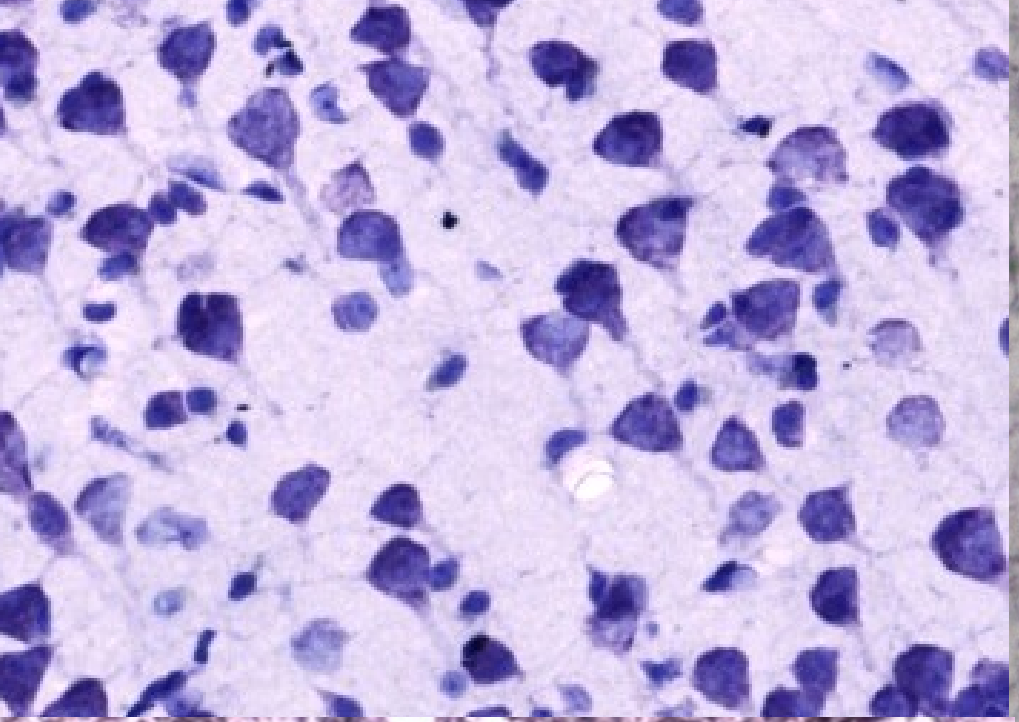
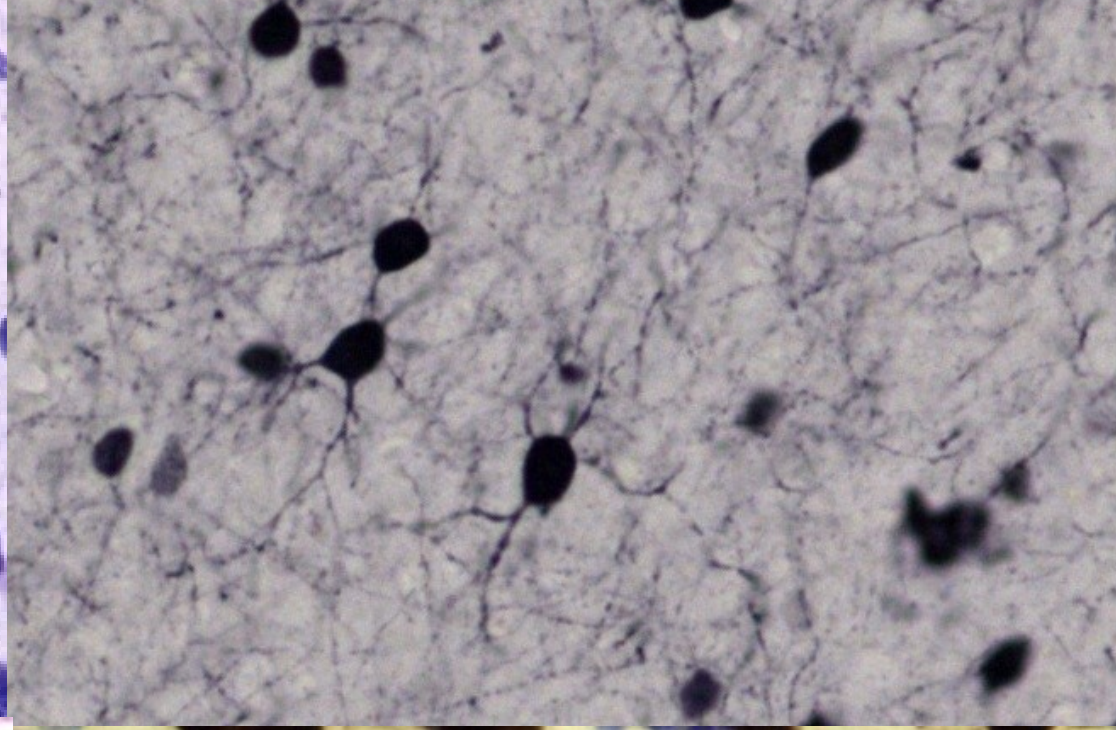
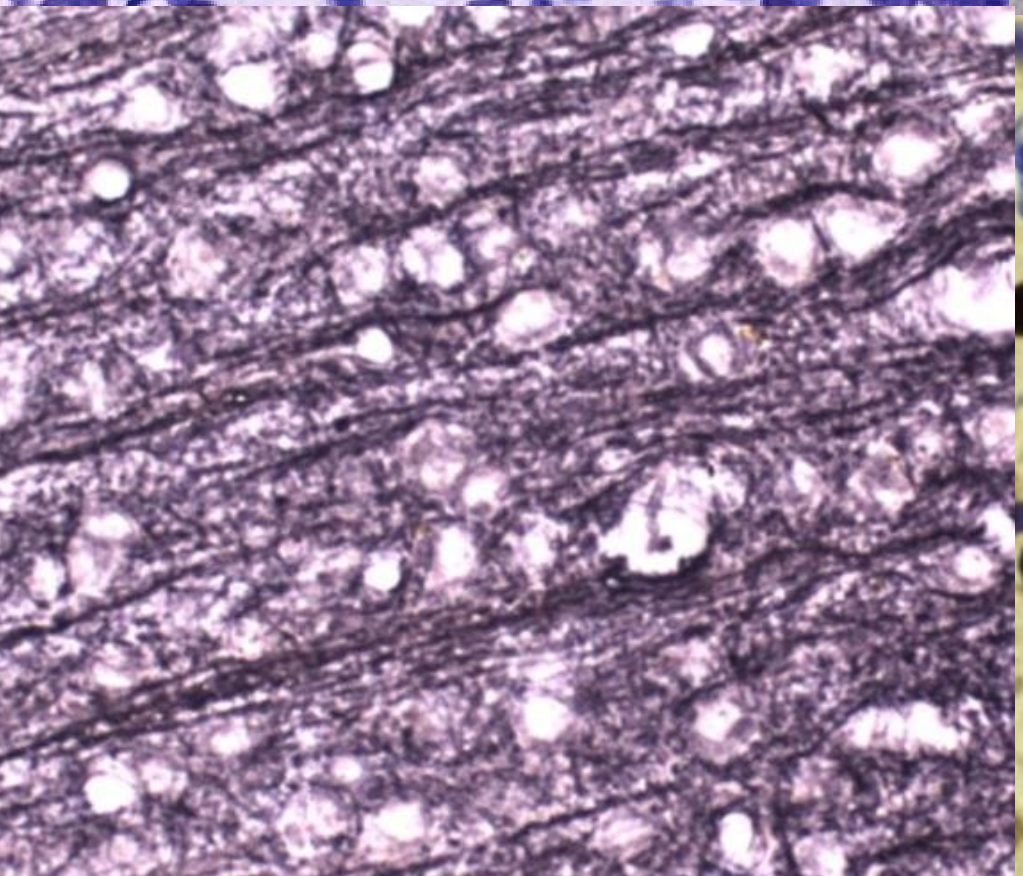
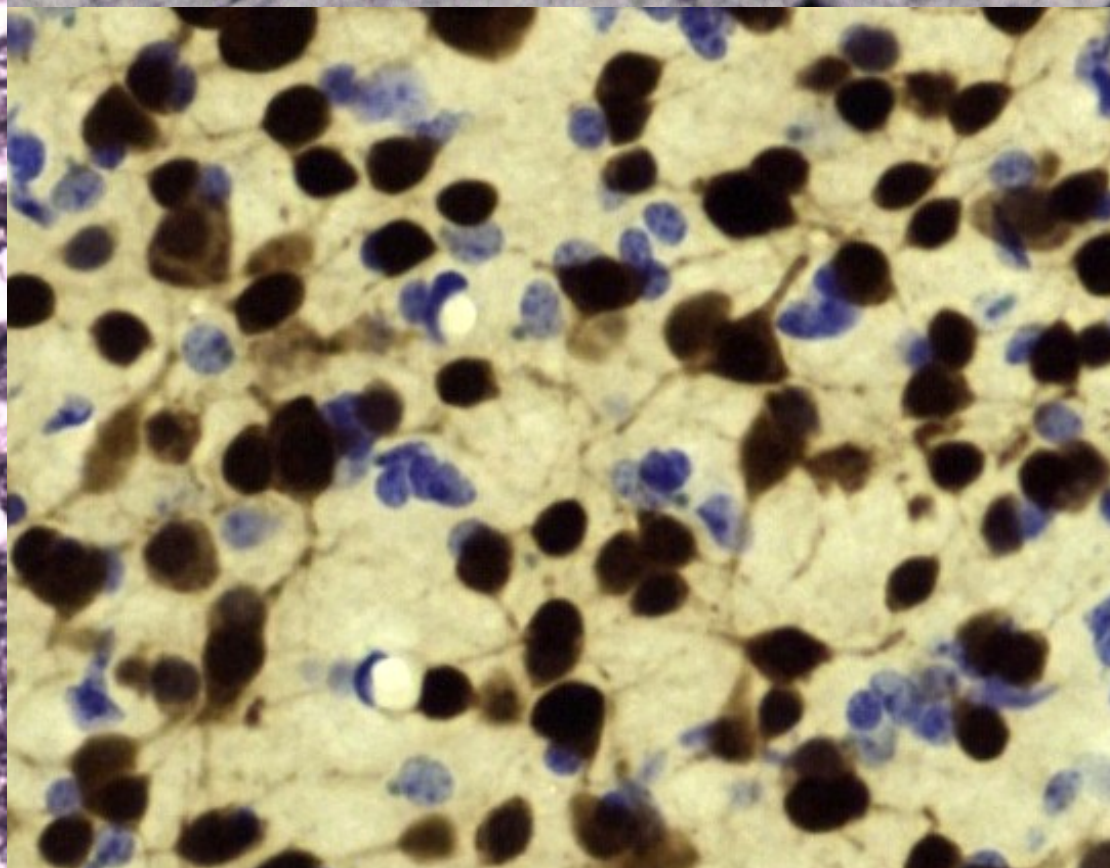

Changes in brain during Development

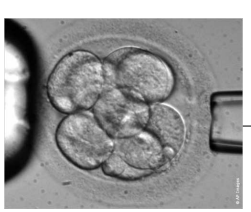

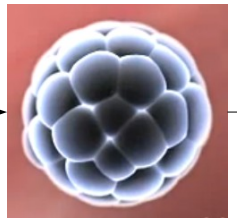

7 days

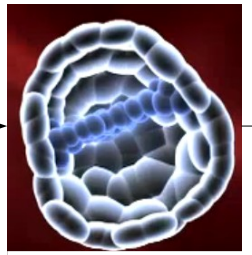

14 days

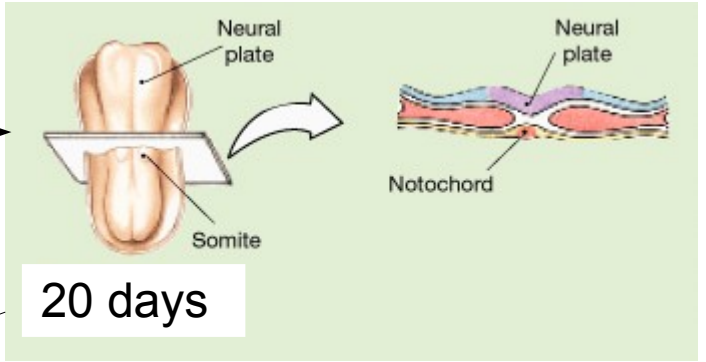

20 days

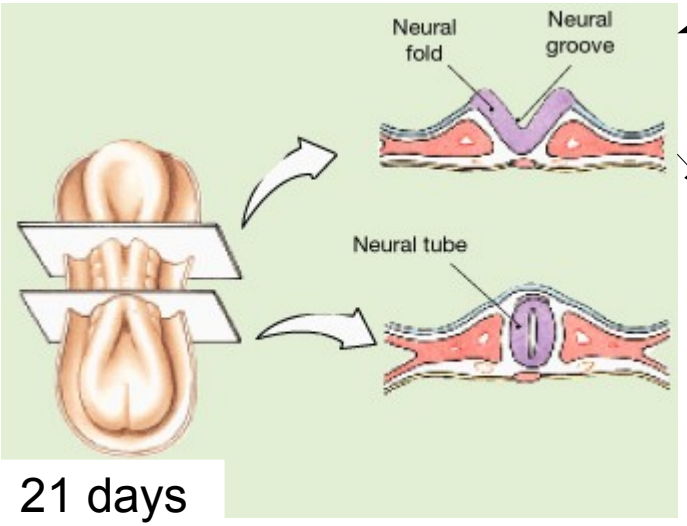

21 days

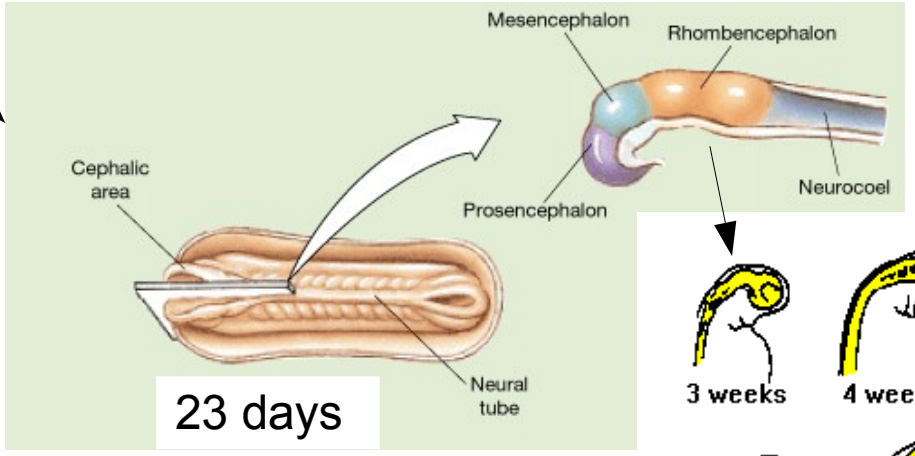

23 days

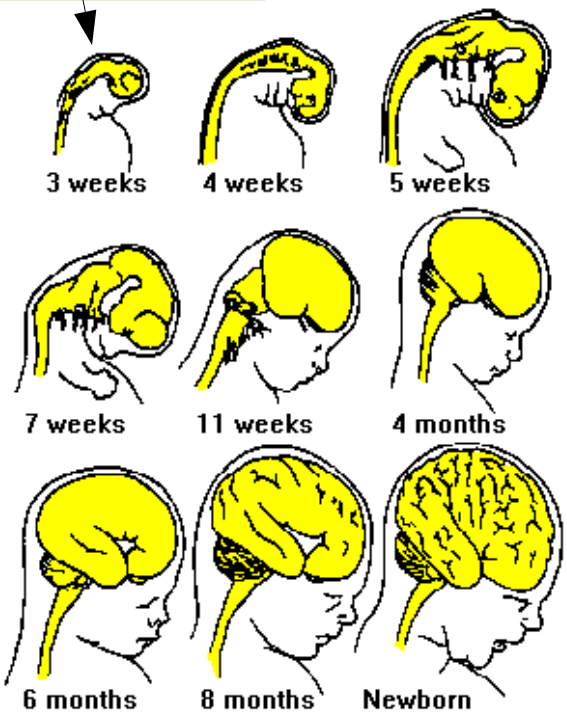

~10^5 cells in 20 days
~10^8 cells at birth (9 months)
~250,000 cells are generated *per minute*

Sources: Howard Huges Medical Institute, Prentice Hall, U.Wash. Neuroscience for Kids.

Changes in brain during Development

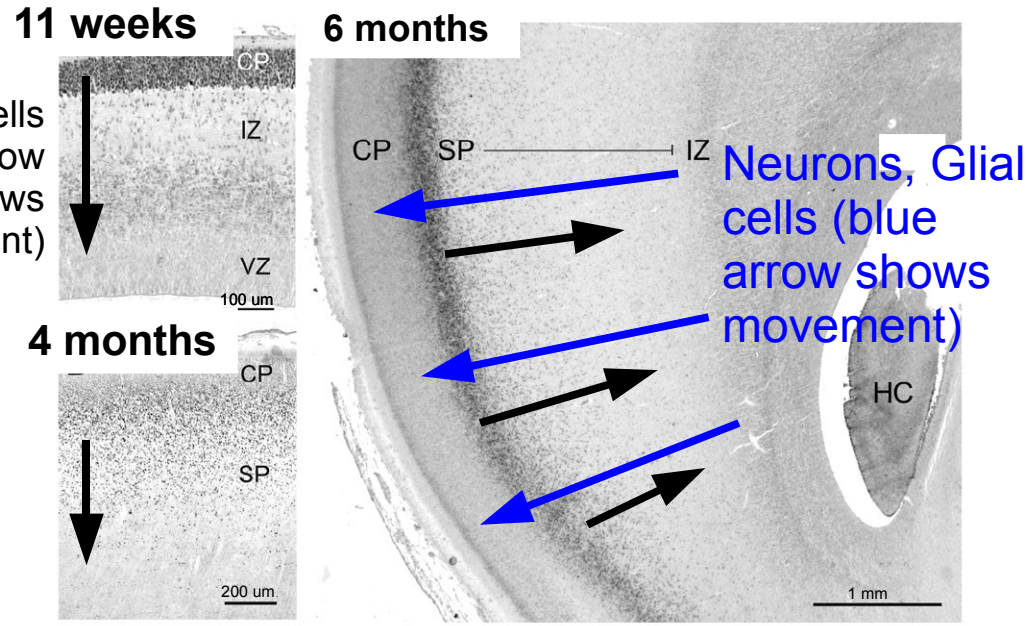

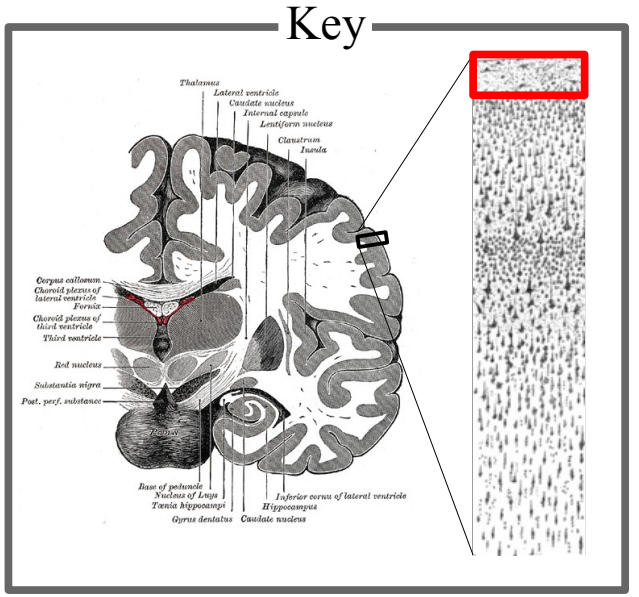

Abbreviations: (CP) cortical plate, (IP) intermediate zone, (VZ) ventricular zone, (SP) sub-plate, (HC) hippocampus

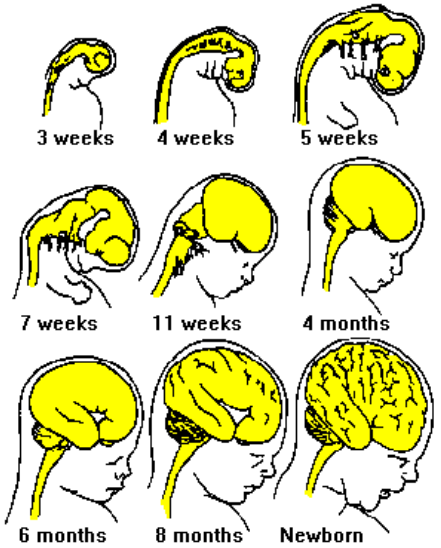

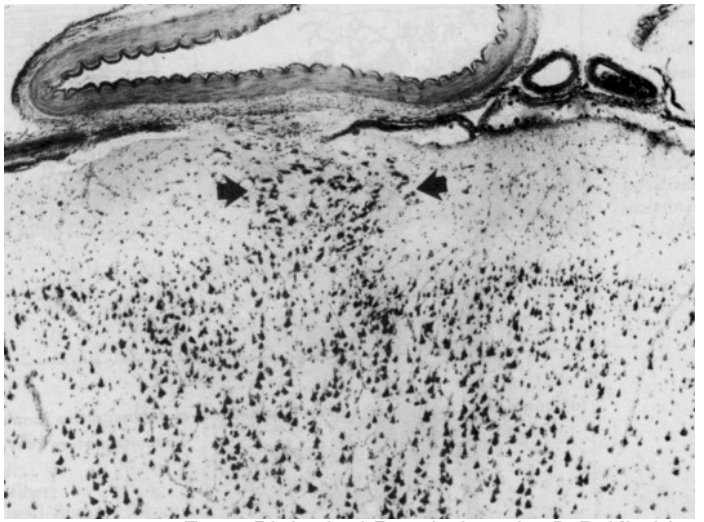

From Biological Psychology by D.P. Kimble

Suarez-Sol, et al. Frontiers in Neuroanatomy, 3, 2009

Changes in brain during Development

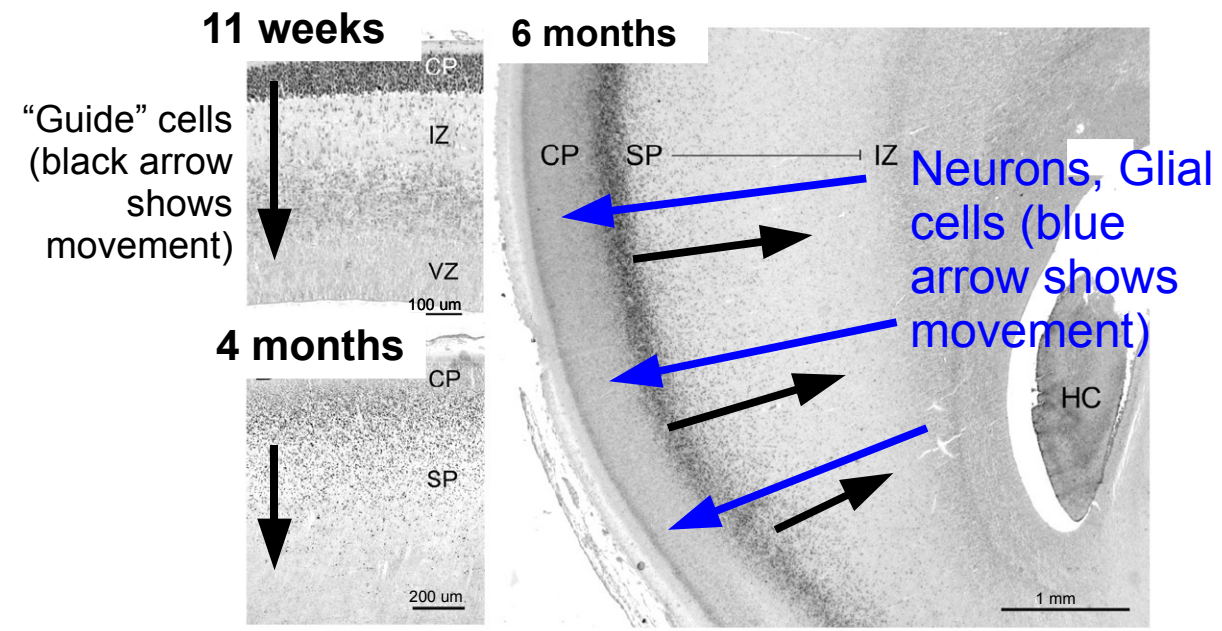

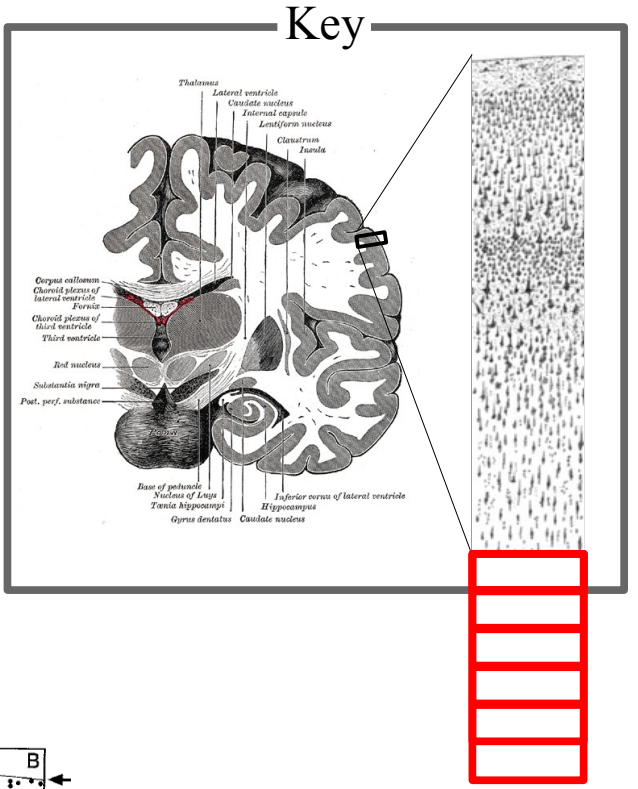

Abbreviations: (CP) cortical plate, (IP) intermediate zone, (VZ) ventricular zone, (SP) sub-plate, (HC) hippocampus

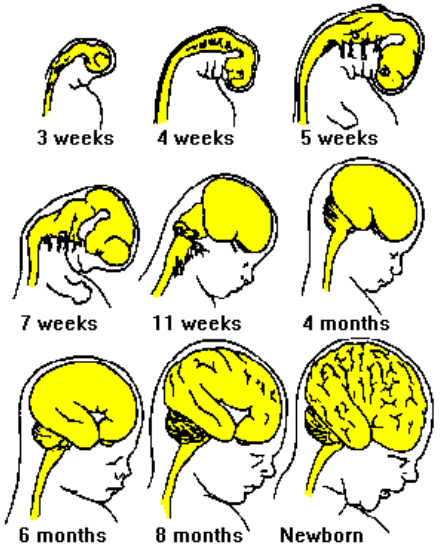

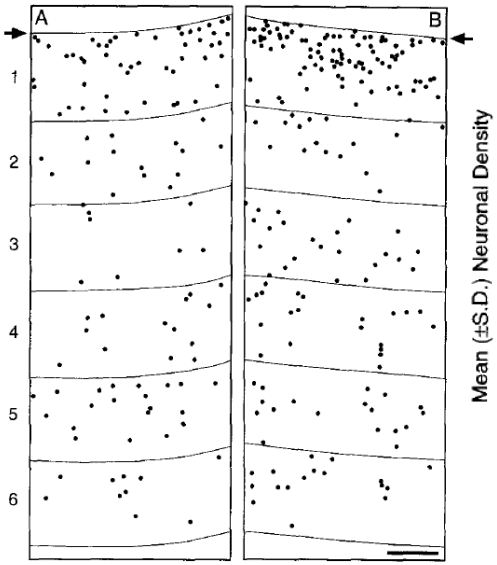

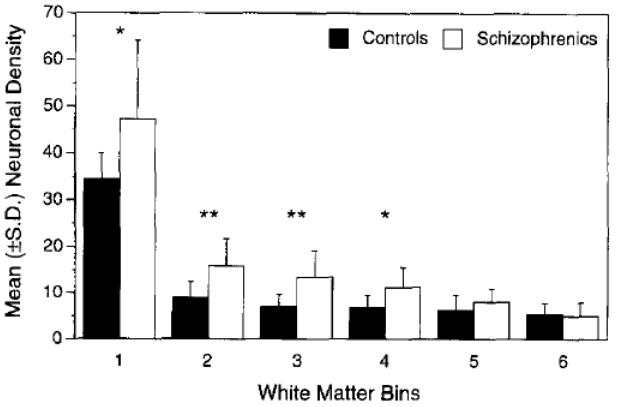

Suarez-Sol, et al. Frontiers in Neuroanatomy, 3, 2009

Suarez-Sol, et al. Frontiers in Neuroanatomy, 3, 2009

Changes in brain during Normal Aging

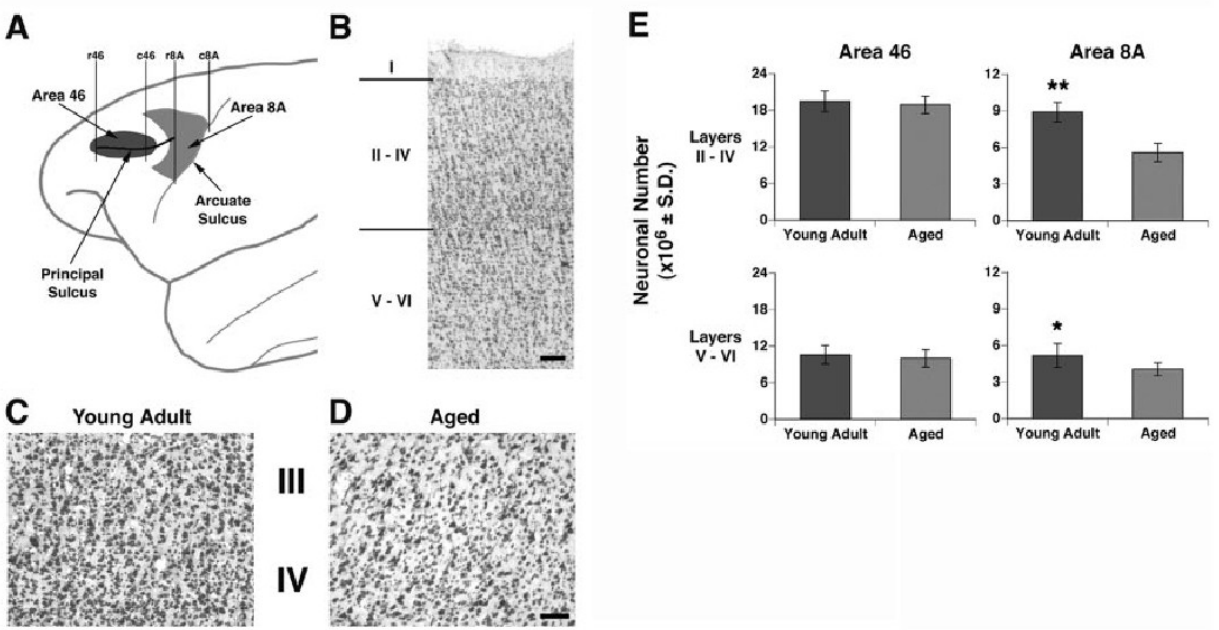

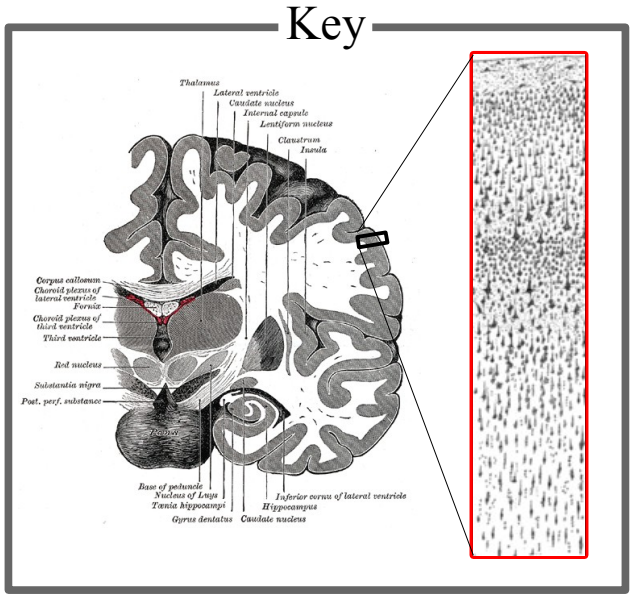

Smith, et al. The Journal of Neuroscience, 24, 2004

$\rho_i(\vec{r})$ density of feature type ***i*** (neuron, glia, surface area, axon length, etc.) at location $\vec{r}$

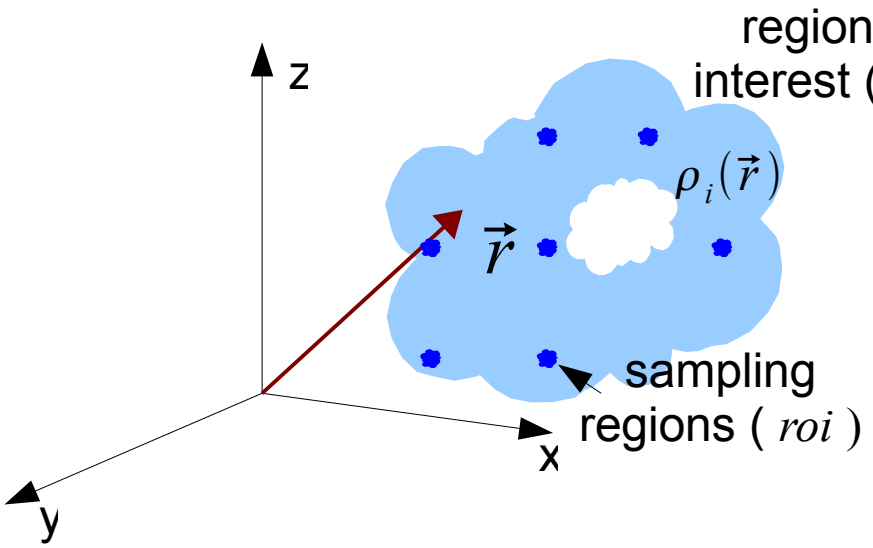

Measurement M of property

$$M = \int_{ROI} \rho_i(\vec{r})\, d\vec{r}$$

alternatively..

$$M = \int_{roi} \rho_i(\vec{r})\, d\vec{r} \cdot \left[\frac{\int_{ROI} d\vec{r}}{\int_{roi} d\vec{r}} \right]$$

Stereology

Stereology example

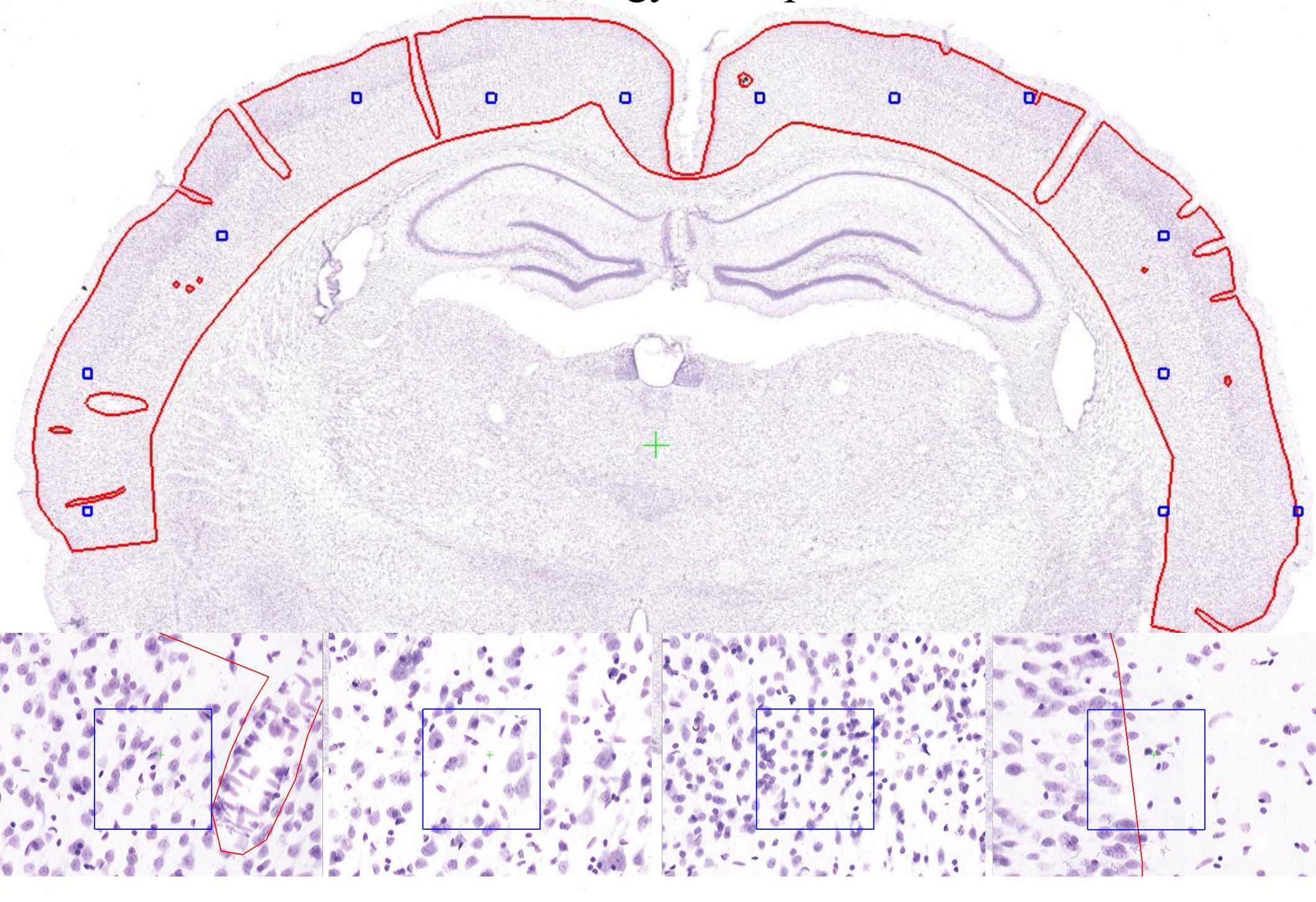

Changes in brain during Disease

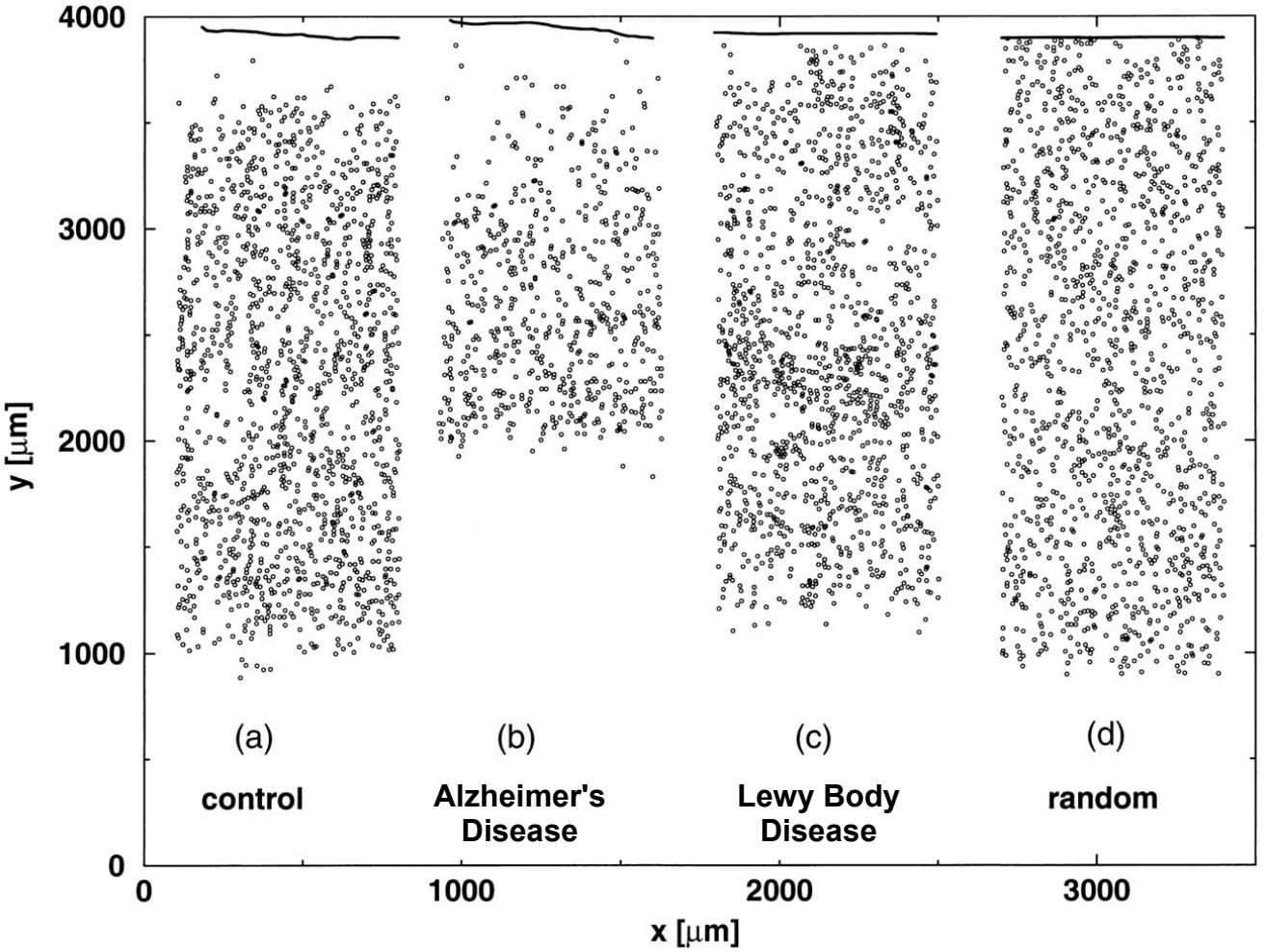

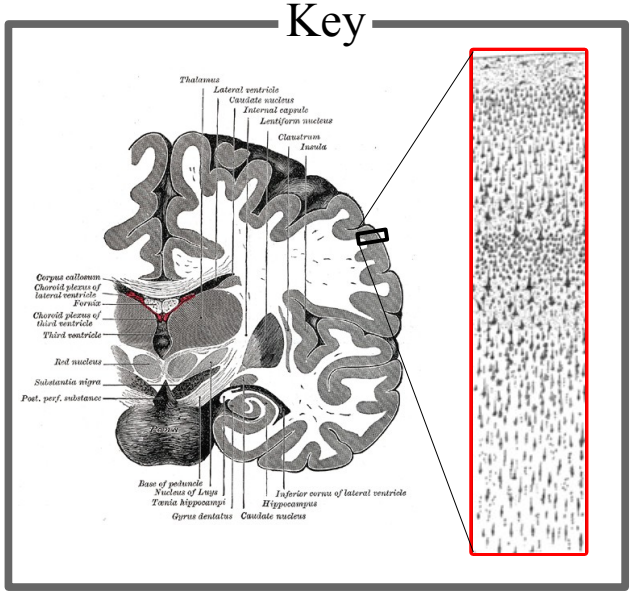

Buldyrev et al. ***PNAS 97****, 5039-5053 (2000)*

Observations

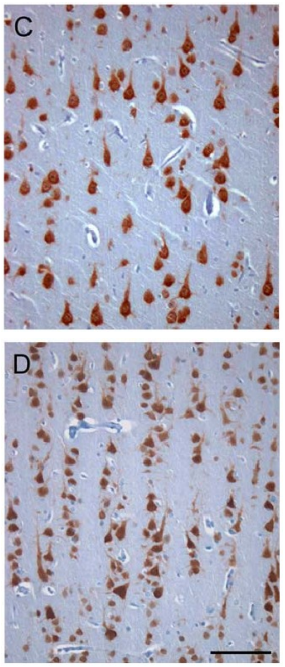

Lewy Body Disease

?

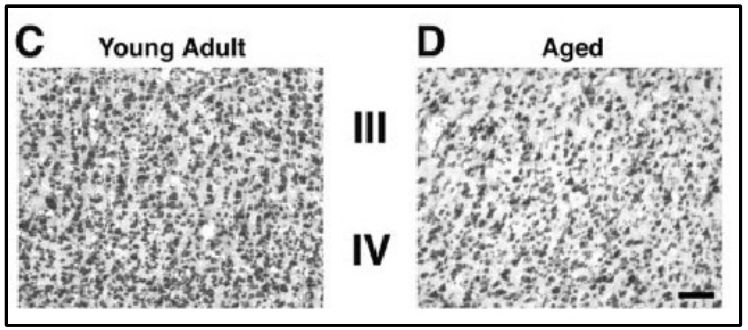

1. Some aberrations in the cortex structure are visually apparent, some are not, and some cannot be observed using sampling theory (stereology). Such aberrations still correspond to meaningful changes in brain function. *It is possible that there are many such aberrations or patterns that are unknown.*
   - No systematic way to measure spatial patterns of cellular or other properties. This leads to only measuring what can be seen by eye or hypothesized and measured via stereology.

2. Full breadth of brains are not being utilized in studies.
   - Analysis studies, even with the power of stereology, are labor intensive and can only be performed in local regions.
   - Even when being studied, a brain region is only sampled in small amounts (using stereology) due to the overwhelming number of cells that exist.
   - hypothesis driven research disallows exploratory correlative analysis of focused studies in very different brain regions.

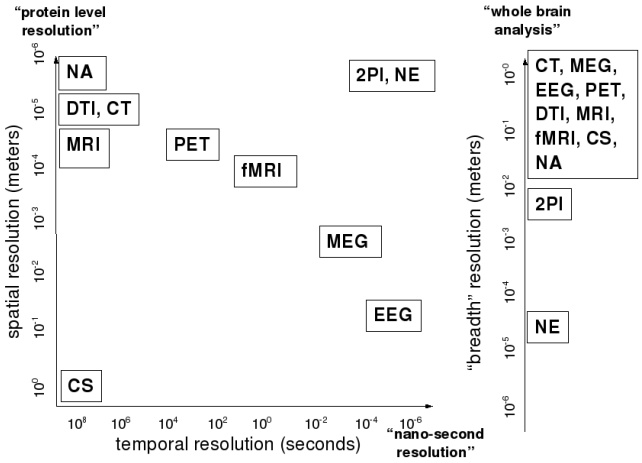

Goal: new experimental tool

1. Acquire and analyze of neuroanatomical measurements from the entire cortex.
   - Allows for exploration of unknown and un-hypothesized relationships of quantitative measurements within the brain (more data driven exploration).
   - Can (potentially) reduce the amount of tissue and subjects tested.

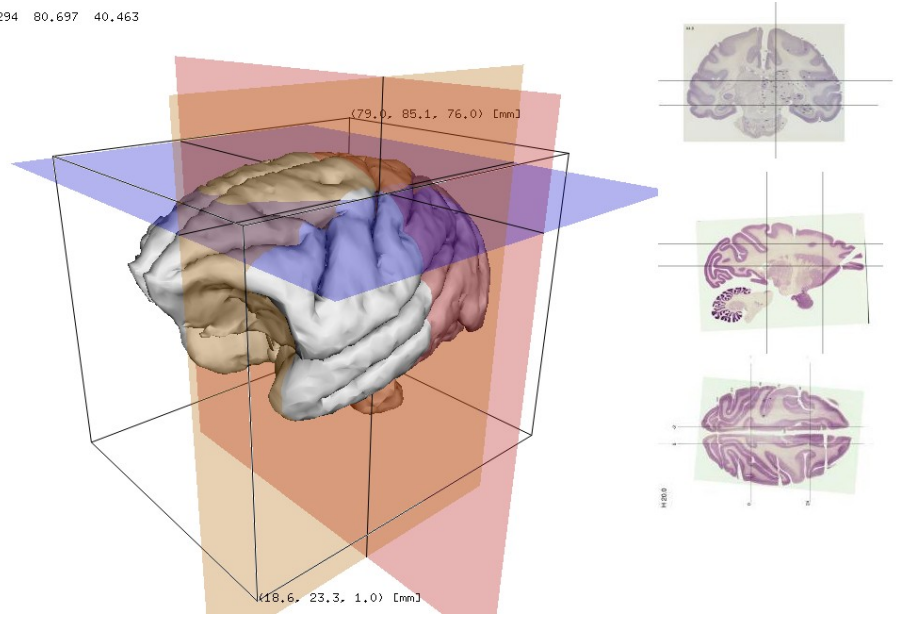

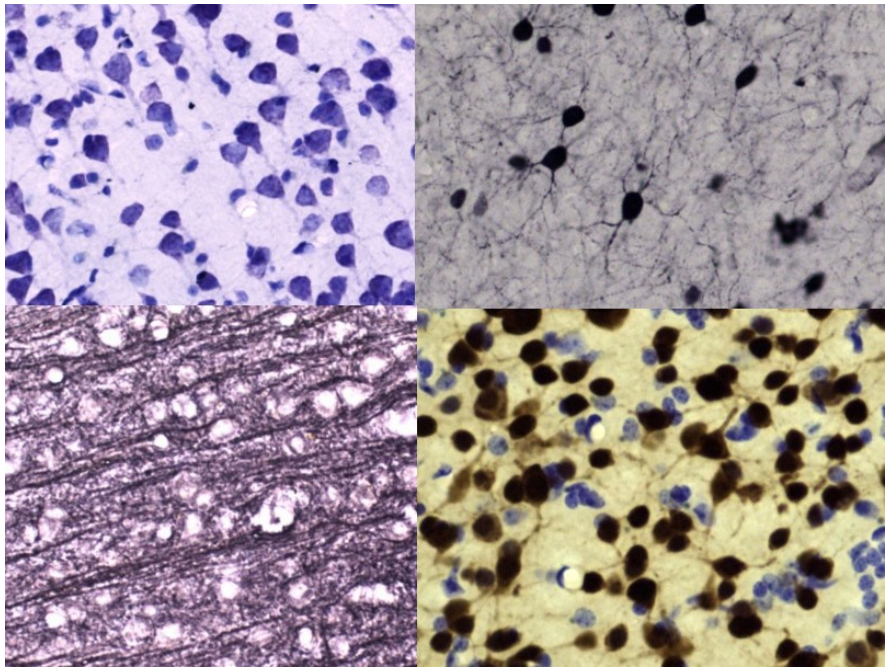

2. Using concepts from statistical physics, create measurement tools that measure tissue patterns which exist right above biological noise.
   - Allows for more understanding of the role of tissue structure on function of the cortex in any neuroanatomical study.
   - Allows for more data driven research.

Theory

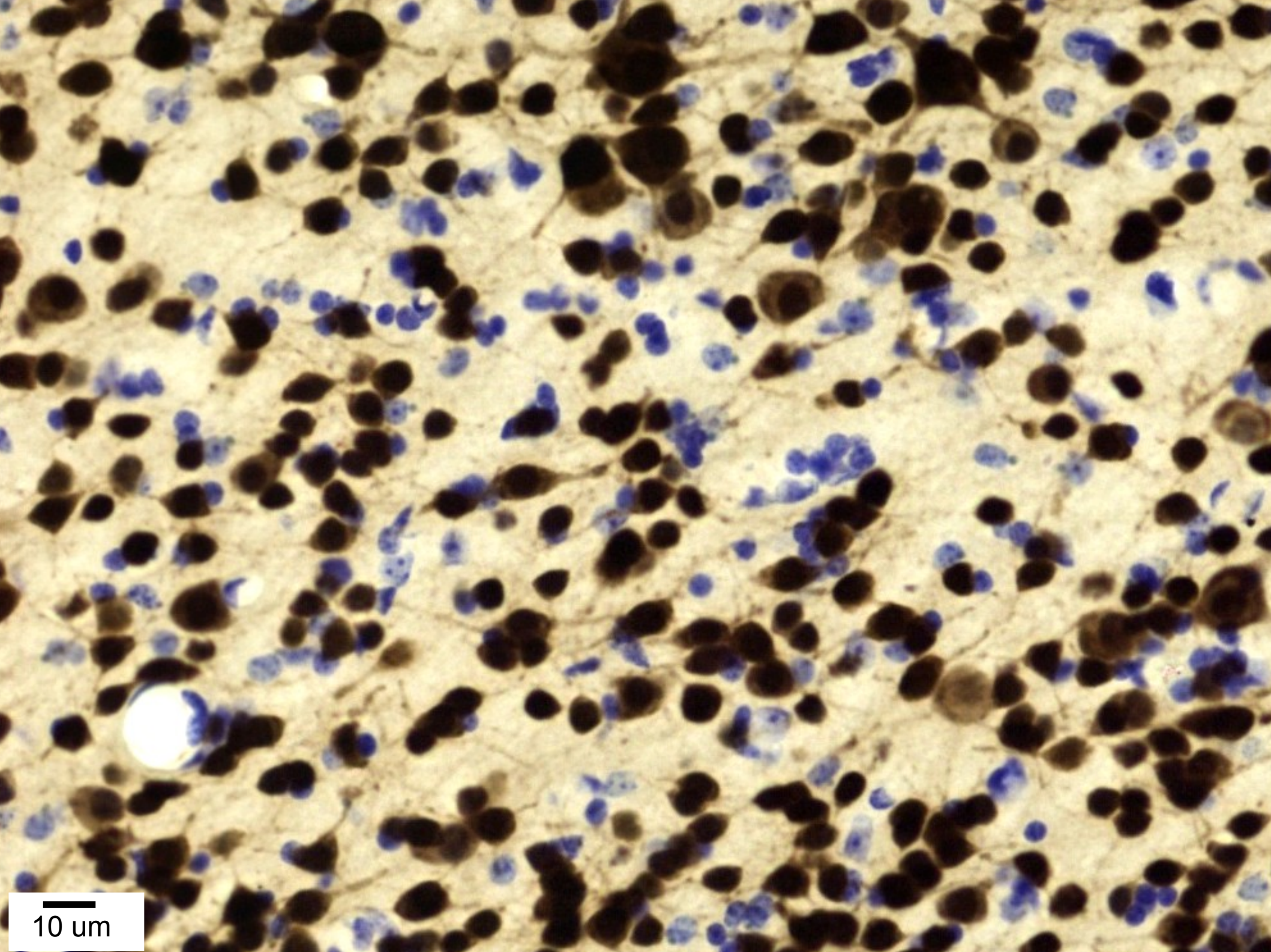
10 um

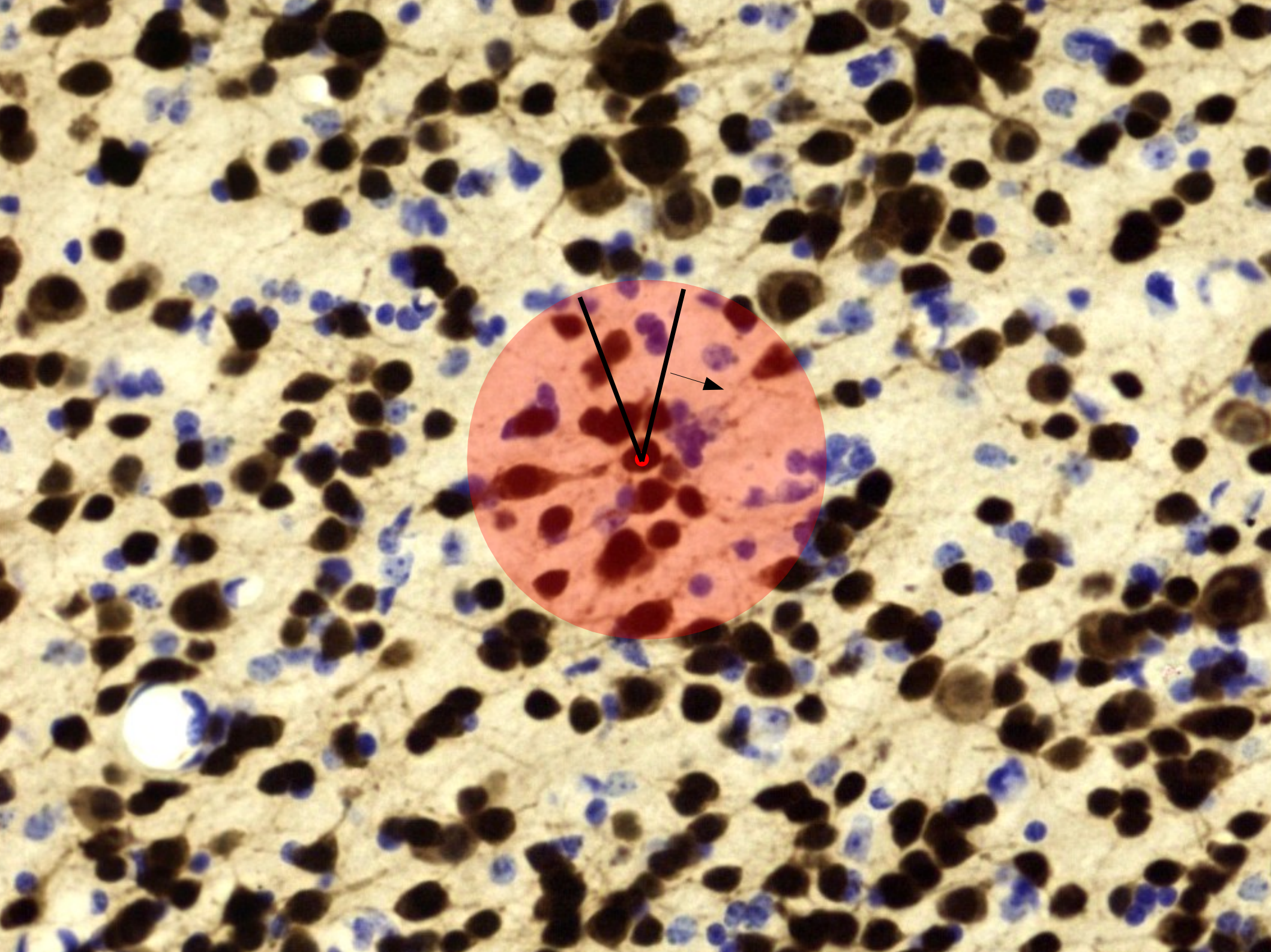

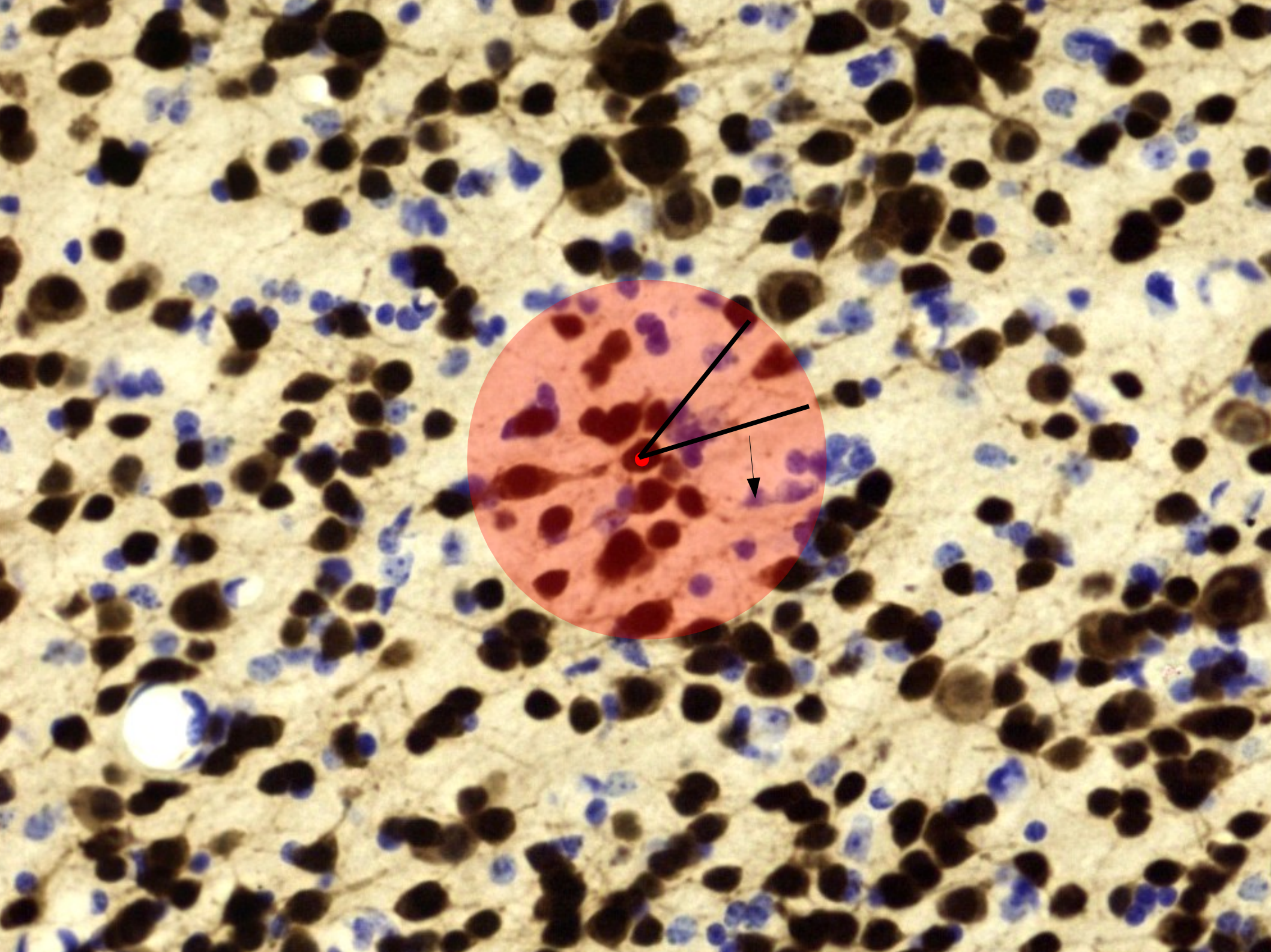

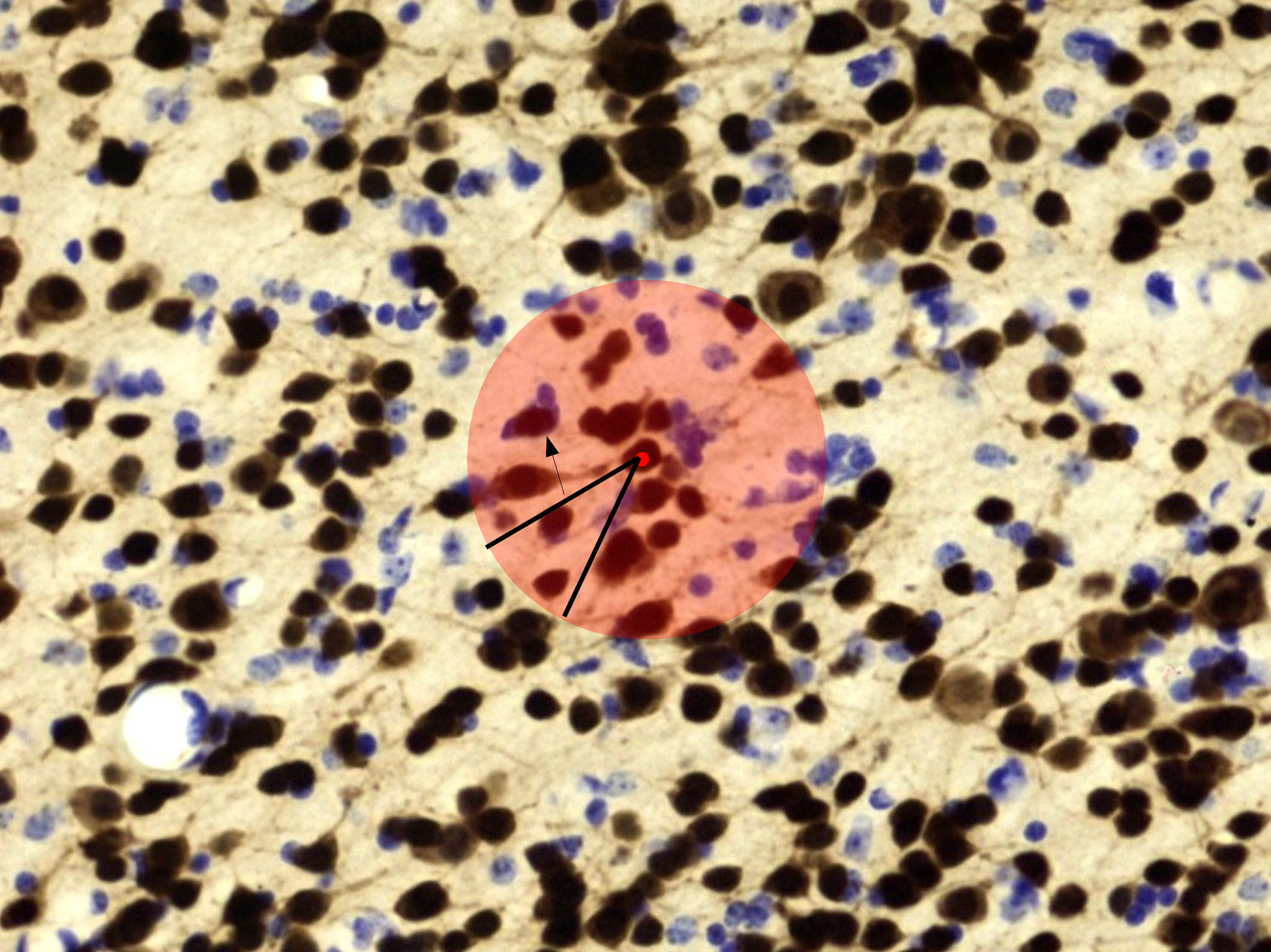

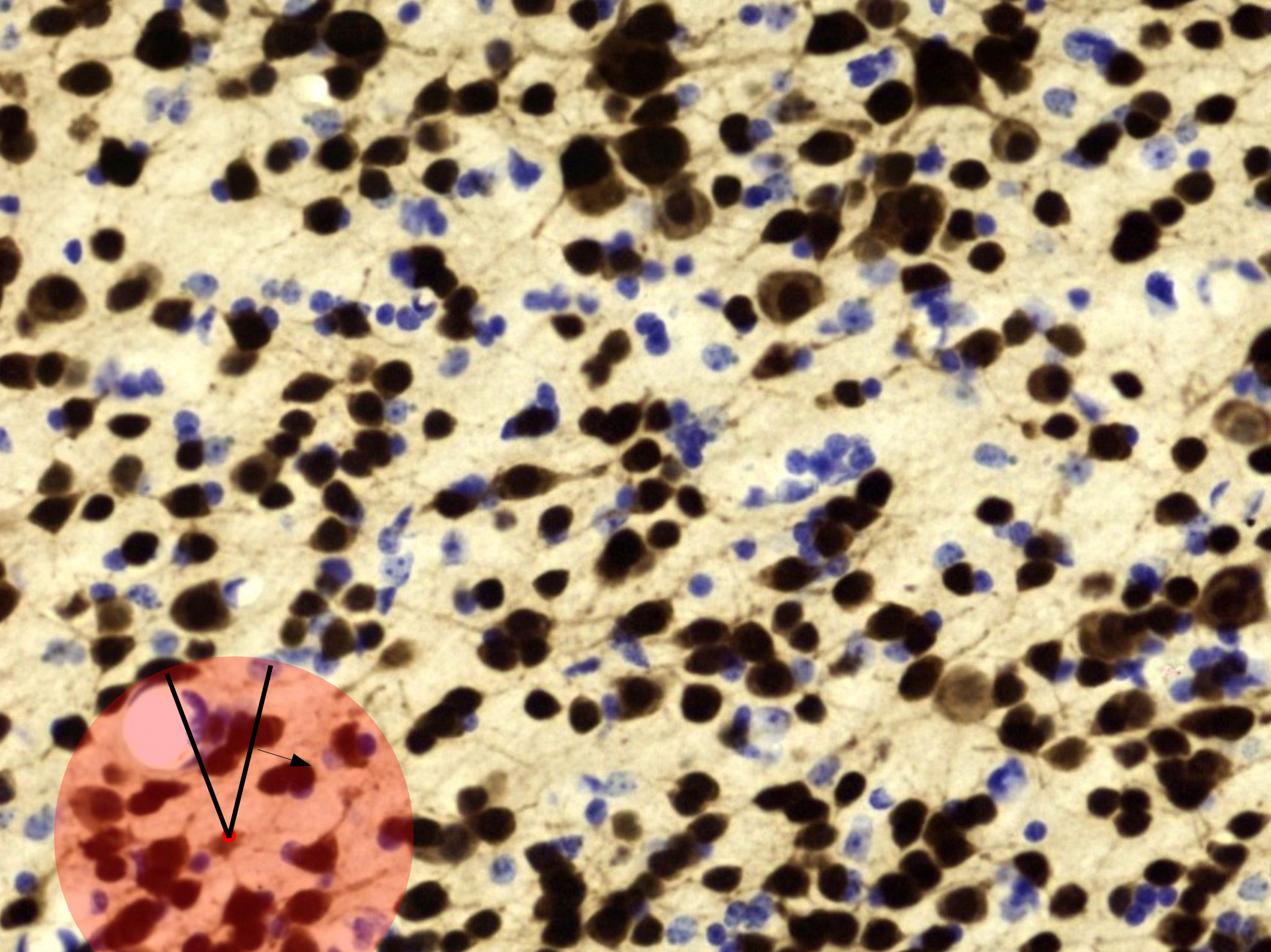

Theory – density map

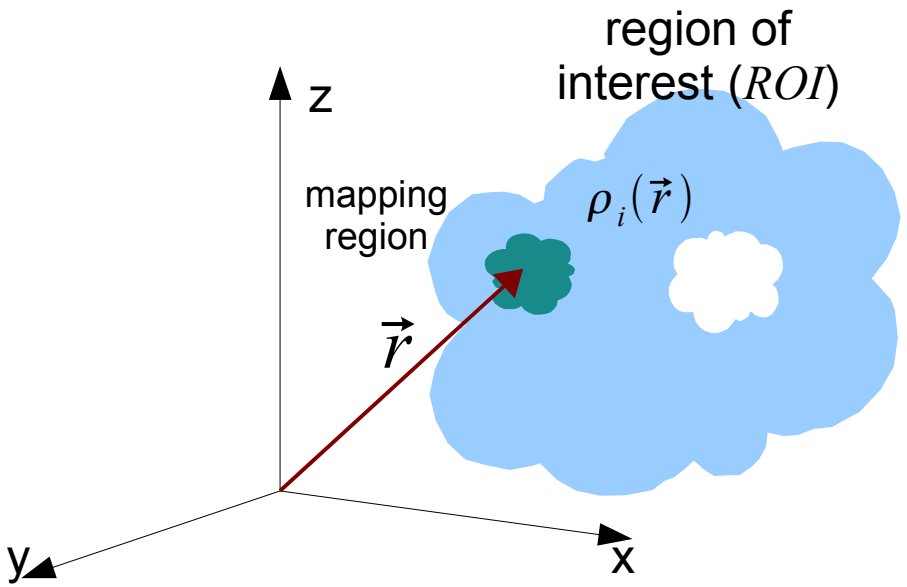

$\rho_i(\vec{r})$ density of feature type ***i*** (neuron, glia, surface area, axon length, etc.) at location $\vec{r}$

Measurement M of property

$$M = \int_{ROI} \rho_i(\vec{r})\, d\vec{r}$$

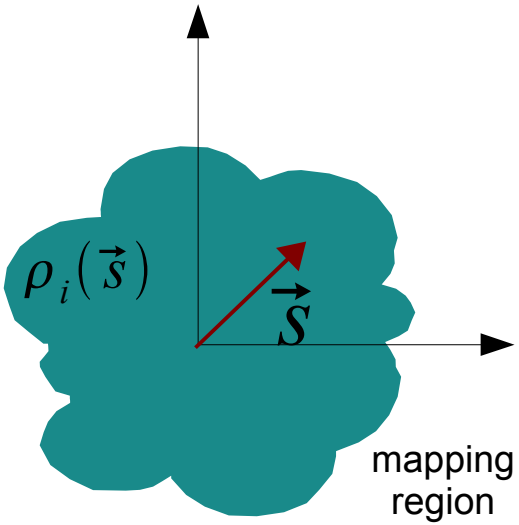

$$d(\vec{s}) = \int_{ROI} \rho_i(\vec{s}\,')\,\rho_j(\vec{s}\,' - \vec{s})\, d\vec{s}\,'$$

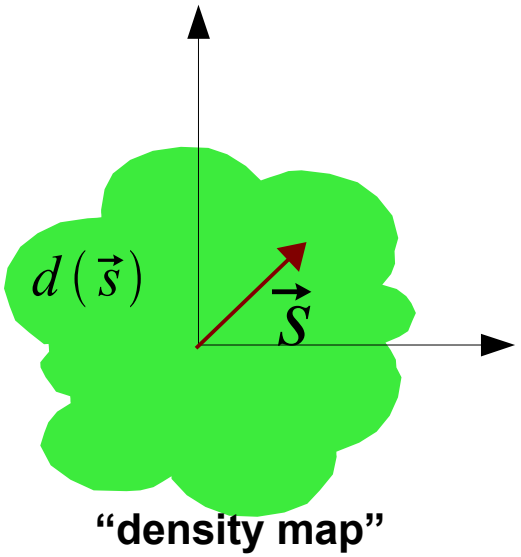

“density map”

Theory – density map

1

$$\rho_i(\vec{r}) \quad i \equiv neuron \quad \vec{r} \equiv \{x, y\}$$

$$d(x, y) = \iint_{ROI} \rho_{neuron}(x', y')\, \rho_{neuron}(x'-x, y'-y)\, dx'\, dy'$$

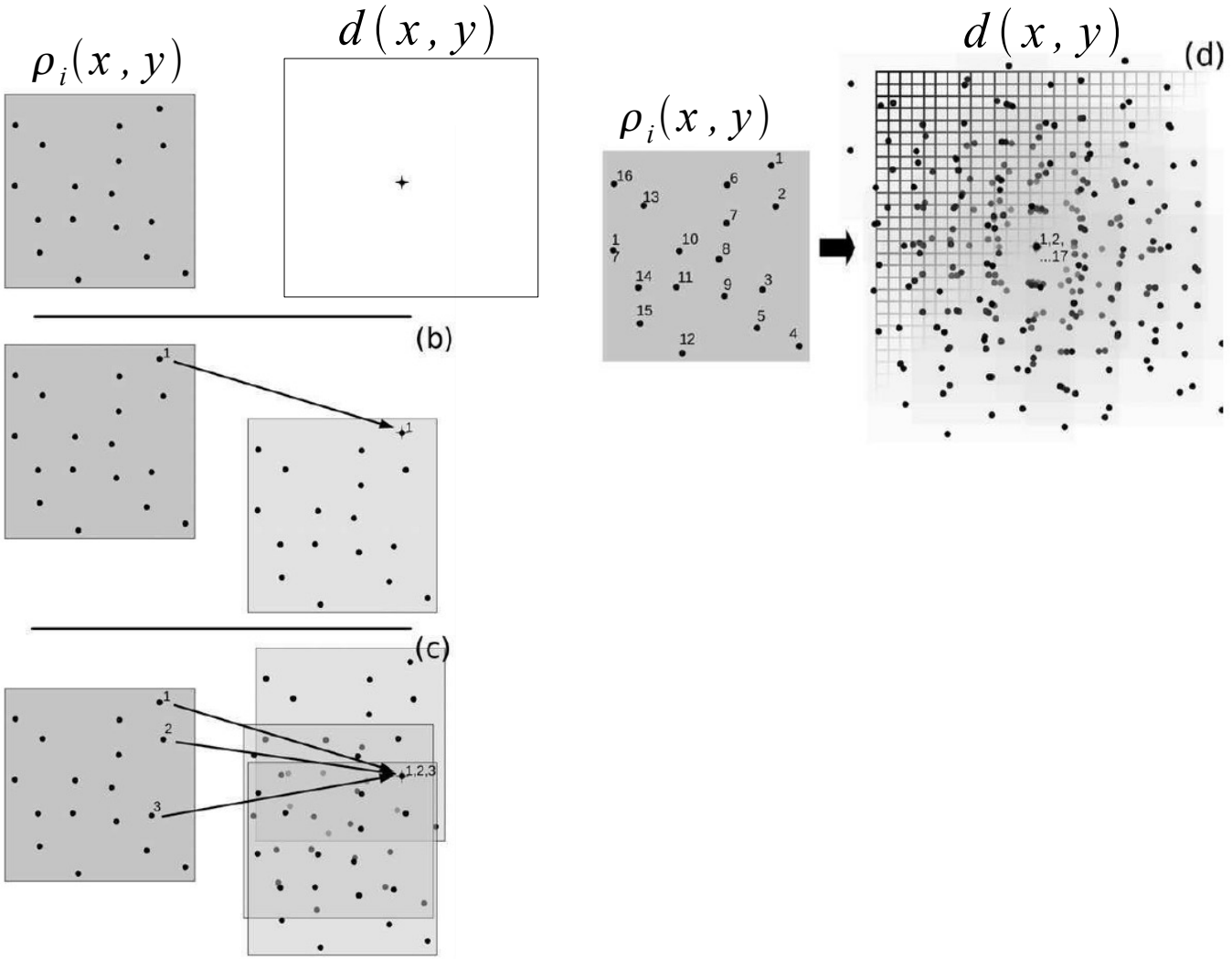

Cruz et al. ***Neuroscience*** *158, 1509-1520 (2009)*

Theory – density map

1

$\rho_i(\vec{r}) \quad i \equiv neuron \quad \vec{r} \equiv \{x, y\}$

$$d(x,y) = \iint_{ROI} \rho_{neuron}(x',y')\,\rho_{neuron}(x'-x, y'-y)\,dx'\,dy'$$

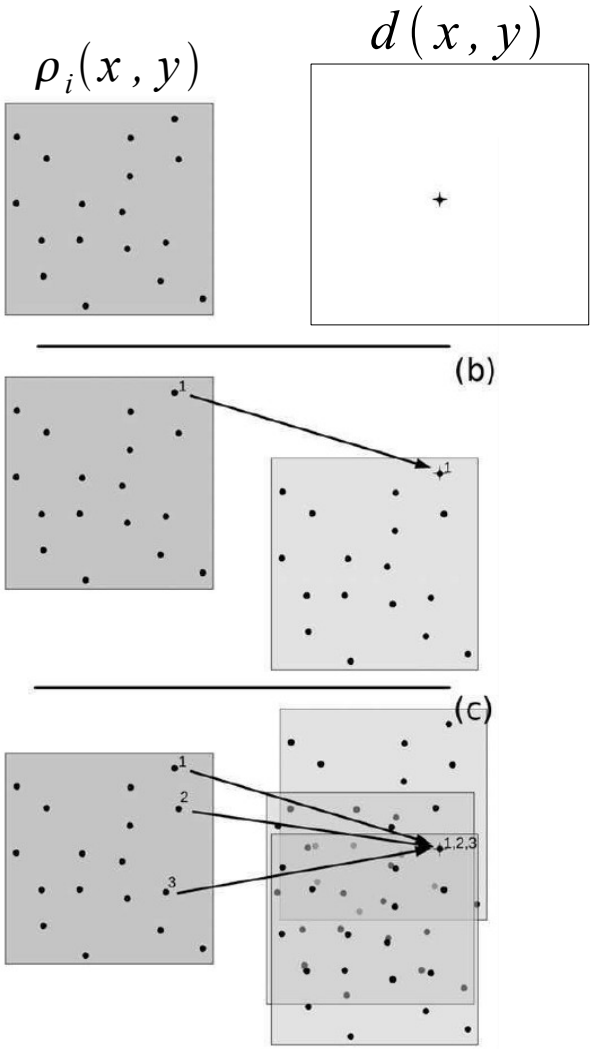

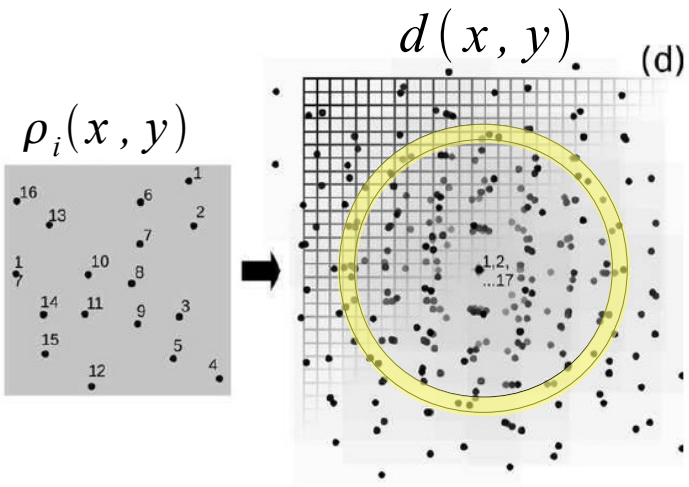

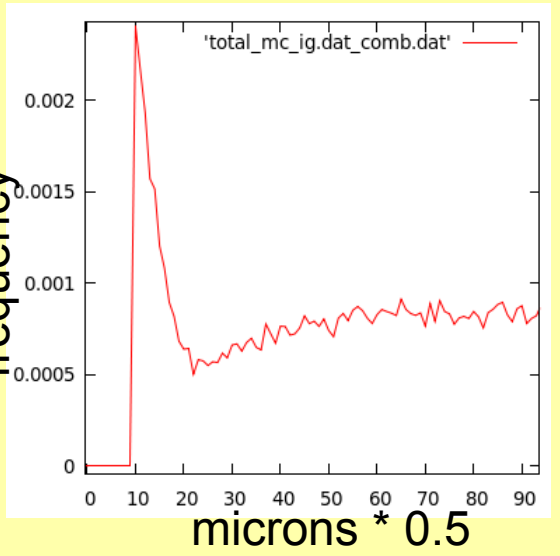

2

$$d(x,y) = \iint_{ROI} \rho_{neuron}(x',y')\,\rho_{glial}(x'-x, y'-y)\,dx'\,dy'$$

$$d(r) = \oint_{surface} d(x,y)\,d\vec{r}\,'$$

Cruz et al. ***Neuroscience*** *158, 1509-1520 (2009)*

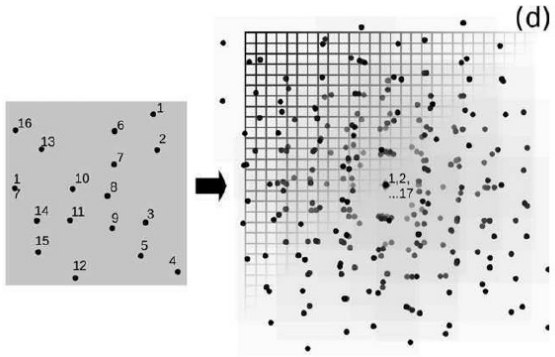

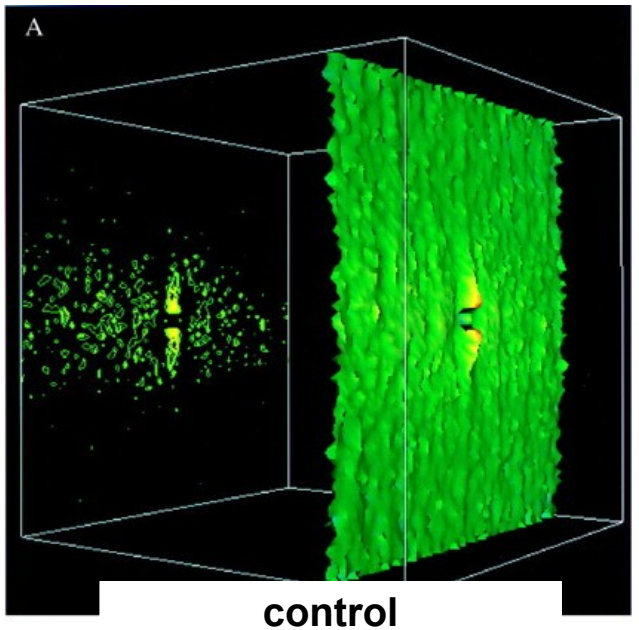

control

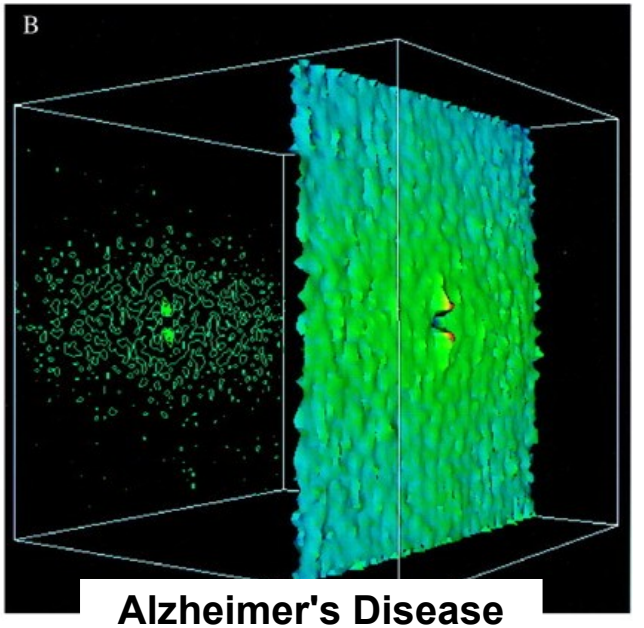

Alzheimer's Disease

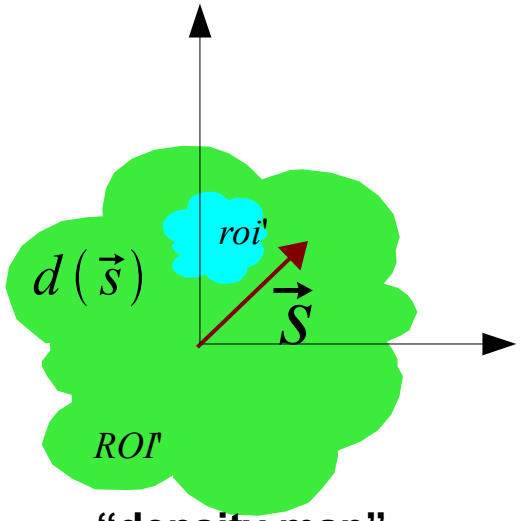

"density map"

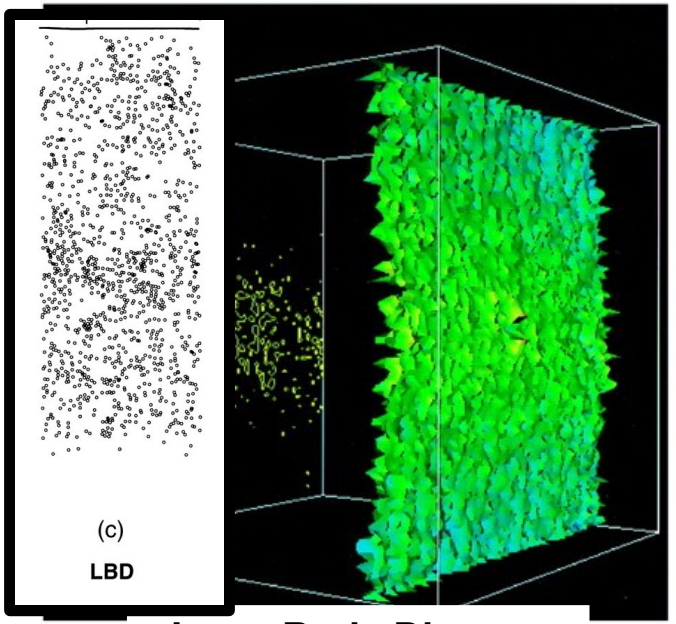

Lewy Body Disease

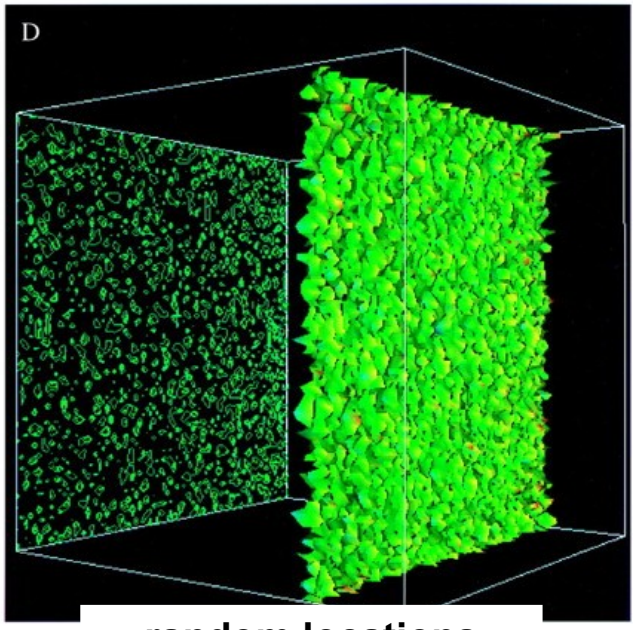

random locations

$$M = \frac{\int_{roi'} d(\vec{s}\,')\, d\vec{s}\,'}{\int_{ROI'} d(\vec{s}\,')\, d\vec{s}\,'}$$

"measurement of density map"

Buldyrev et al. ***PNAS 97****, 5039-5053 (2000)*

Theory – density map

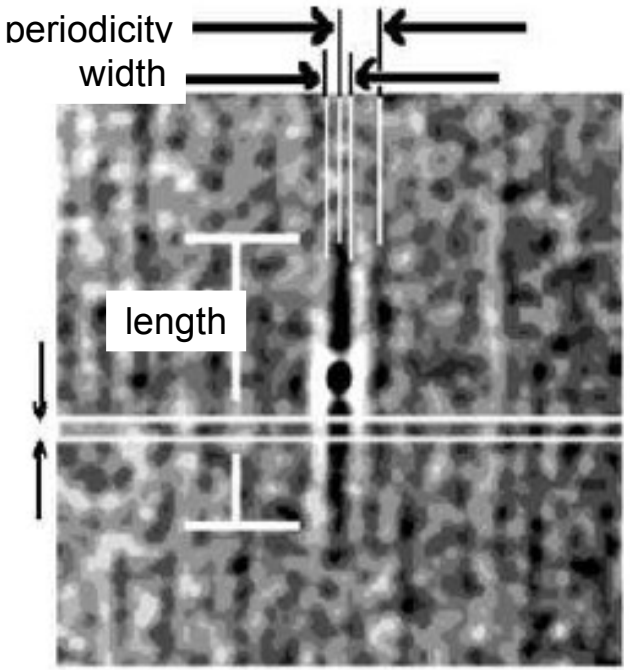

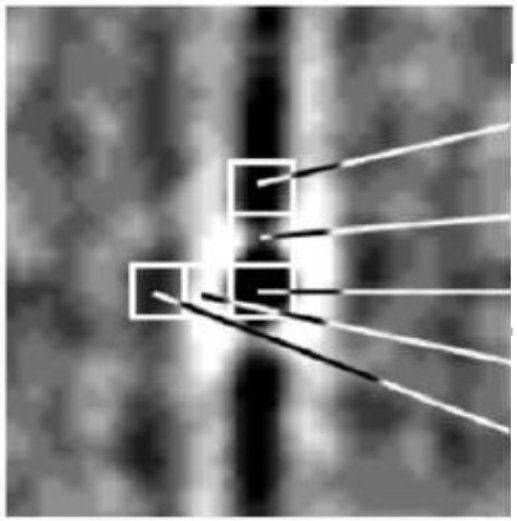

column strength

intra-column depletion

origin

inter-column depletion

neighboring column strength

Cruz et al. ***J. Neuro. Meth****. 141, 321 (2005)*

glial – neuron attachment strength

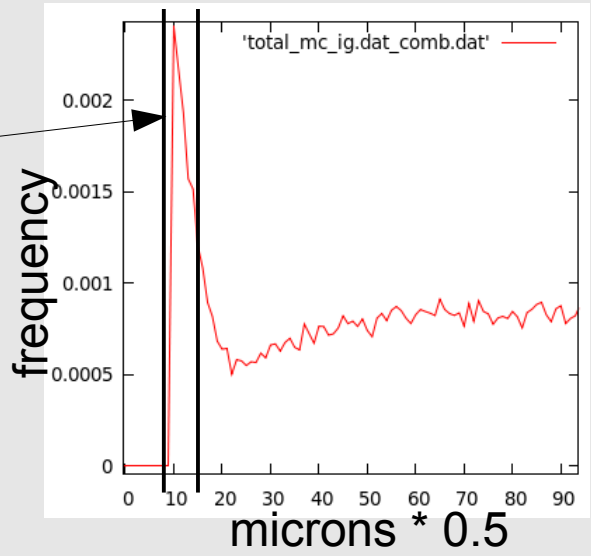

Theory – density map

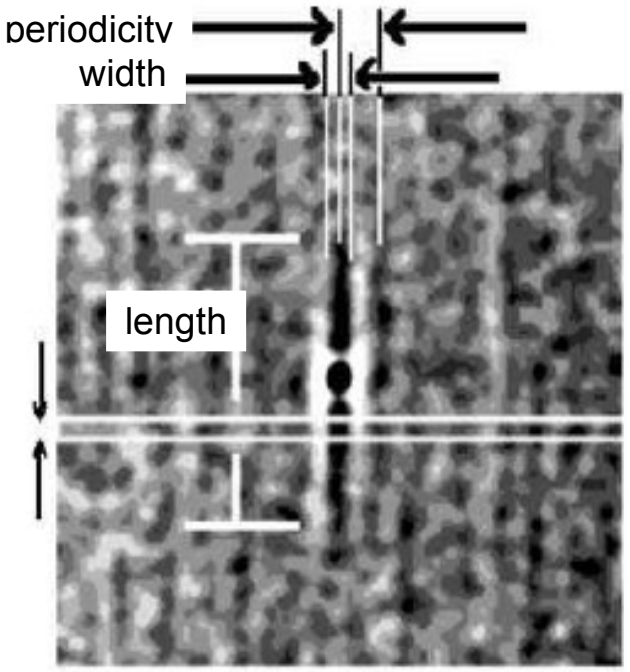

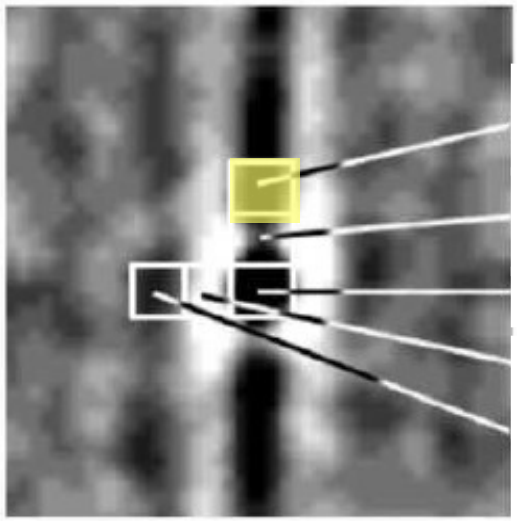

column strength

intra-column depletion

origin

inter-column depletion

neighboring column strength

$$N = \frac{1}{\rho e^2 a}$$

ρ = density of cells (0.002 cells/micron^2)

e = desired error (**10%/5%/1%**)

a = area of measurement 100 microns^2

N = 500/2000/50000 cells per measurement

Cruz et al. ***J. Neuro. Meth****. 141, 321 (2005)*

$$N = \frac{1}{2\pi r \rho e^2 l}$$

r = distance from origin (7 microns)

l = length of measurement (20 microns)

N = 60/230/5700 cells per measurement

glial – neuron attachment strength

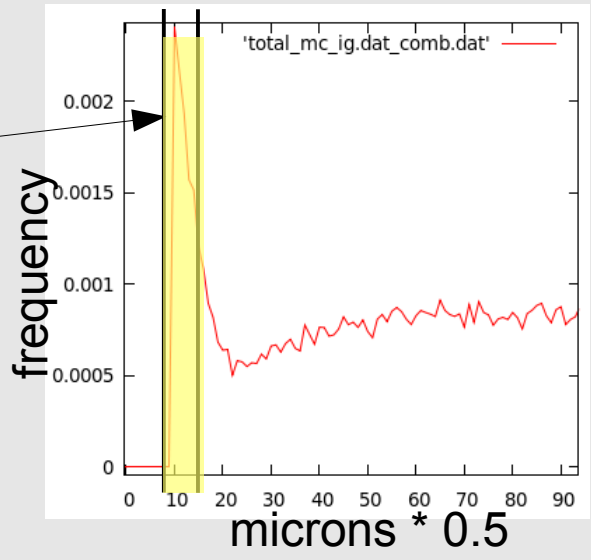

Theory – density map

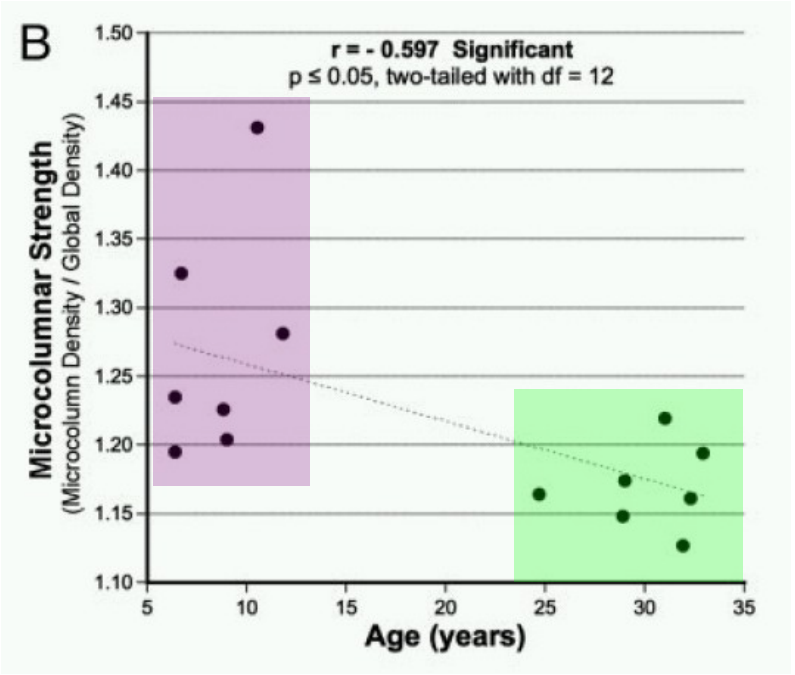

Cruz et al. ***PNAS****. 101 (2004)*

$$N = \frac{1}{\rho e^2 a}$$

ρ = density of cells
(0.002 cells/micron^2)
e = desired error
(**10%/5%/1%**)
a = area of measurement
100 microns^2

N **= 500/2000/50000 cells per measurement**

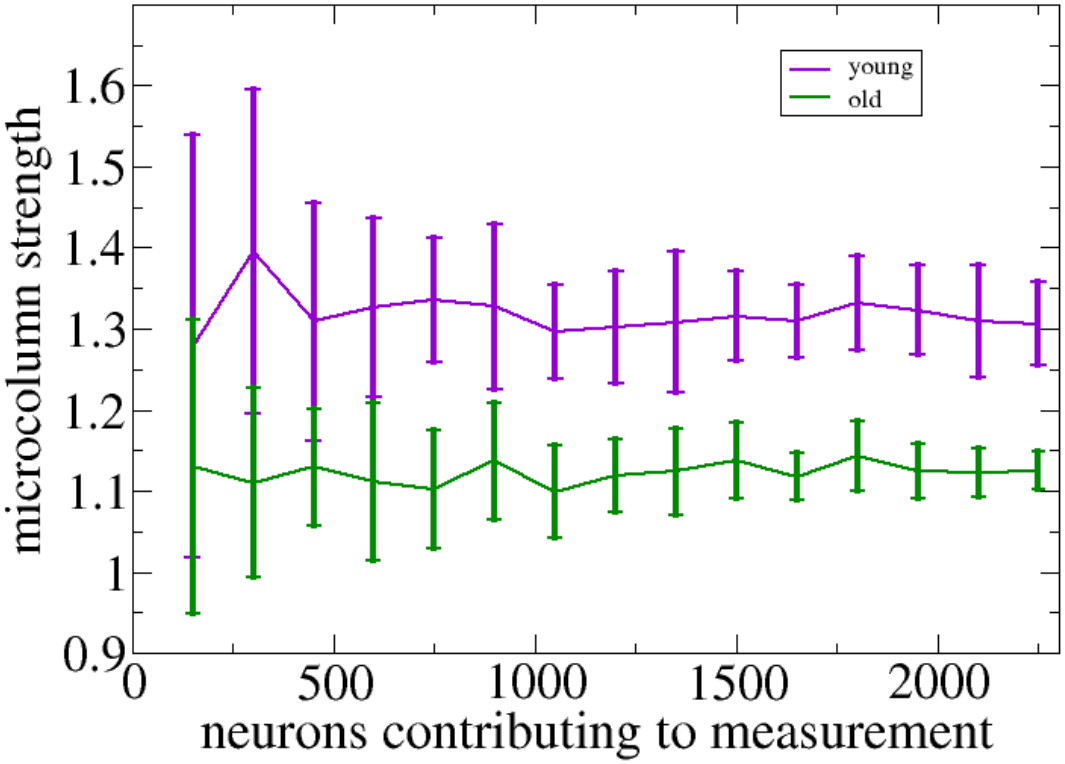

Method

Method

- Brain life and experiment
- Death and brain preservation
- Tissue preparation and staining

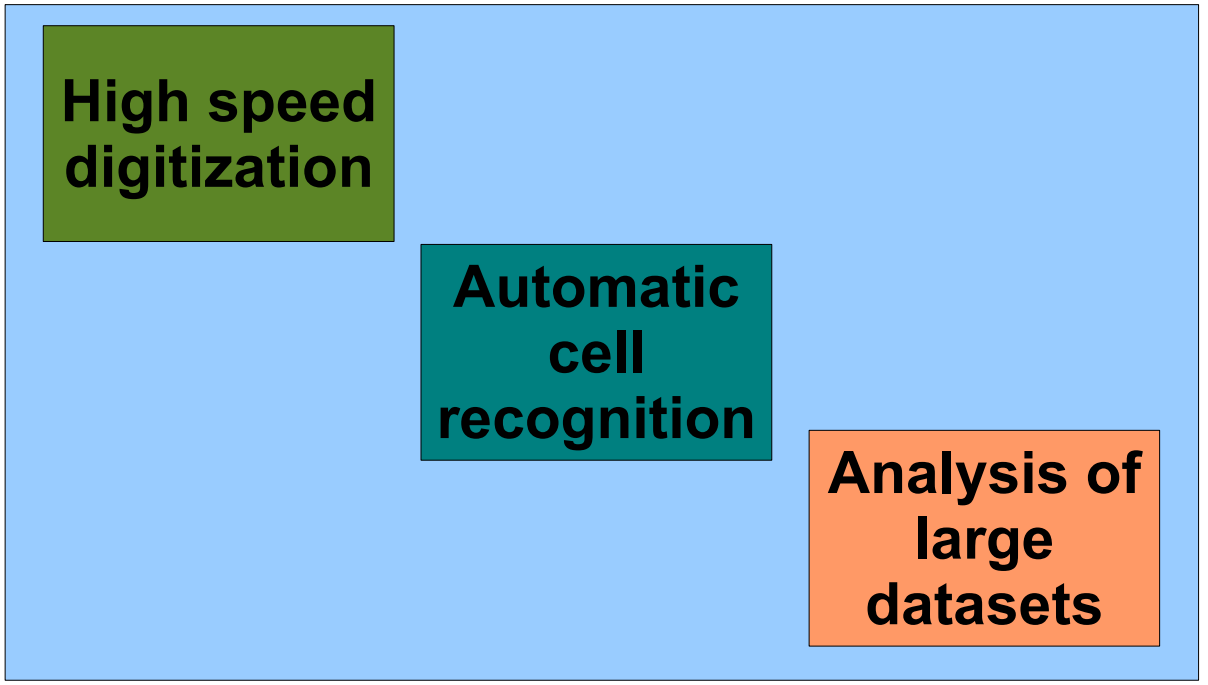

- Evaluation
- Deciding on next experiment


Von Braunmühls Series
Myelin Trials
AM 7
AM7
Koelle
AM8
AM15
Heidenhain Trials
Thionin
TAGO
AM-12
"ROSETTA"
AM 12
"Rosetta"
BM-22
BM-23
BM-21
"zelig"
BM 30
Luke
BM 33
BM 11

Method - digitization

Evelyn F. McKnight Brain Institute

d·metrix
MICROSCOPY MULTIPLIED

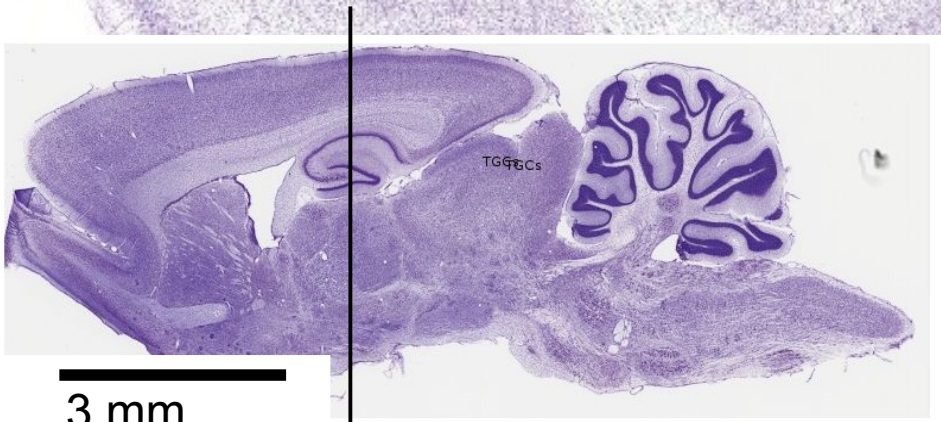

1 mm

Method - digitization

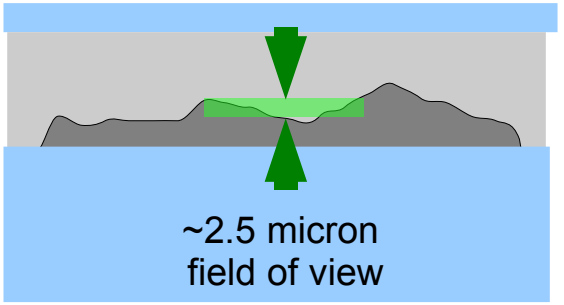

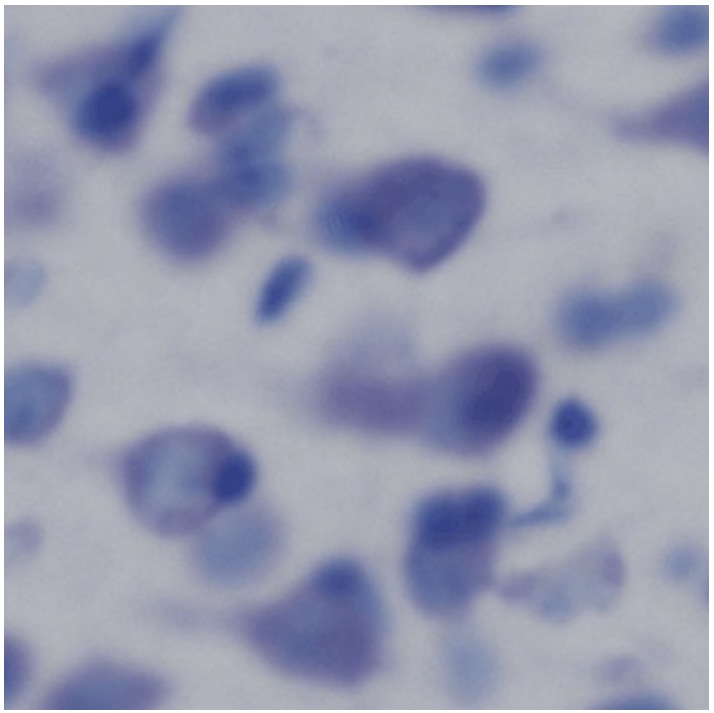

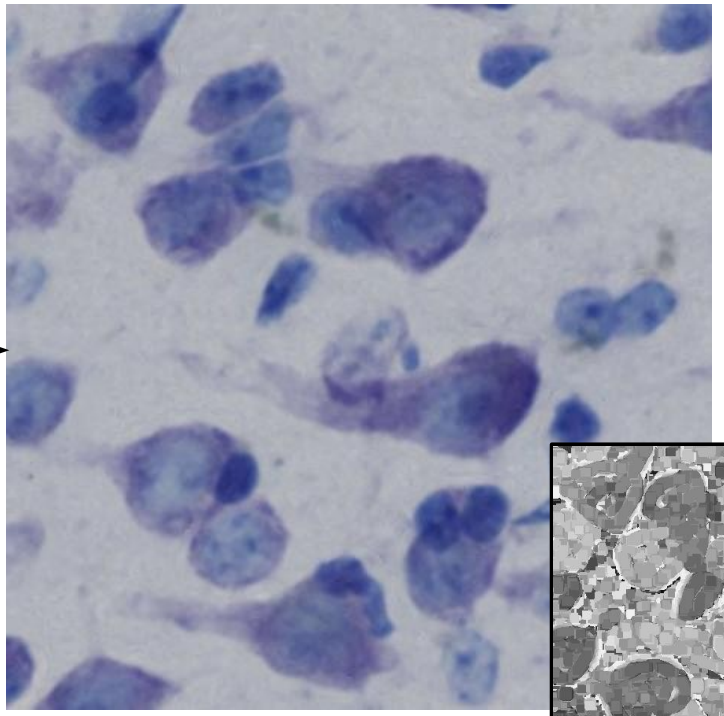

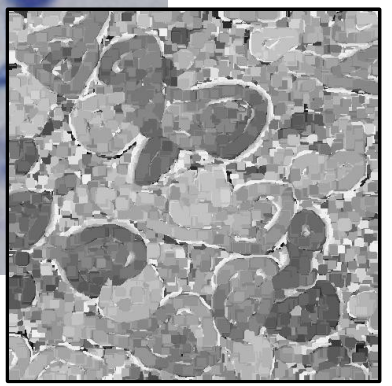

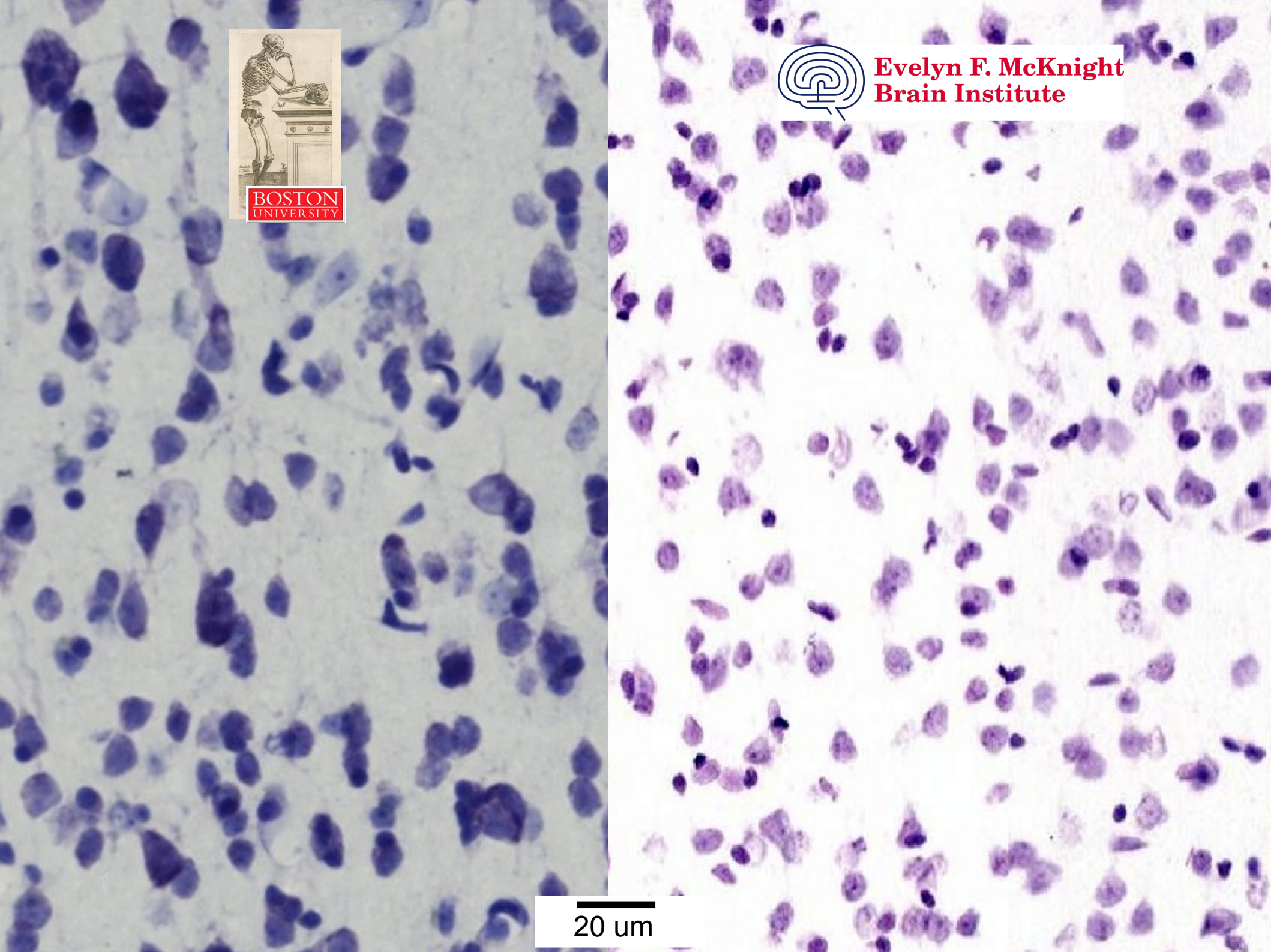
BOSTON
UNIVERSITY
Evelyn F. McKnight
Brain Institute
20 um

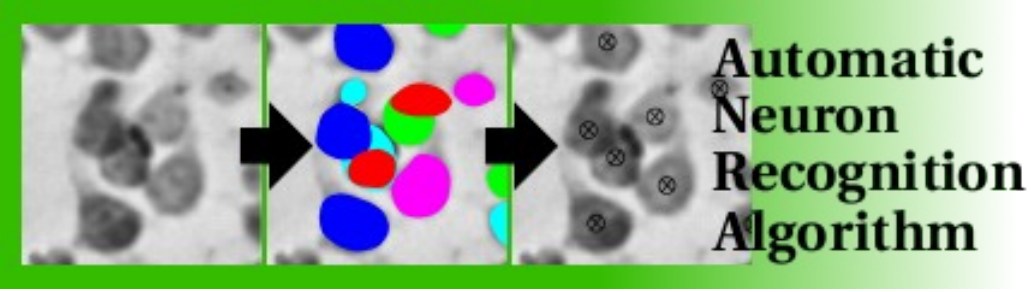

Method - visualization

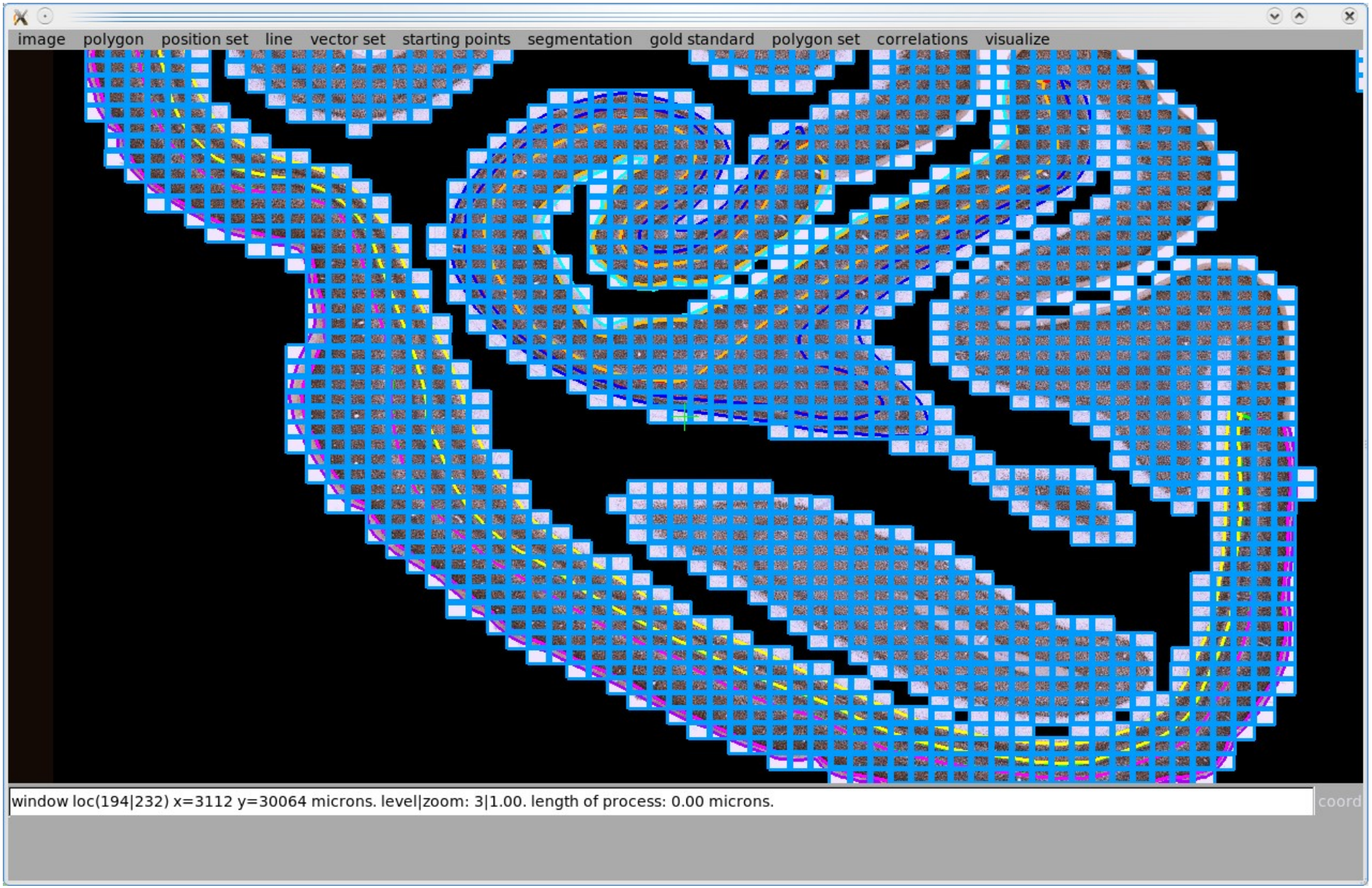

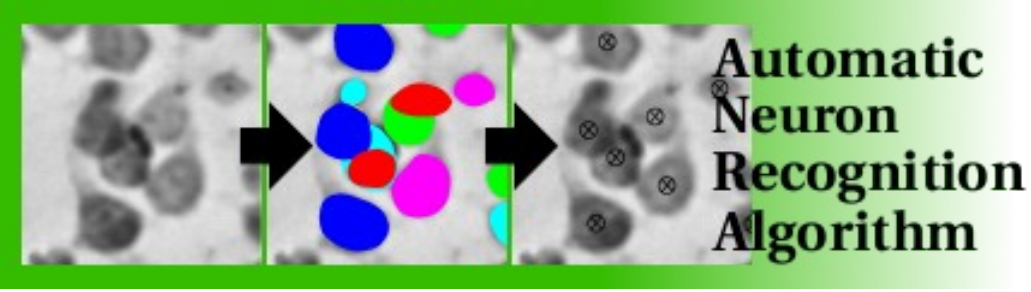

Method - visualization

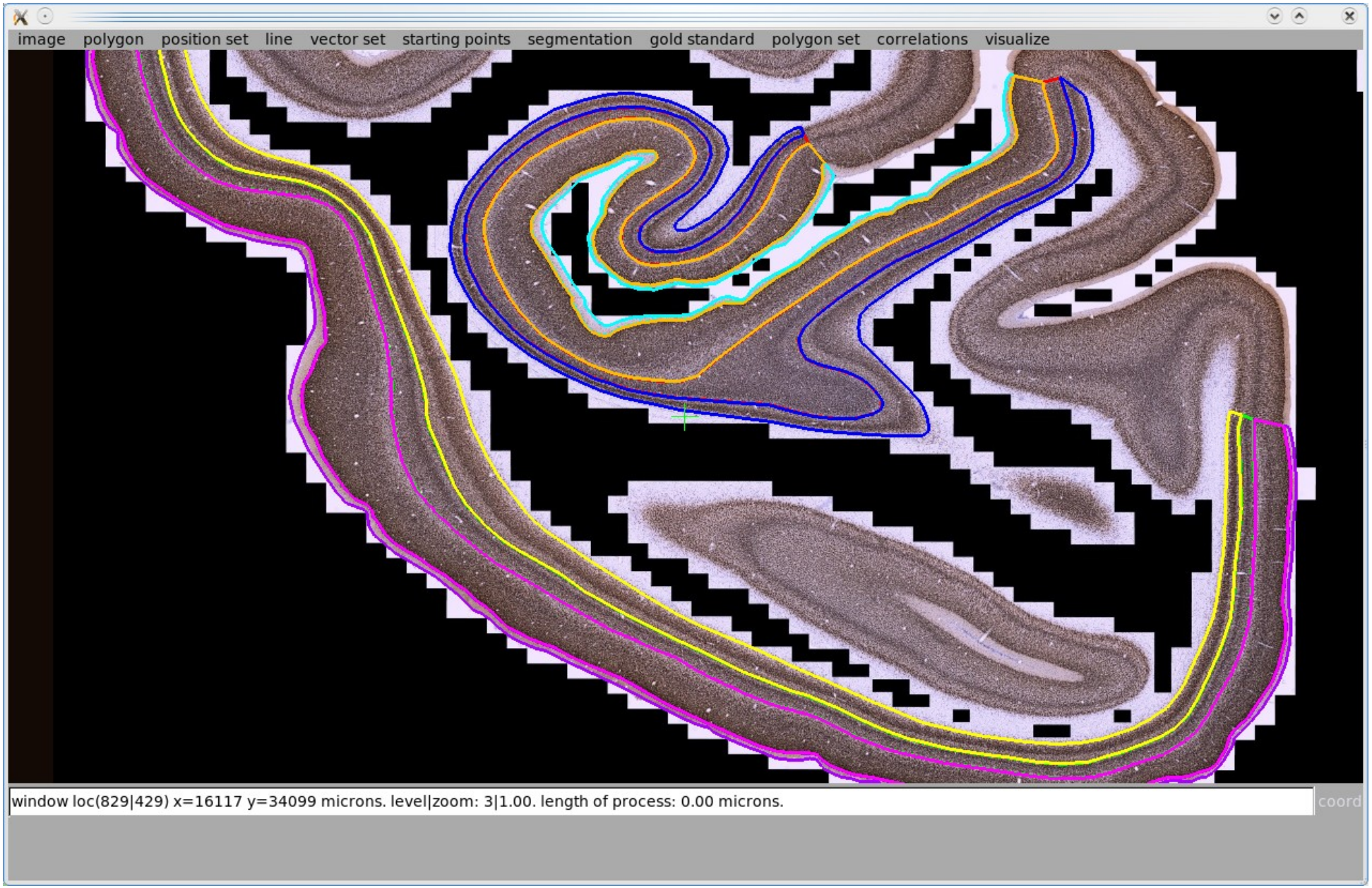

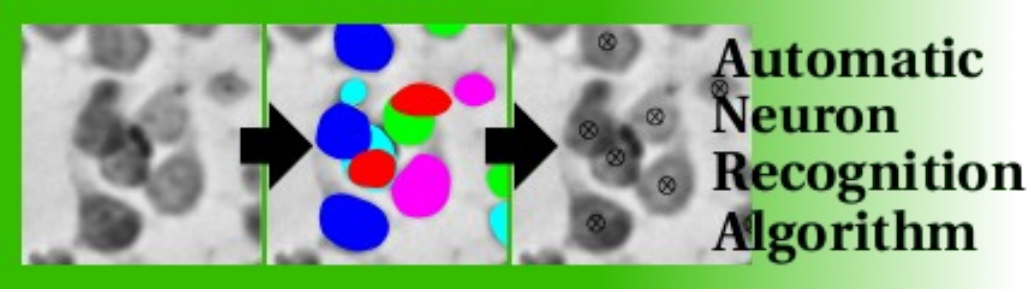

Method - visualization

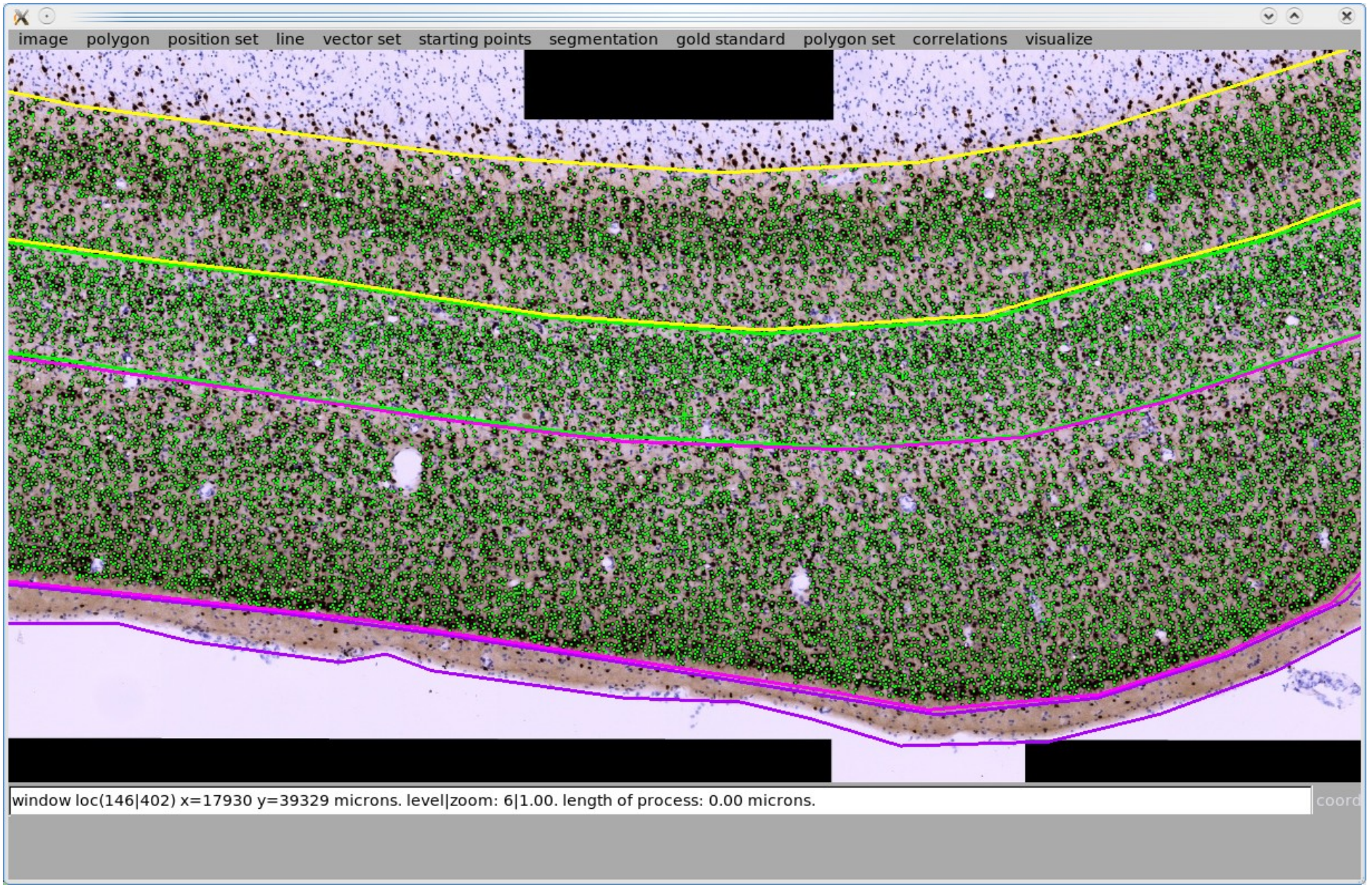

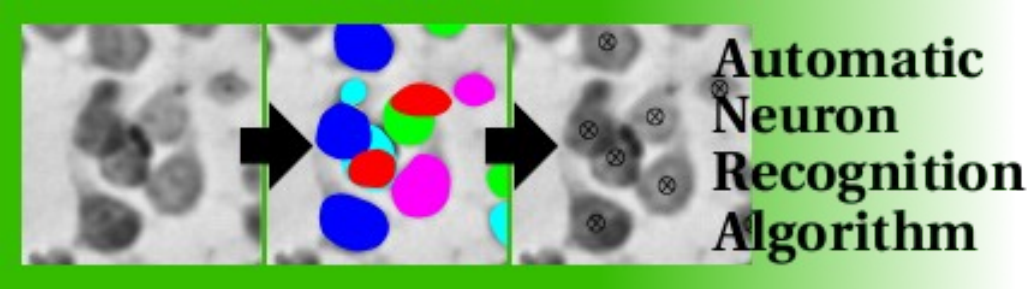

Method - visualization

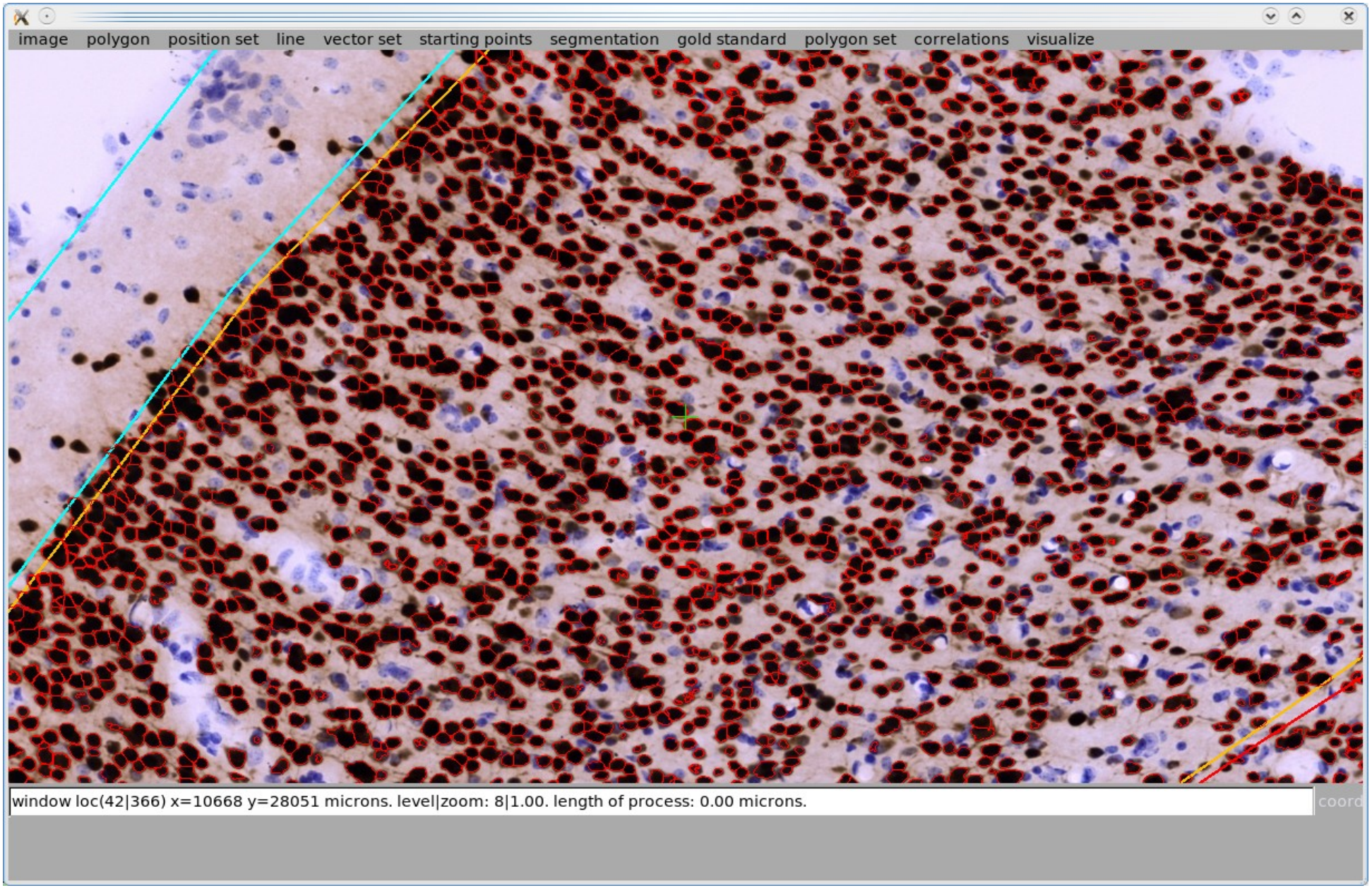

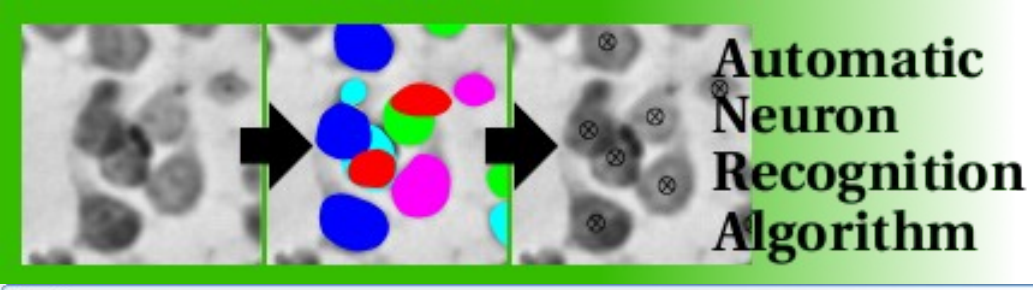

Method - visualization

image polygon position set line vector set starting points segmentation gold standard polygon set correlations visualize

window loc(462|388) x=6488 y=3376 microns. level|zoom: 5|1.00. length of process: 0.00 microns.

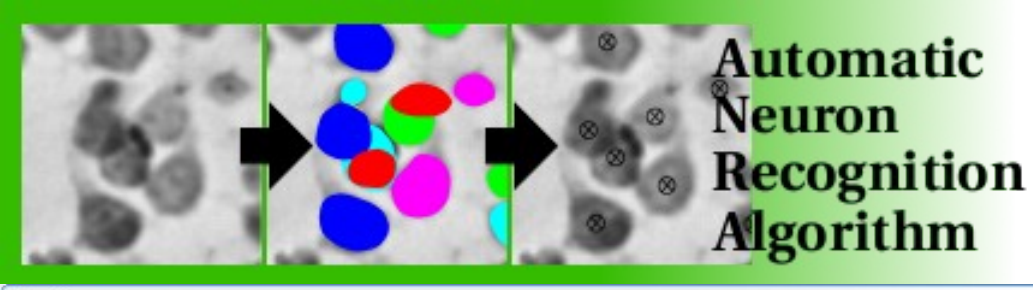

Method - visualization

image polygon position set line vector set starting points segmentation gold standard polygon set correlations visualize

window loc(232|236) x=4648 y=2160 microns. level|zoom: 5|1.00. length of process: 0.00 microns.

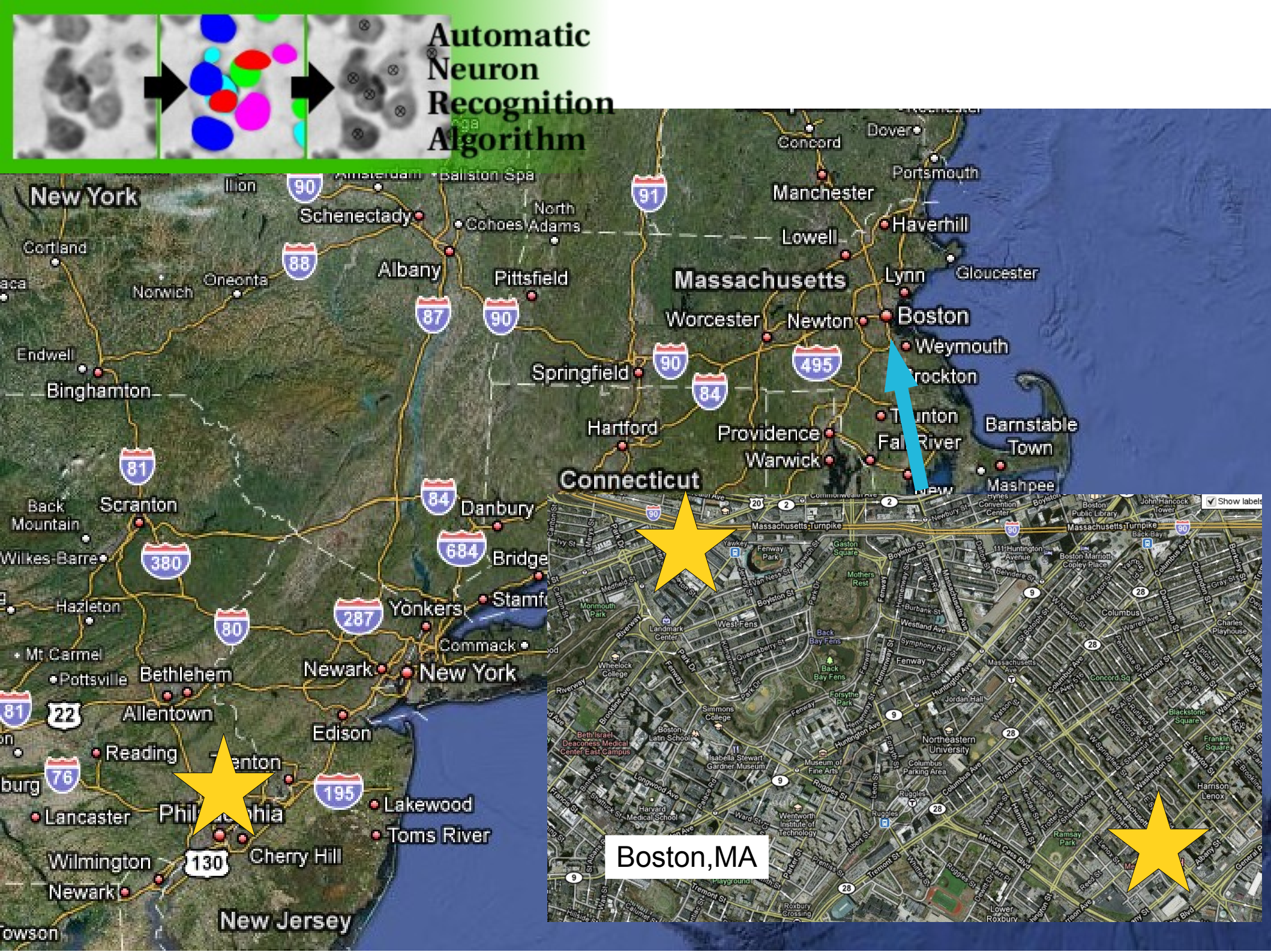
Automatic
Neuron
Recognition
Algorithm
New York
Schenectady
Albany
Pittsfield
Cohoes
North Adams
Manchester
Concord
Dover
Portsmouth
Haverhill
Lowell
Lynn
Gloucester
Massachusetts
Worcester
Newton
Boston
Weymouth
Springfield
Hartford
Providence
Warwick
Barnstable Town
Mashpee
Connecticut
Cortland
Oneonta
Norwich
Endwell
Binghamton
Scranton
Back Mountain
Wilkes-Barre
Hazleton
Danbury
Bridgeport
Yonkers
Stamford
Commack
Mt Carmel
Pottsville
Bethlehem
Allentown
Newark
New York
Edison
Reading
Lakewood
Toms River
Lancaster
Philadelphia
Cherry Hill
Wilmington
Newark
New Jersey
Towson
Boston,MA

Method - recognition

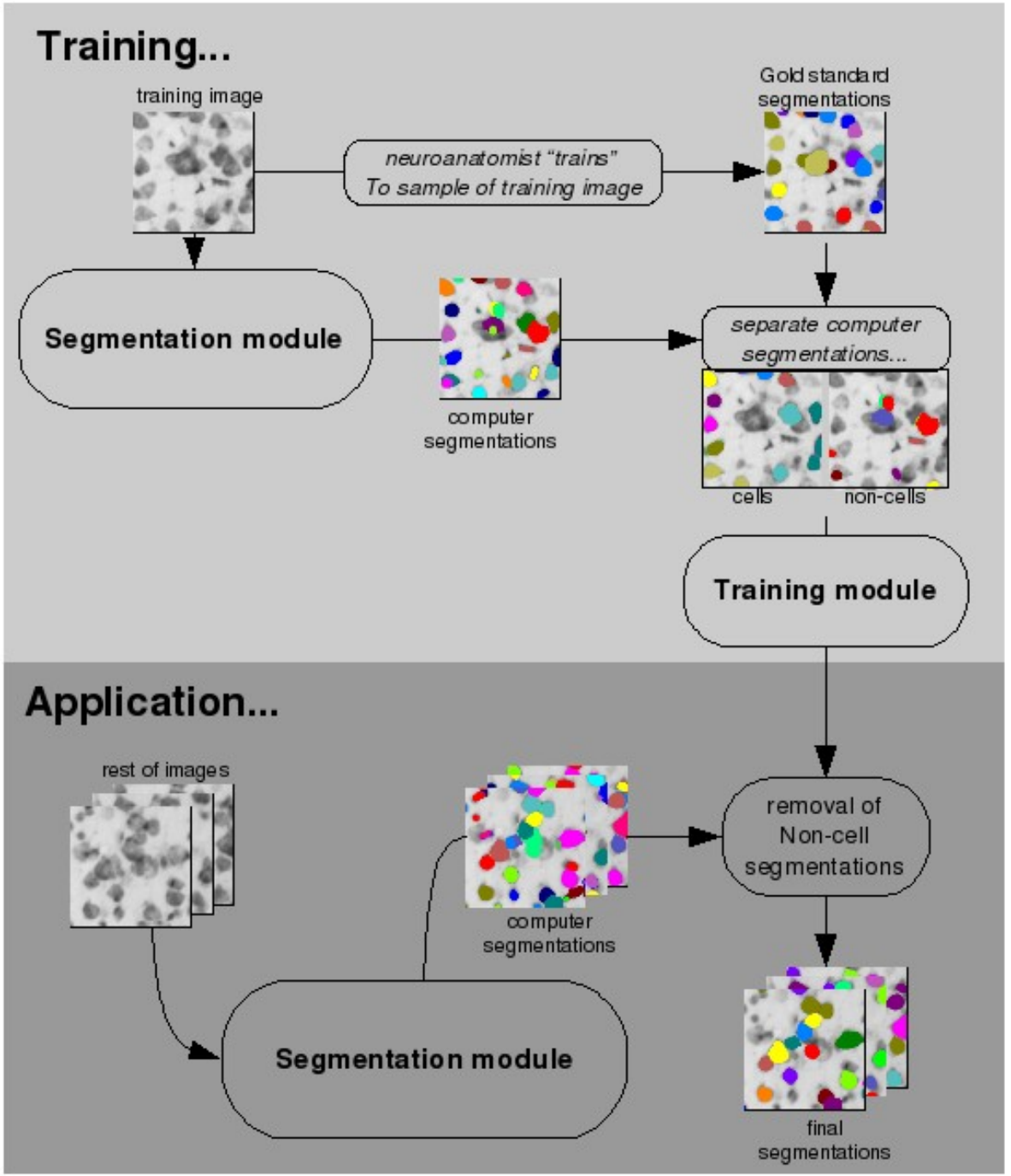

Inglis et al. ***J. Microscopy*** *230, 339 (2008)*

Method - recognition

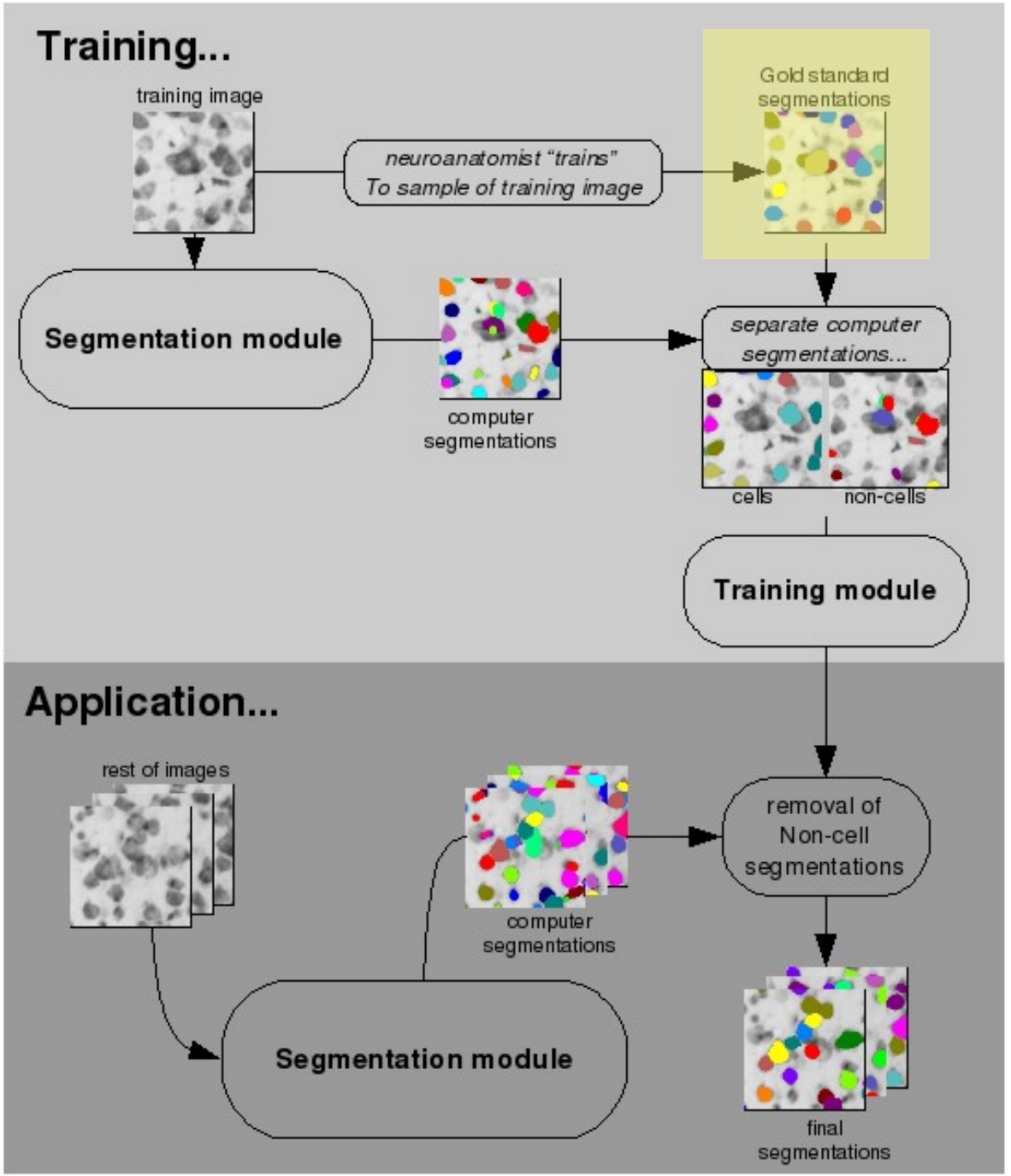

Inglis et al. ***J. Microscopy*** *230, 339 (2008)*

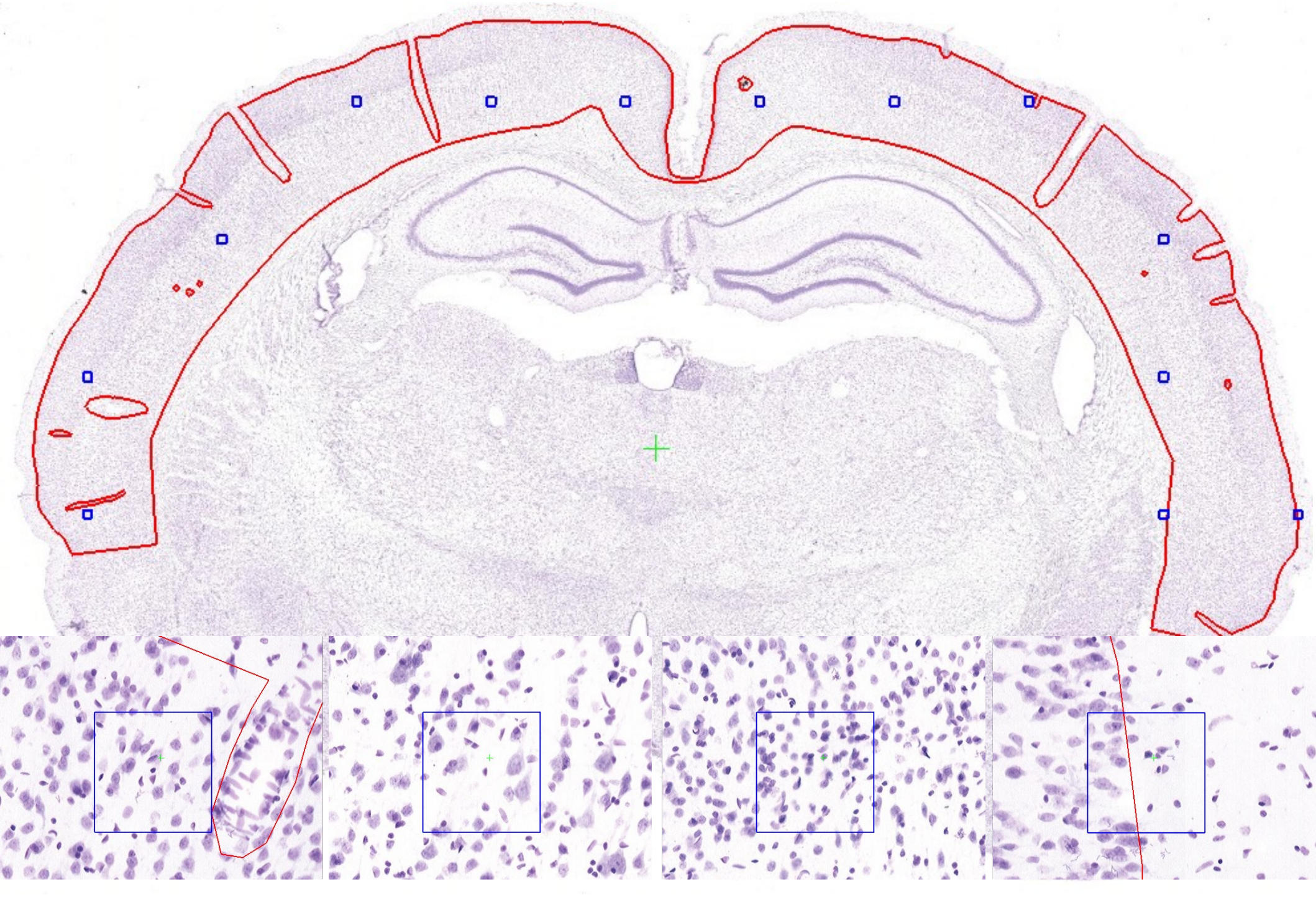

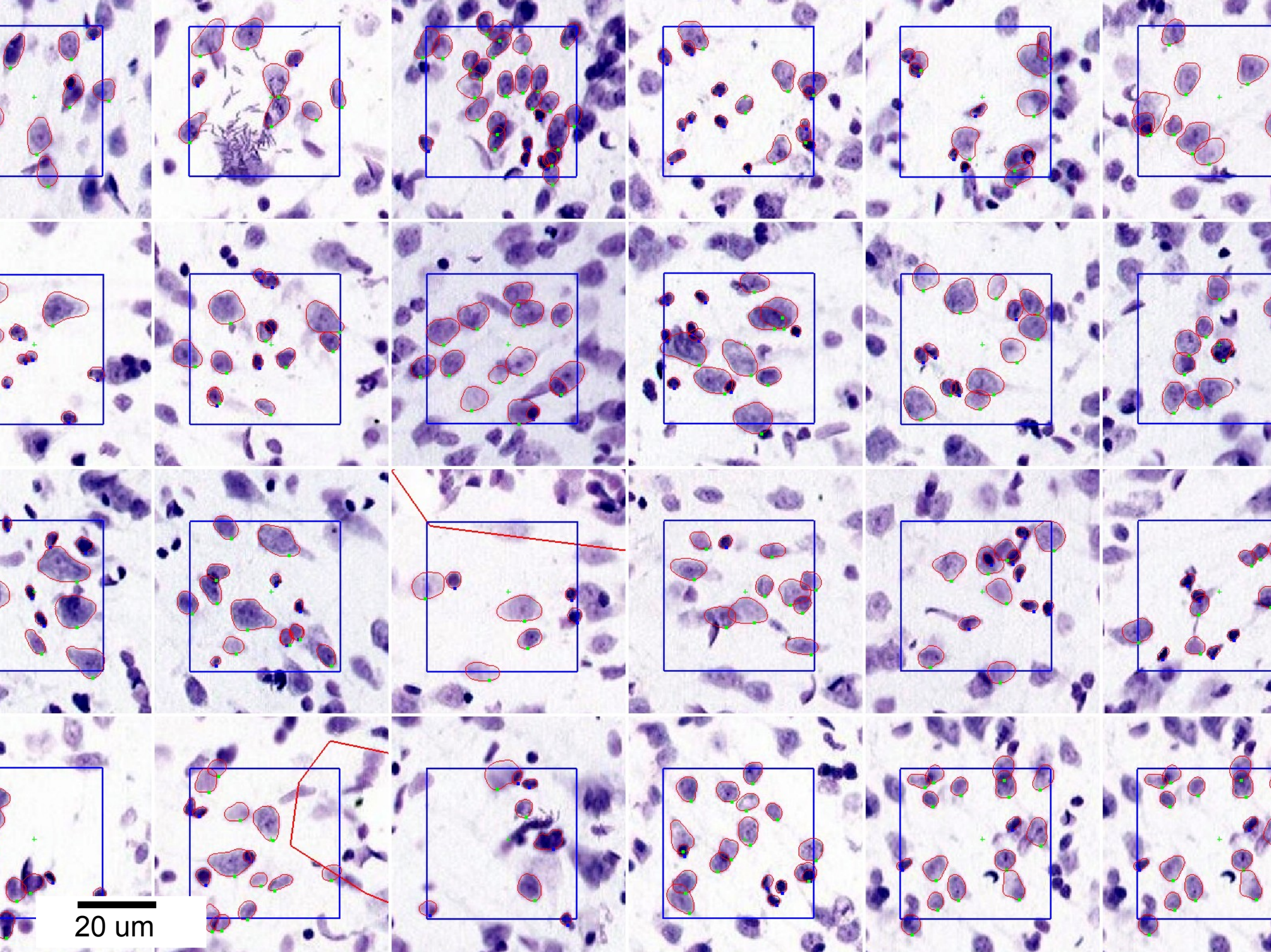
20 um

Method - recognition

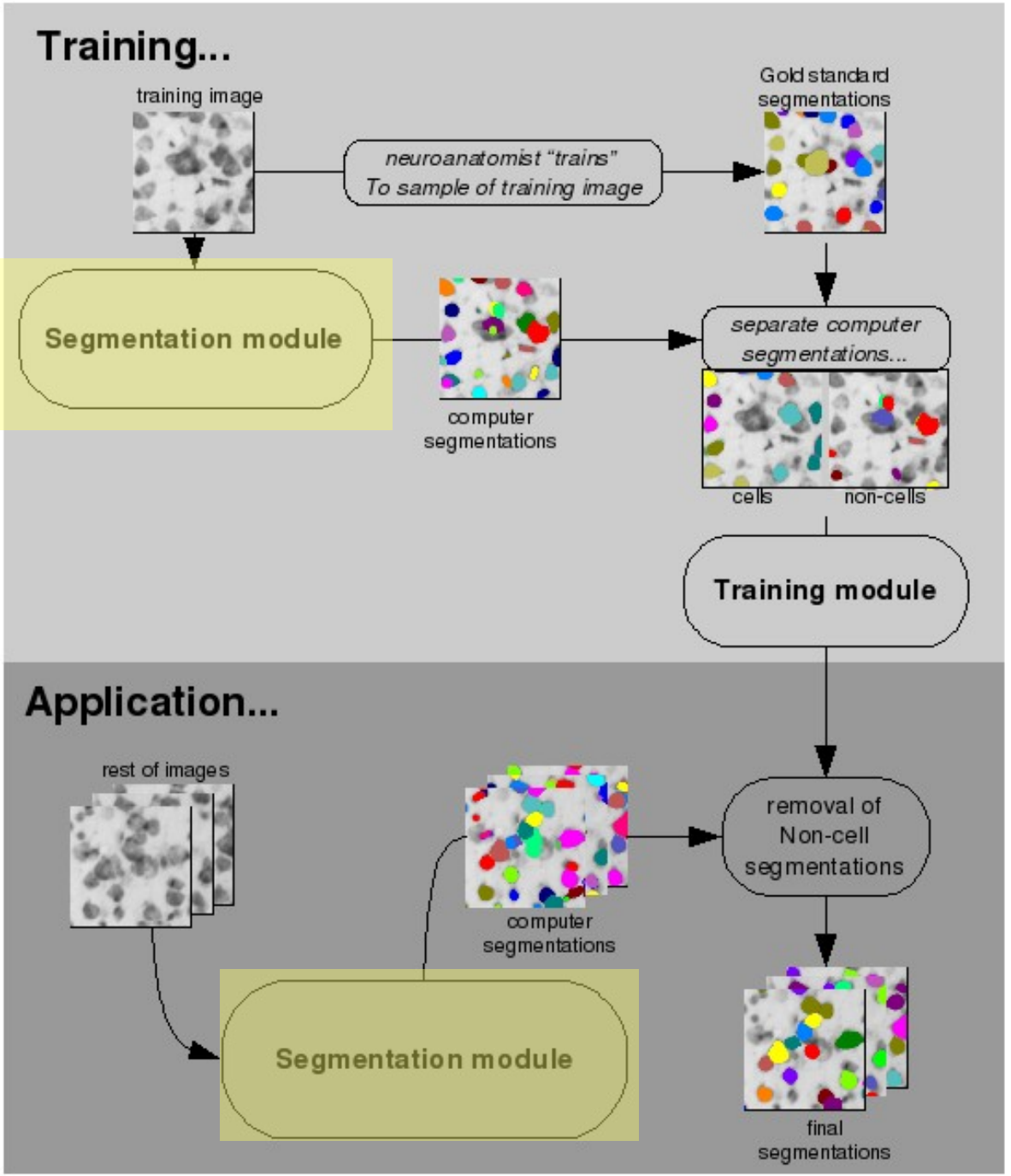

Inglis et al. ***J. Microscopy*** *230, 339 (2008)*

Method - recognition

1

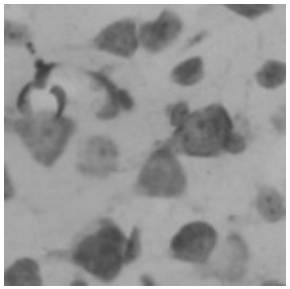
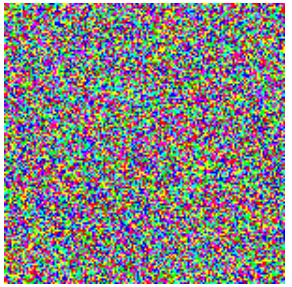
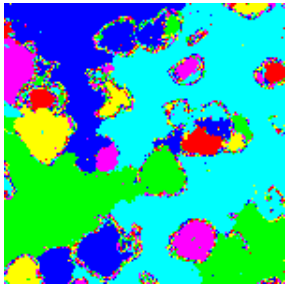

Peng et al. PNAS 100 (2003)

2

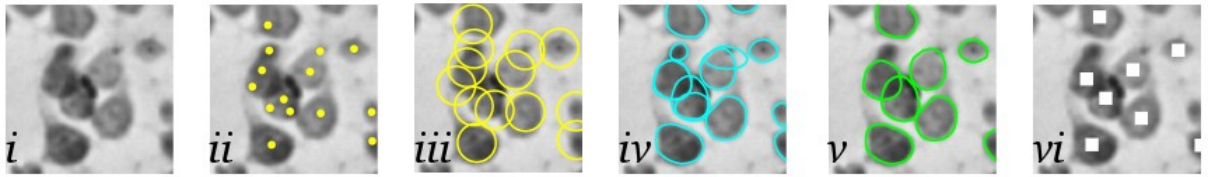

Inglis et al. ***J. Microscopy*** *230, 339 (2008)*

3

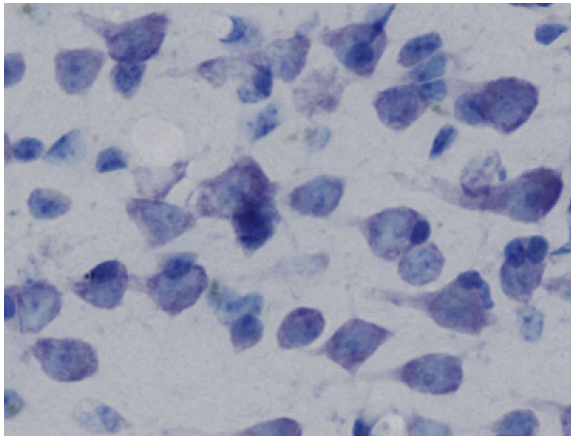
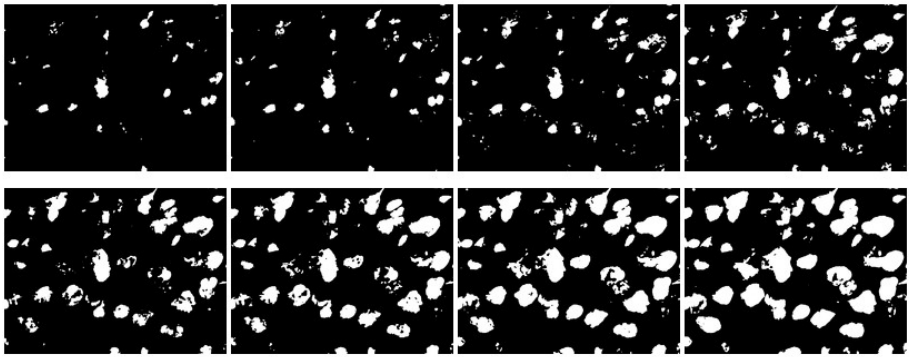

4 "

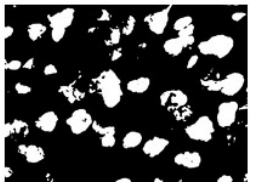

Segmentation: Multithresholding/Watershed

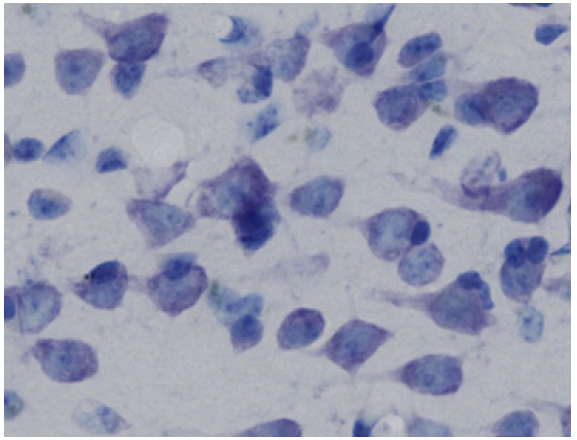

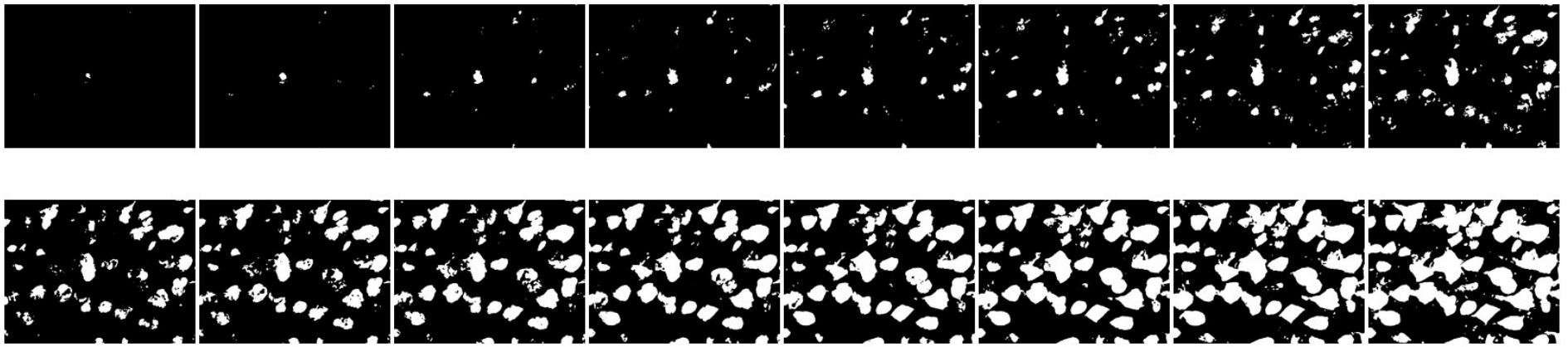

Divide grayscale information into ~15 levels. Perform watershed on each level. Save white regions as segmentations.

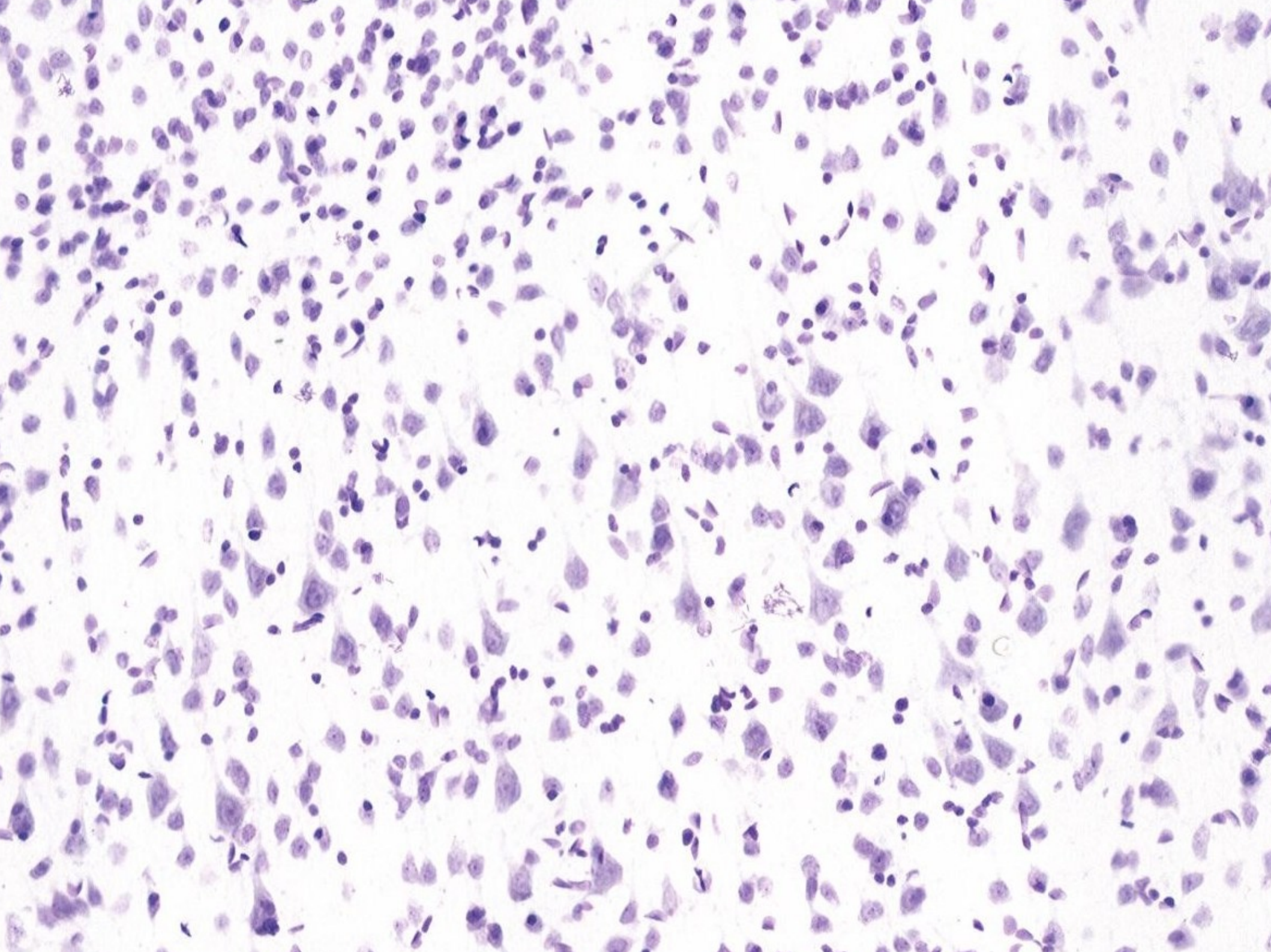

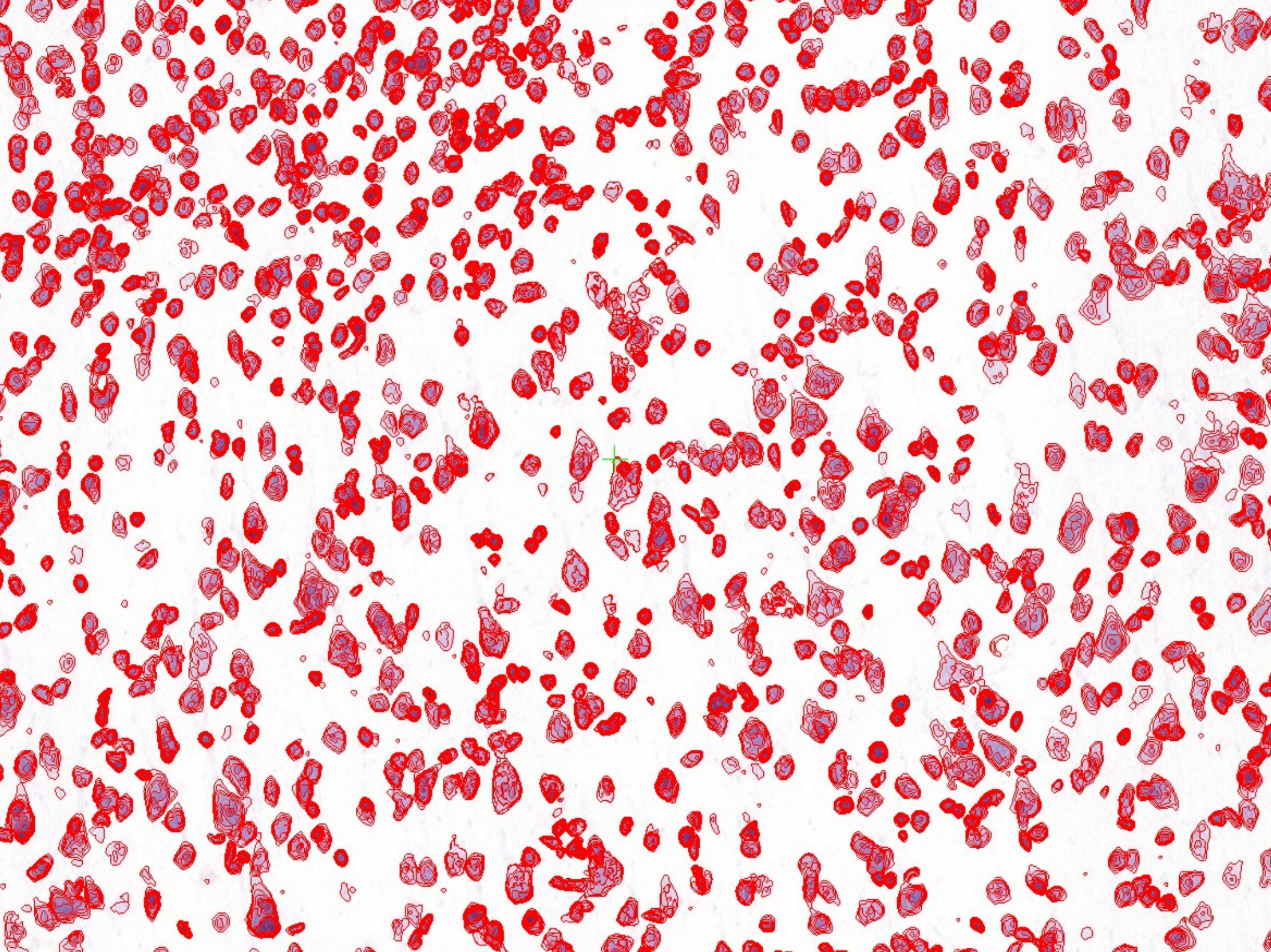

Method - recognition

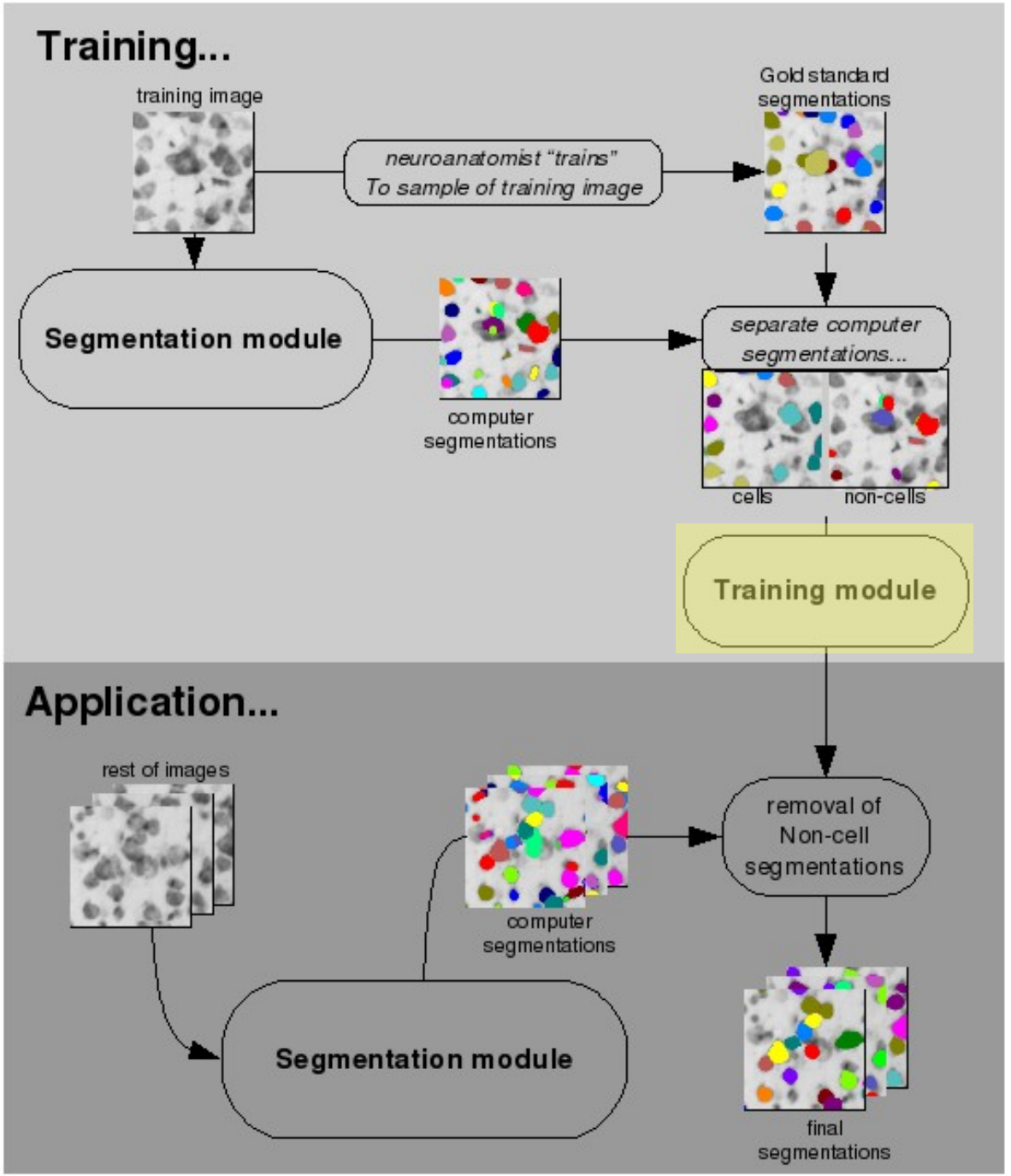

Inglis et al. ***J. Microscopy*** *230, 339 (2008)*

Method - recognition

Central moments

Central moments are defined as

$$\mu_{pq} = \int_{-\infty}^{\infty}\int_{-\infty}^{\infty}(x-\bar{x})^p(y-\bar{y})^q f(x,y)\,dx\,dy$$

where $\bar{x} = \frac{M_{10}}{M_{00}}$ and $\bar{y} = \frac{M_{01}}{M_{00}}$ are the components of the centroid.

If $f(x, y)$ is a digital image, then the previous equation becomes

$$\mu_{pq} = \sum_x \sum_y (x-\bar{x})^p(y-\bar{y})^q f(x,y)$$

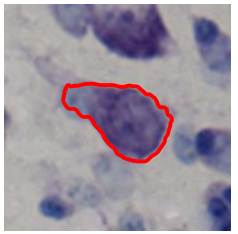

Scale invariant moments

Moments η_{ij} where $i + j \geq 2$ can be constructed to be invariant to both translation and changes in scale by dividing the corresponding central moment by the properly scale

$$\eta_{ij} = \frac{\mu_{ij}}{\mu_{00}^{\left(1+\frac{i+j}{2}\right)}}$$

Rotation invariant moments

It is possible to calculate moments which are invariant under translation, changes in scale, and also *rotation*. Most frequently used are the Hu set of invariant moments [1]:

$$I_1 = \eta_{20} + \eta_{02}$$

$$I_2 = (\eta_{20} - \eta_{02})^2 + (2\eta_{11})^2$$

$$I_3 = (\eta_{30} - 3\eta_{12})^2 + (3\eta_{21} - \eta_{03})^2$$

$$I_4 = (\eta_{30} + \eta_{12})^2 + (\eta_{21} + \eta_{03})^2$$

$$I_5 = (\eta_{30} - 3\eta_{12})(\eta_{30} + \eta_{12})[(\eta_{30} + \eta_{12})^2 - 3(\eta_{21} + \eta_{03})^2] + (3\eta_{21} - \eta_{03})(\eta_{21} + \eta_{03})[3(\eta_{30} + \eta_{12})^2 - (\eta_{21} + \eta_{03})^2]$$

$$I_6 = (\eta_{20} - \eta_{02})[(\eta_{30} + \eta_{12})^2 - (\eta_{21} + \eta_{03})^2] + 4\eta_{11}(\eta_{30} + \eta_{12})(\eta_{21} + \eta_{03})$$

$$I_7 = (3\eta_{21} - \eta_{03})(\eta_{30} + \eta_{12})[(\eta_{30} + \eta_{12})^2 - 3(\eta_{21} + \eta_{03})^2] - (\eta_{30} - 3\eta_{12})(\eta_{21} + \eta_{03})[3(\eta_{30} + \eta_{12})^2 - (\eta_{21} + \eta_{03})^2].$$

From Wikipedia article “Image Moments”

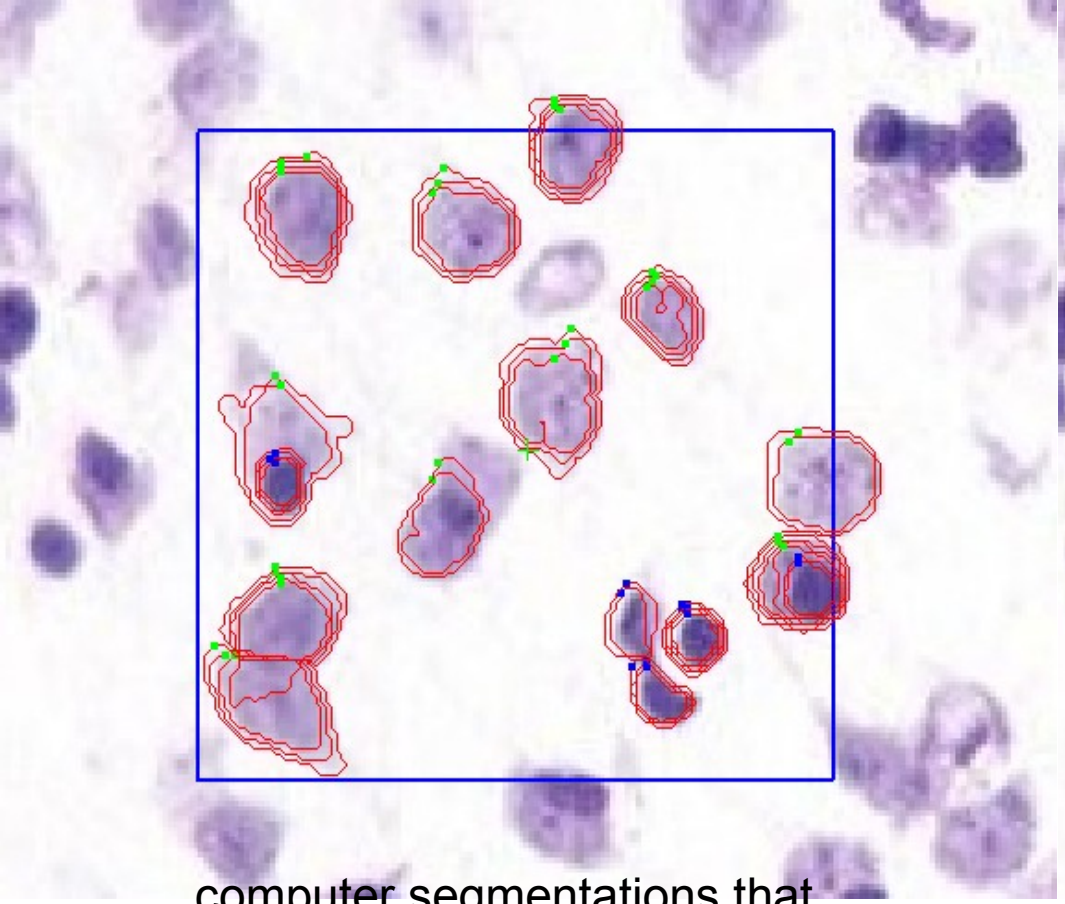

computer segmentations that match the (human) gold standard neurons and glial

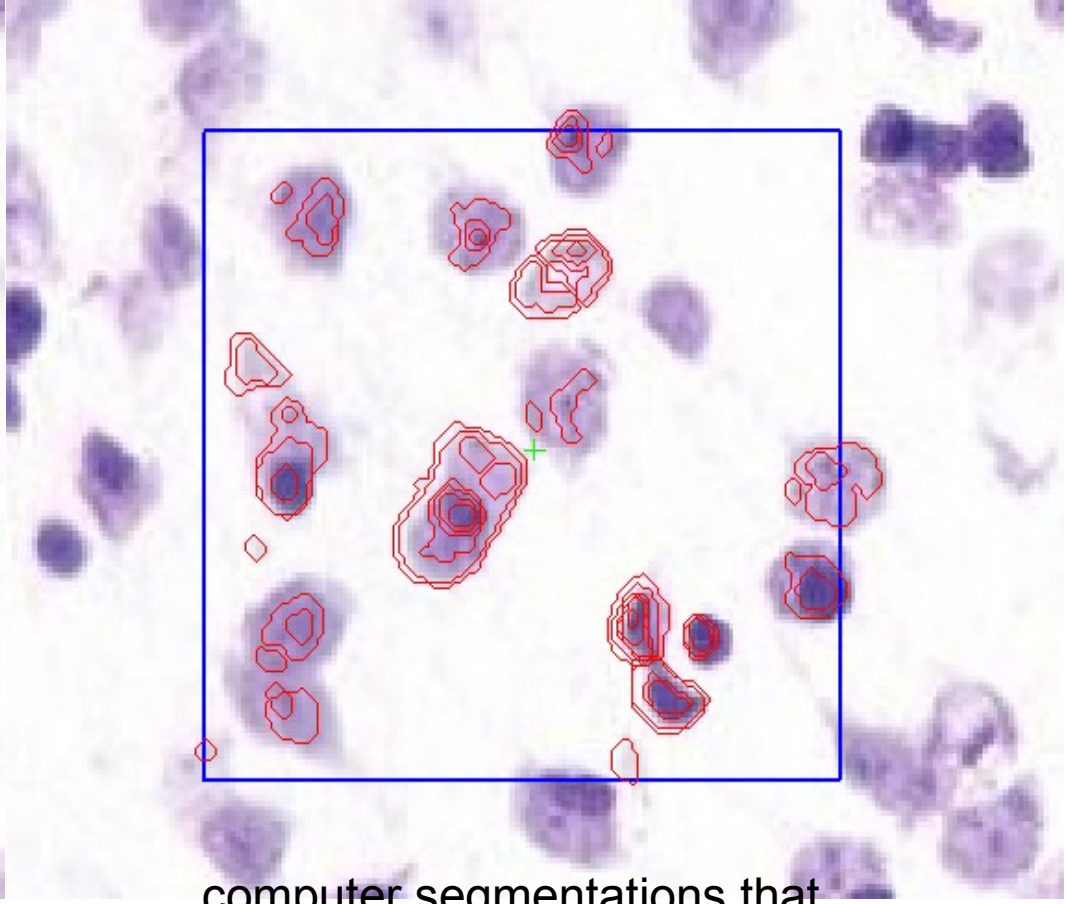

computer segmentations that don't match the (human) gold standard neurons or

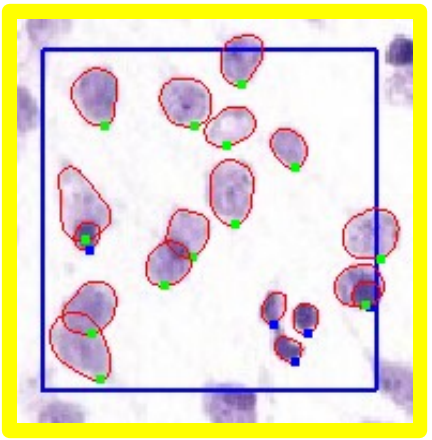

Gold Standard

Training Methodology

Central moments

Central moments are defined as

$$\mu_{pq} = \int_{-\infty}^{\infty}\int_{-\infty}^{\infty}(x-\bar{x})^p(y-\bar{y})^q f(x,y)\,dx\,dy$$

where $\bar{x} = \frac{M_{10}}{M_{00}}$ and $\bar{y} = \frac{M_{01}}{M_{00}}$ are the components of the centroid.

If $f(x, y)$ is a digital image, then the previous equation becomes

$$\mu_{pq} = \sum_x \sum_y (x-\bar{x})^p(y-\bar{y})^q f(x,y)$$

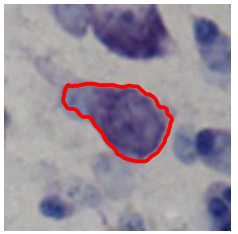

Scale invariant moments

Moments η_{ij} where $i + j \geq 2$ can be constructed to be invariant to both translation and changes in scale by dividing the corresponding central moment by the properly scale

$$\eta_{ij} = \frac{\mu_{ij}}{\mu_{00}^{\left(1+\frac{i+j}{2}\right)}}$$

Rotation invariant moments

It is possible to calculate moments which are invariant under translation, changes in scale, and also *rotation*. Most frequently used are the Hu set of invariant moments [1]:

$$I_1 = \eta_{20} + \eta_{02}$$

$$I_2 = (\eta_{20} - \eta_{02})^2 + (2\eta_{11})^2$$

$$I_3 = (\eta_{30} - 3\eta_{12})^2 + (3\eta_{21} - \eta_{03})^2$$

$$I_4 = (\eta_{30} + \eta_{12})^2 + (\eta_{21} + \eta_{03})^2$$

$$I_5 = (\eta_{30} - 3\eta_{12})(\eta_{30} + \eta_{12})[(\eta_{30} + \eta_{12})^2 - 3(\eta_{21} + \eta_{03})^2] + (3\eta_{21} - \eta_{03})(\eta_{21} + \eta_{03})[3(\eta_{30} + \eta_{12})^2 - (\eta_{21} + \eta_{03})^2]$$

$$I_6 = (\eta_{20} - \eta_{02})[(\eta_{30} + \eta_{12})^2 - (\eta_{21} + \eta_{03})^2] + 4\eta_{11}(\eta_{30} + \eta_{12})(\eta_{21} + \eta_{03})$$

$$I_7 = (3\eta_{21} - \eta_{03})(\eta_{30} + \eta_{12})[(\eta_{30} + \eta_{12})^2 - 3(\eta_{21} + \eta_{03})^2] - (\eta_{30} - 3\eta_{12})(\eta_{21} + \eta_{03})[3(\eta_{30} + \eta_{12})^2 - (\eta_{21} + \eta_{03})^2].$$

From Wikipedia article “Image Moments”

Training Methodology

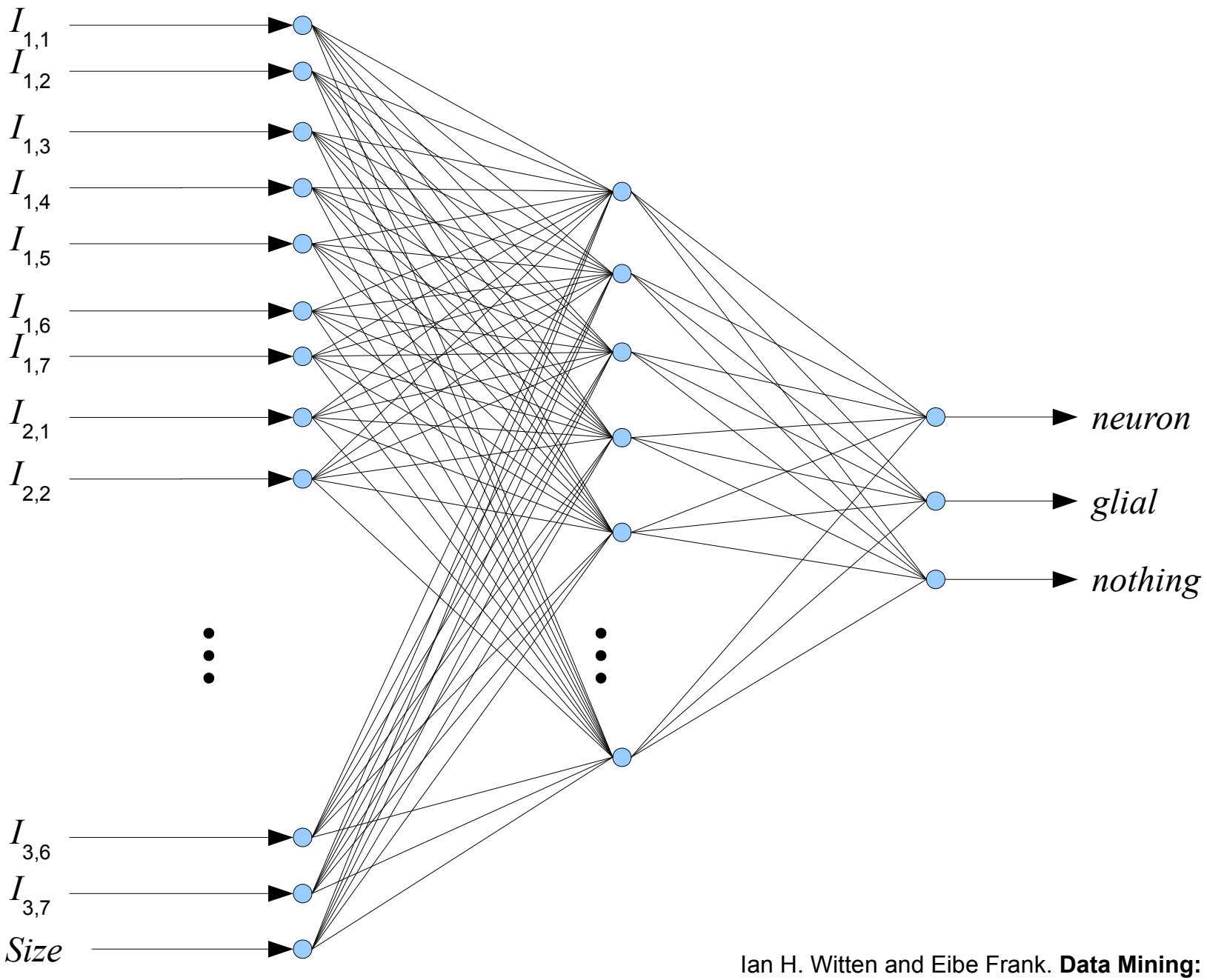

Ian H. Witten and Eibe Frank. **Data Mining: Practical machine learning tools and techniques** (2005).

Training Methodology

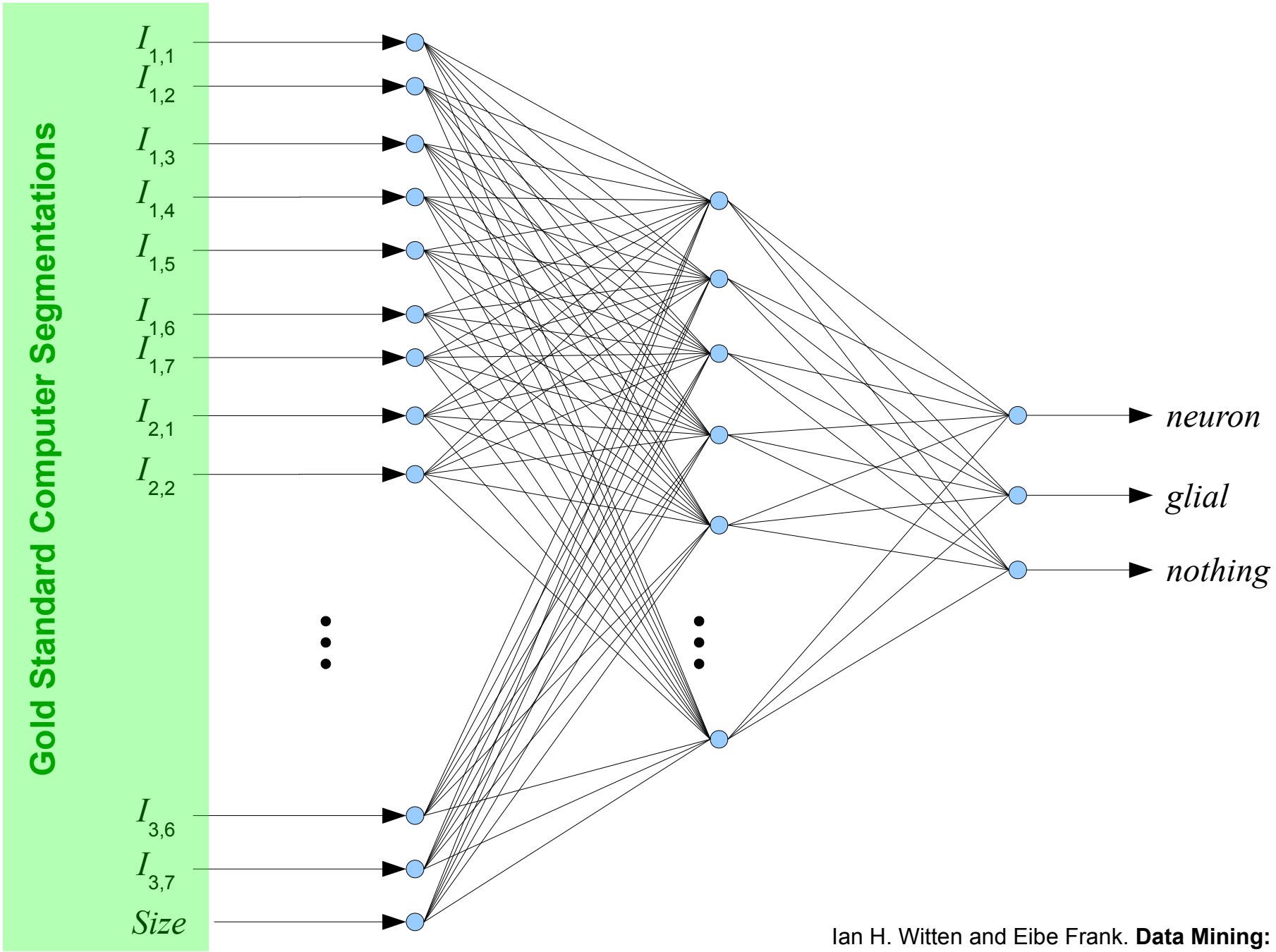

Ian H. Witten and Eibe Frank. **Data Mining: Practical machine learning tools and techniques** (2005).

Training Methodology

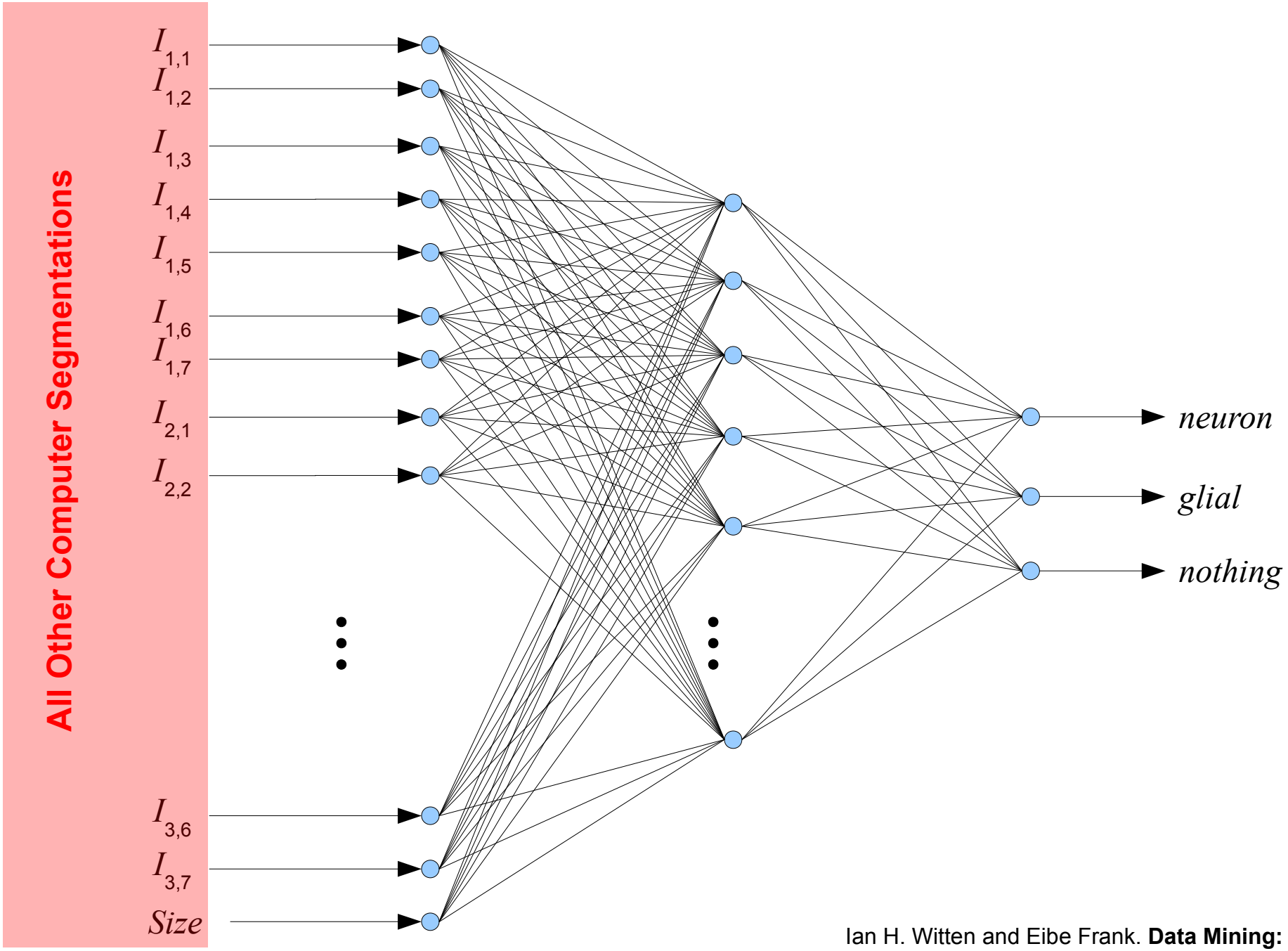

Ian H. Witten and Eibe Frank. **Data Mining: Practical machine learning tools and techniques** (2005).

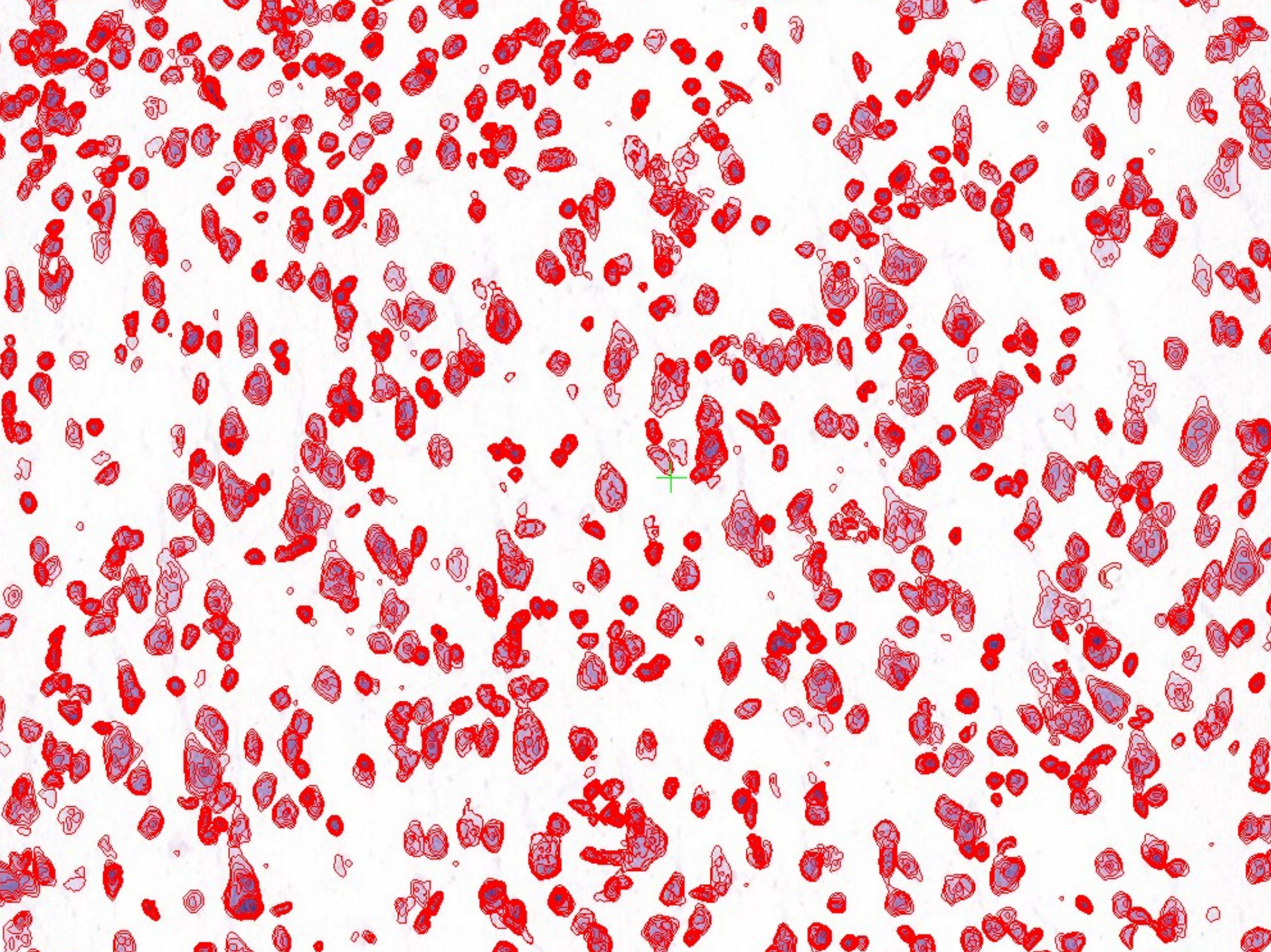

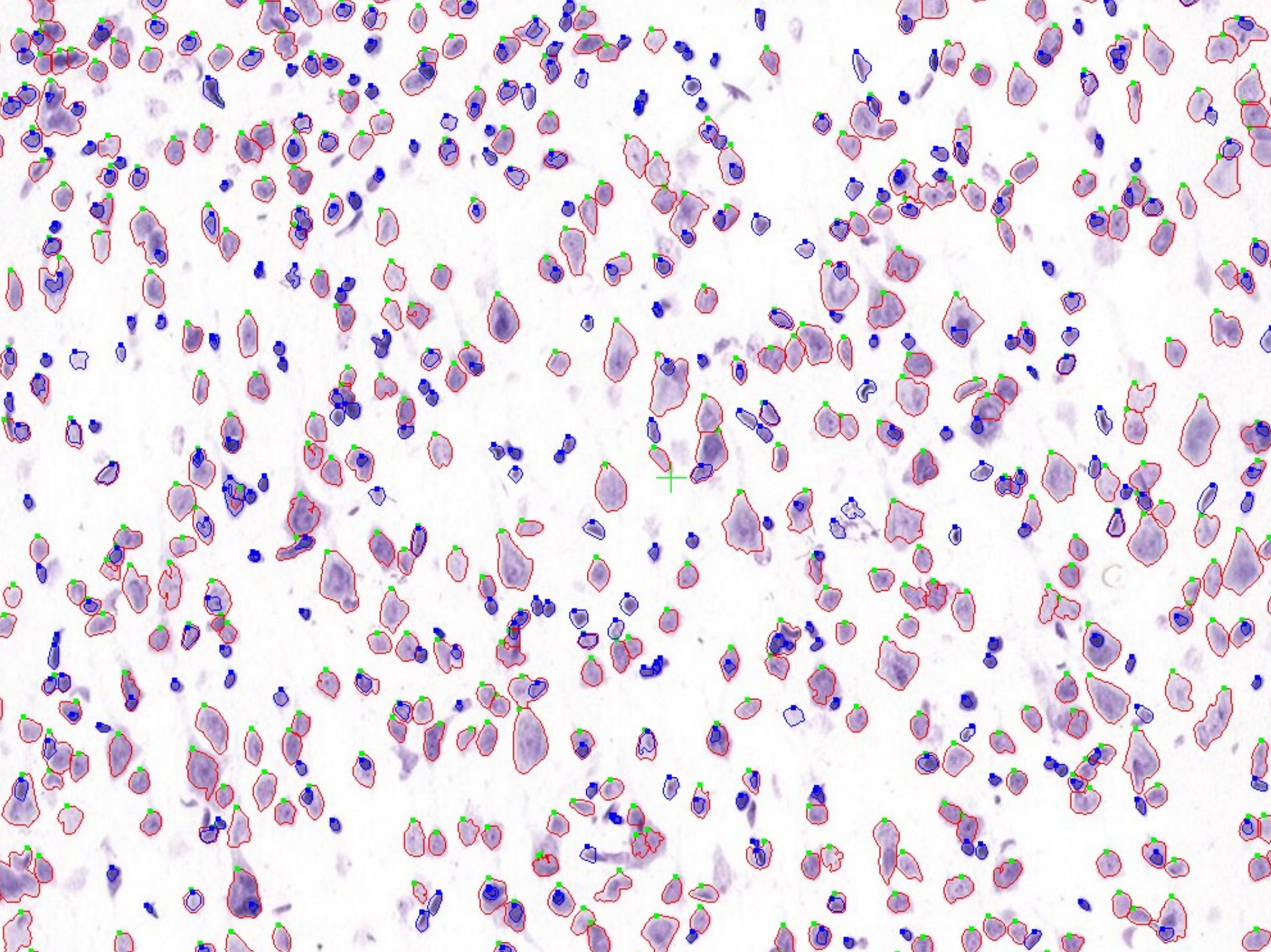

Method – validation 1 of 2

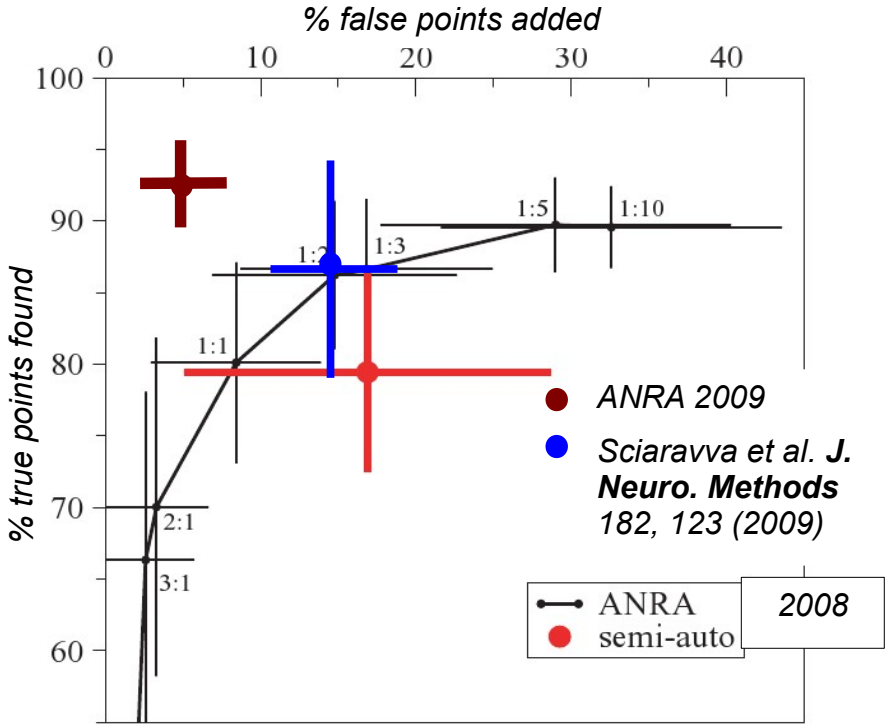

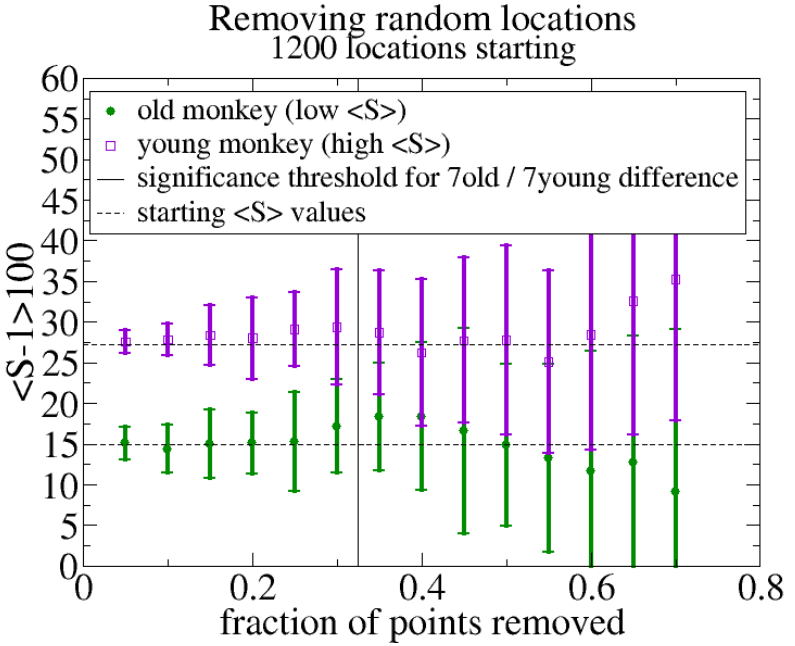

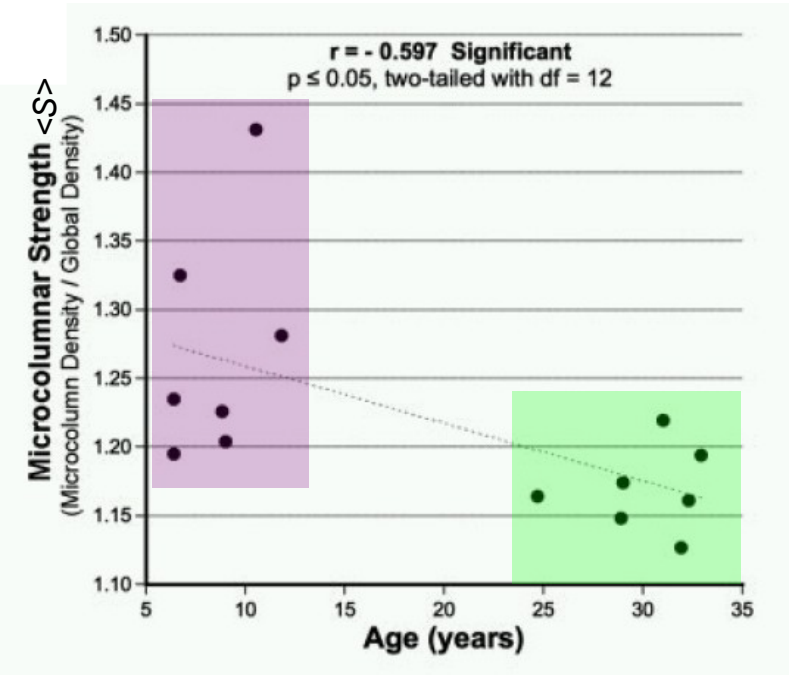

Cruz et al. ***PNAS***. 101 (2004)

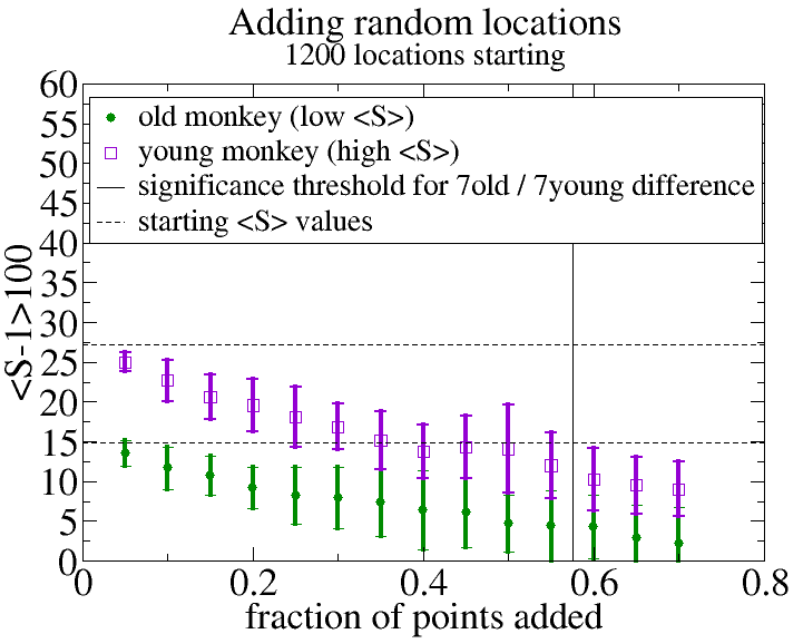

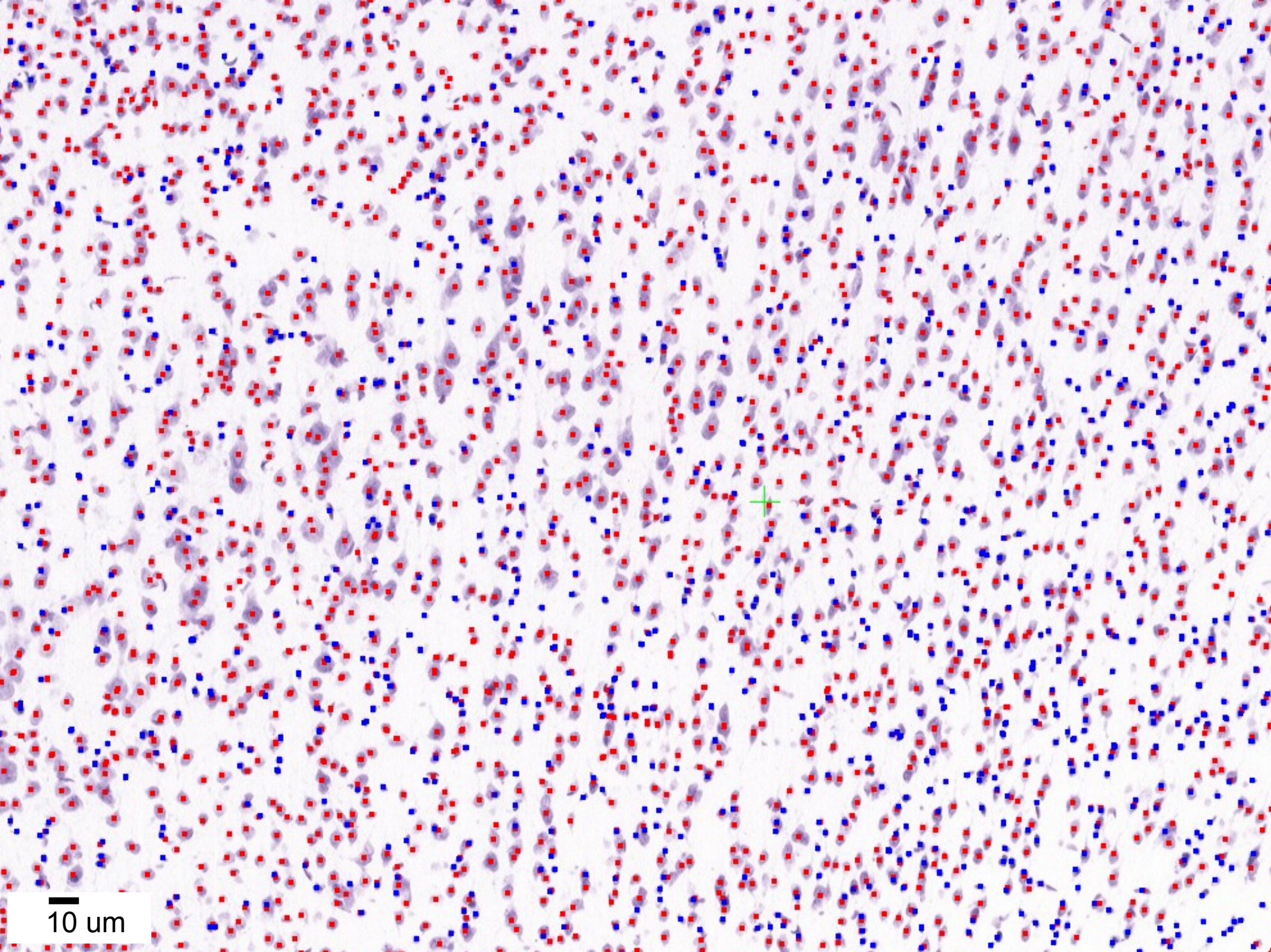
10 um

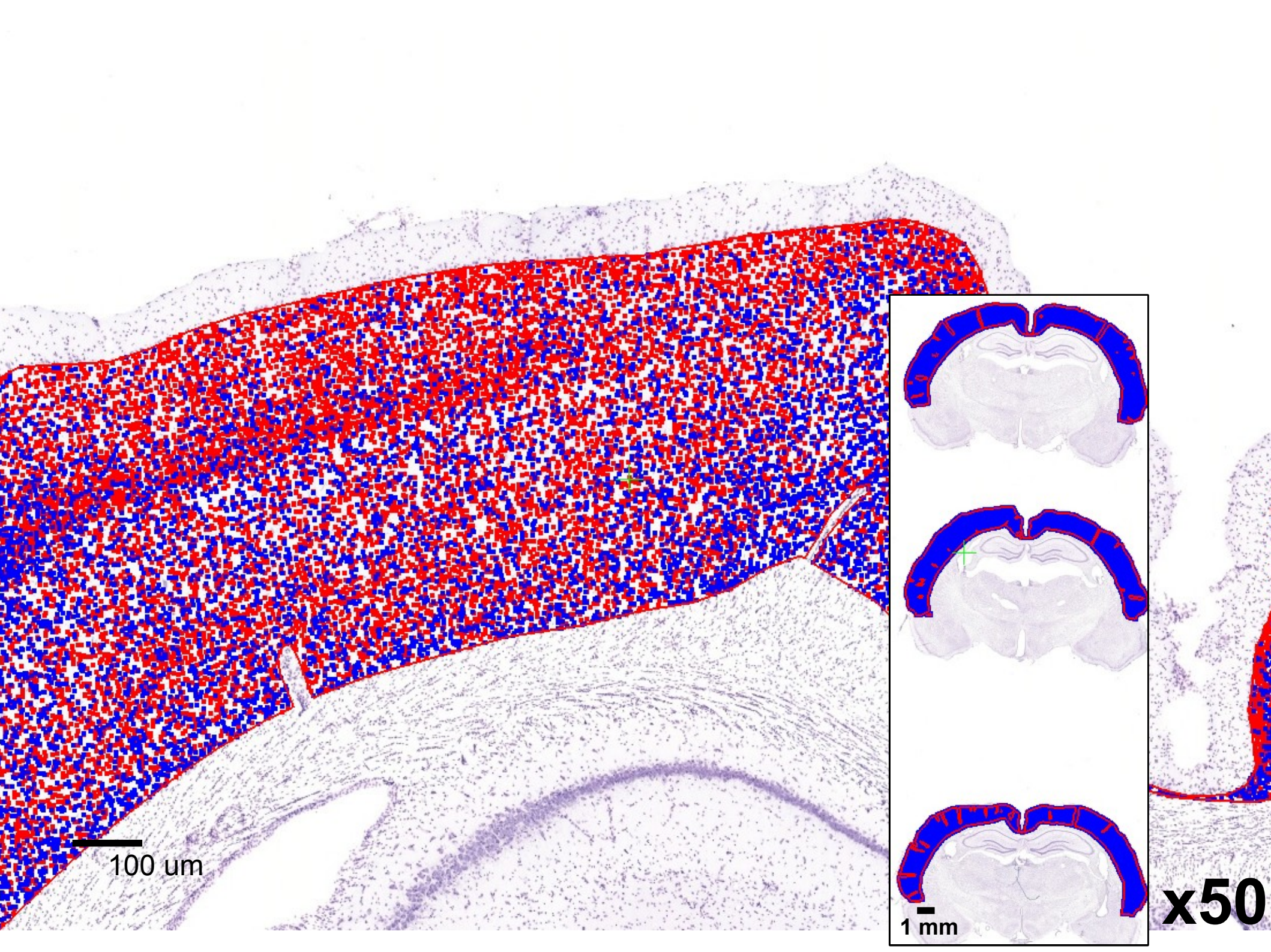
100 um
1 mm
x50

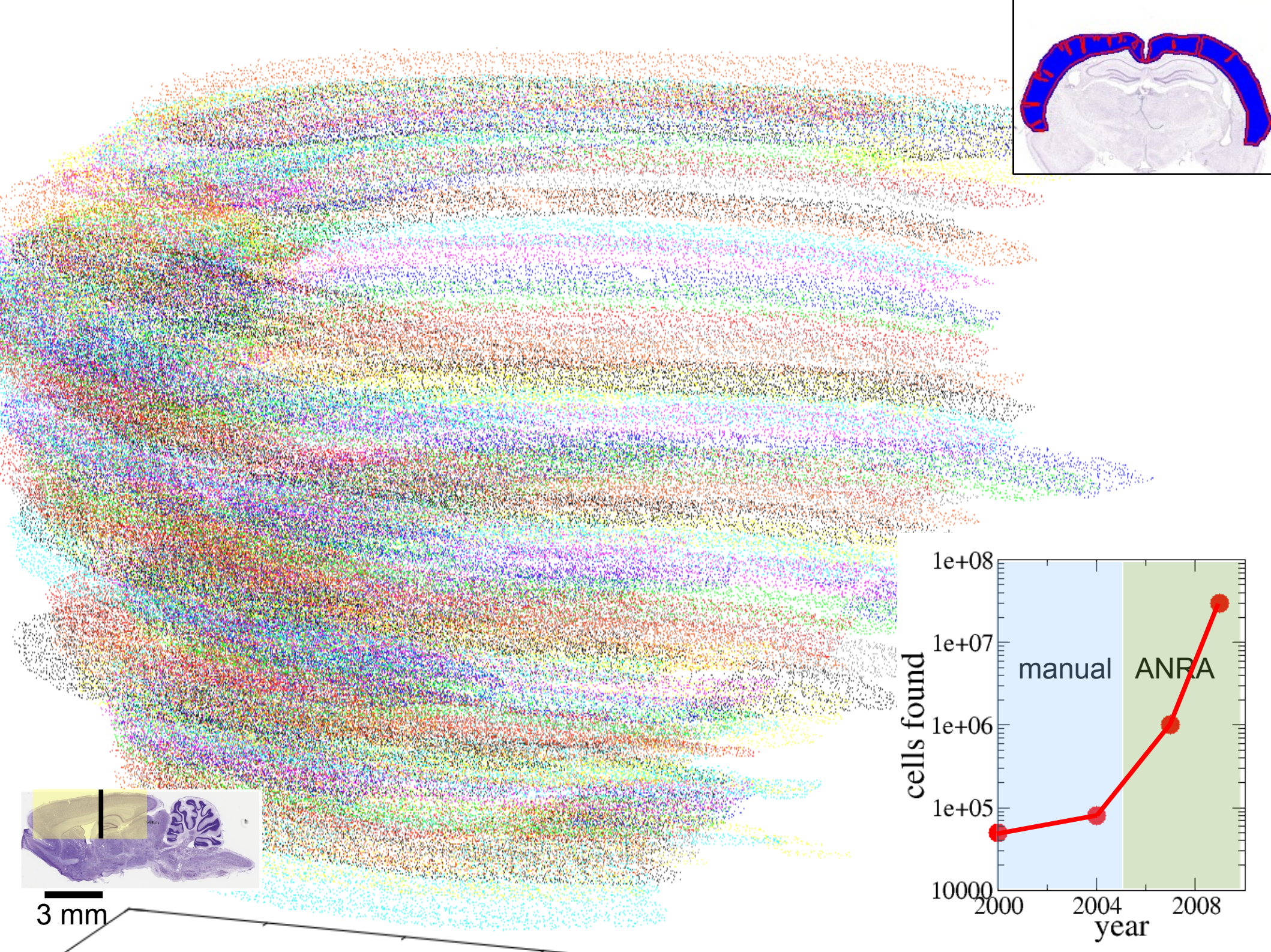
1e+08
1e+07
1e+06
1e+05
10000
cells found
manual
ANRA
2000
2004
2008
year
3 mm

Method – validation 2 of 2

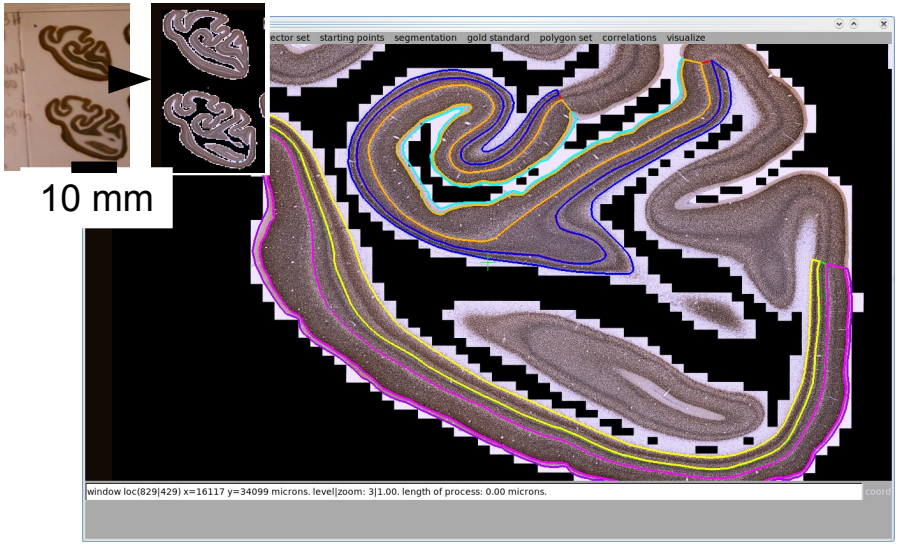

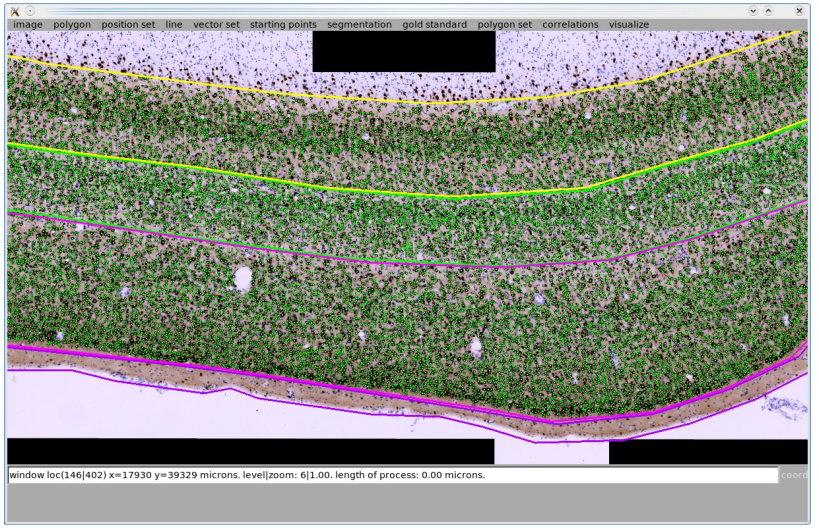

$$N_{stereology} = (objects\ counted)\left(\frac{1}{section\ sampling\ fraction}\right)\left(\frac{1}{area\ sampling\ fraction}\right)\left(\frac{average\ thickness\ of\ tissue}{height\ of\ dissector}\right)$$

$$N_{ANRA} = (objects\ recognized)\left(\frac{1}{area\ sampling\ fraction}\right)\left(\frac{average\ thickness\ of\ tissue}{height\ of\ dissector}\right)$$

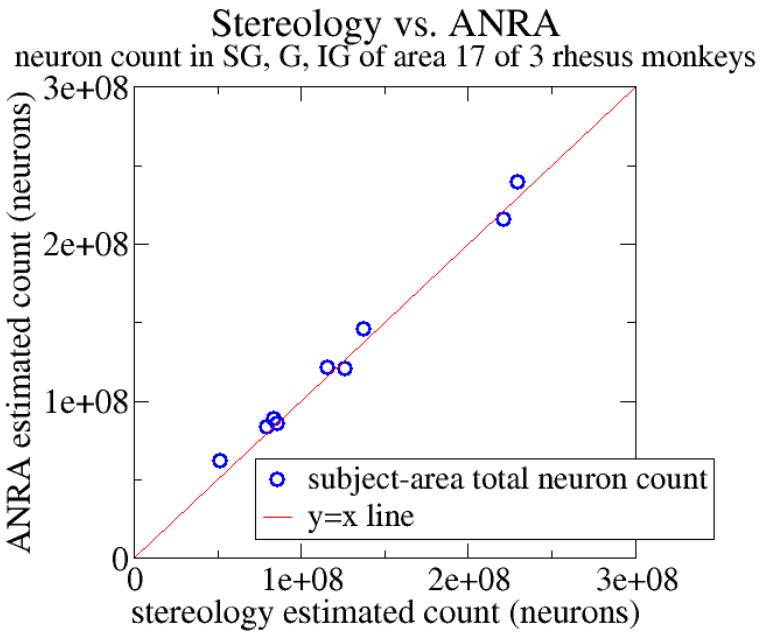

subject-area	$N_{stereology}$	N_{ANRA}
T-SG	230 099 130	239 022 080
Z-SG	137 677 540	146 075 136
HH-SG	221 661 580	215 428 224
T-G	126 382 500	120 815 616
Z-G	79 481 250	83 124 480
HH-G	115 740 000	121 409 152
T-IG	83 652 750	88 364 544
Z-IG	51 282 000	61 650 944
HH-IG	86 204 250	85 948 288

Results

Results – temporal lobe

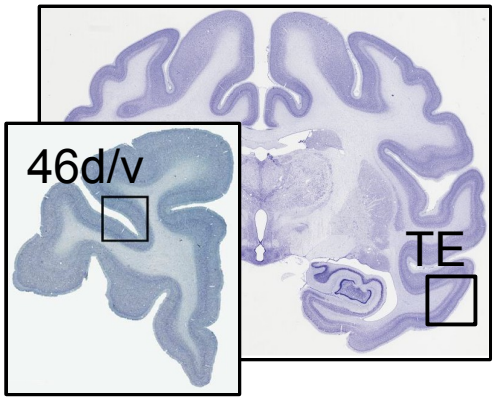

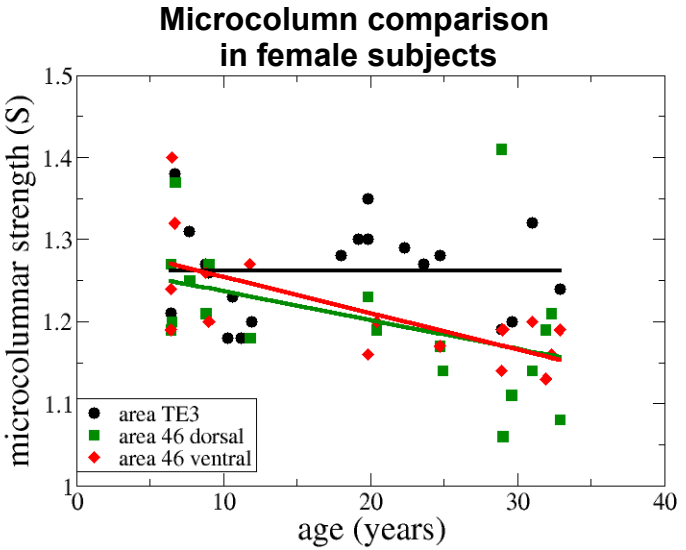

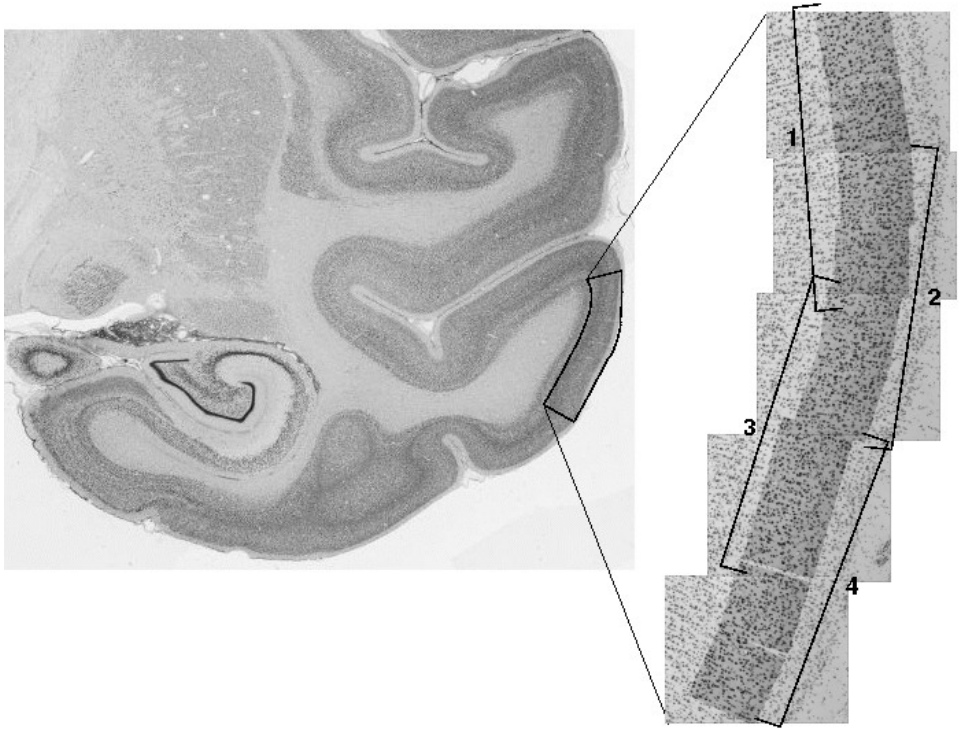

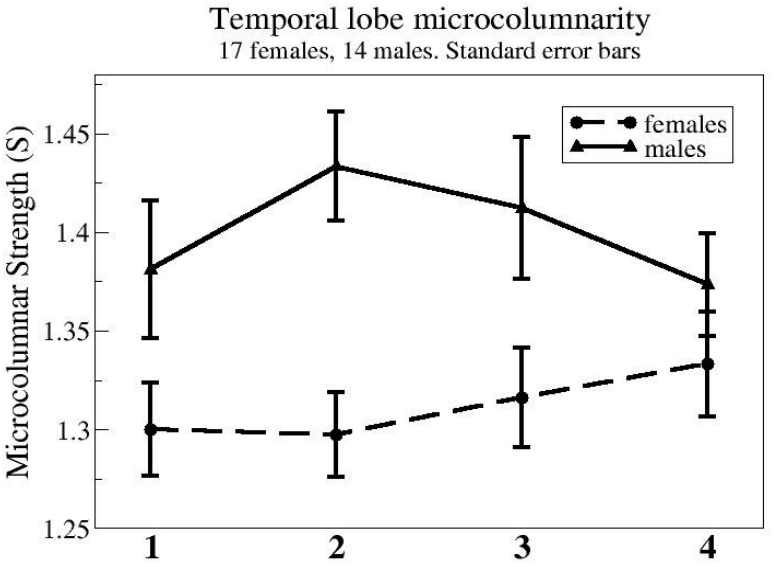

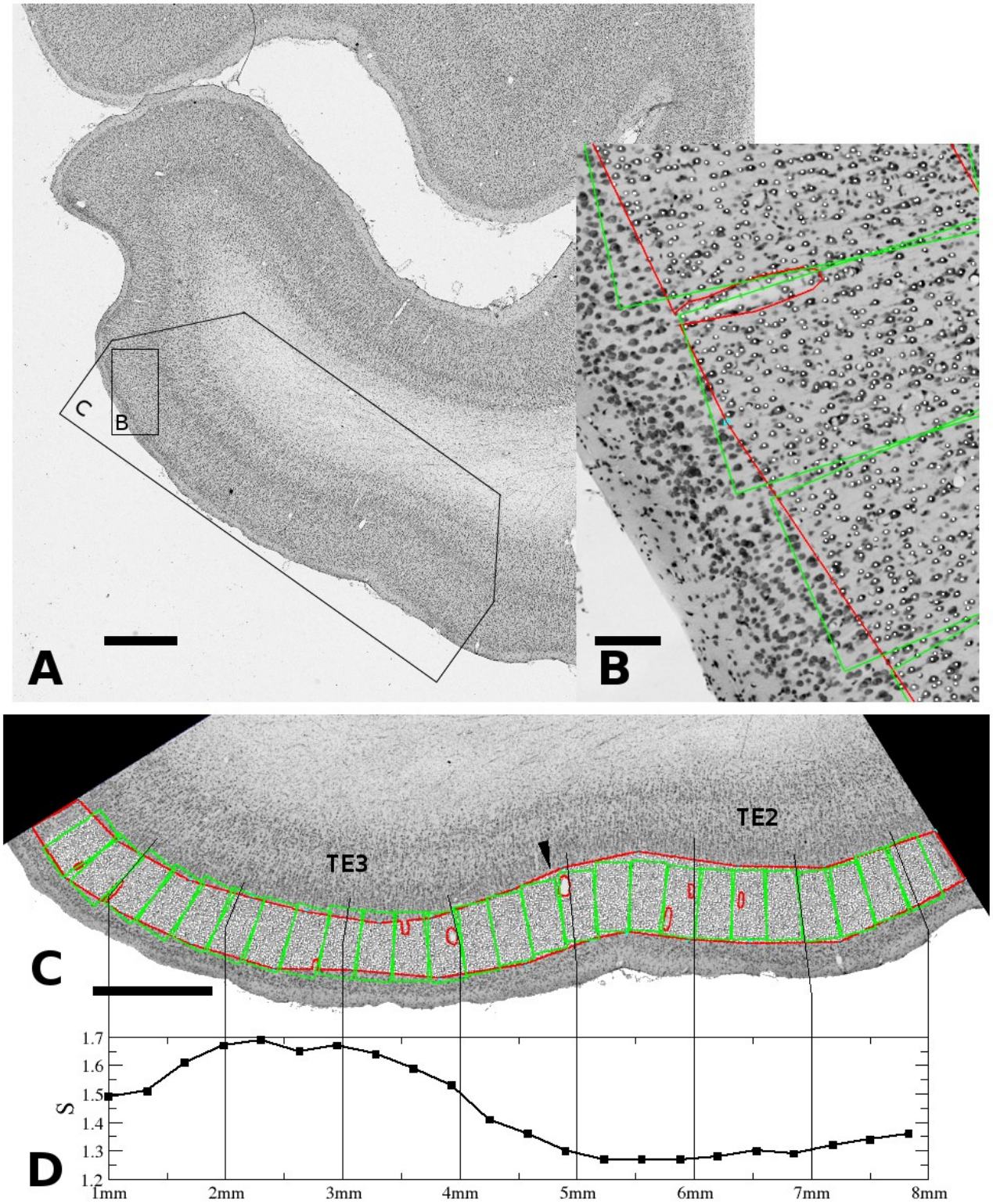
A
B
C
B
TE3
TE2
C
D
S
1.7
1.6
1.5
1.4
1.3
1.2
1mm
2mm
3mm
4mm
5mm
6mm
7mm
8mm

Results – temporal lobe

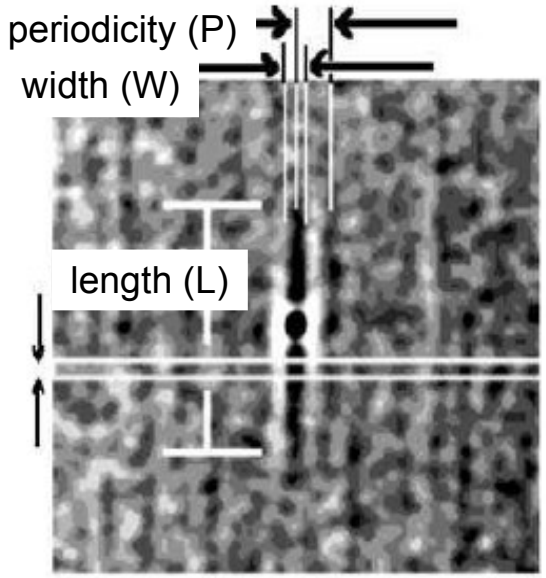

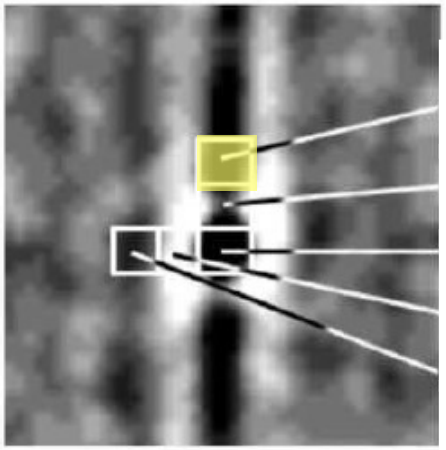

column strength (S)

intra-column depletion origin

inter-column depletion

neighboring column strength (T)

Area TE3 columnar properties
20 female subjects

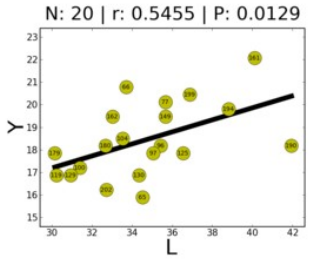

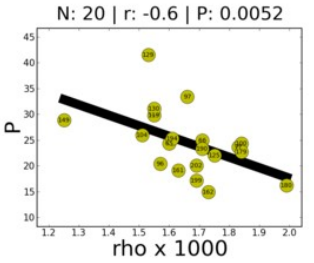

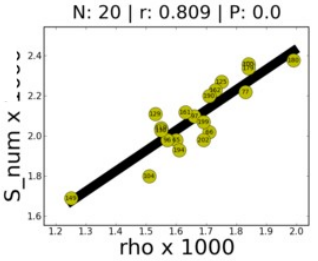

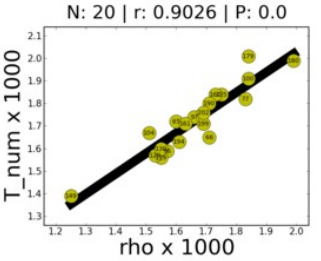

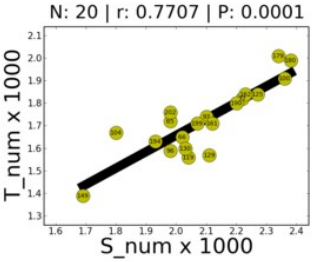

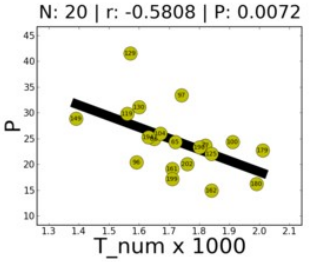

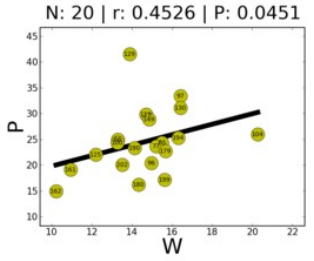

Results – temporal lobe

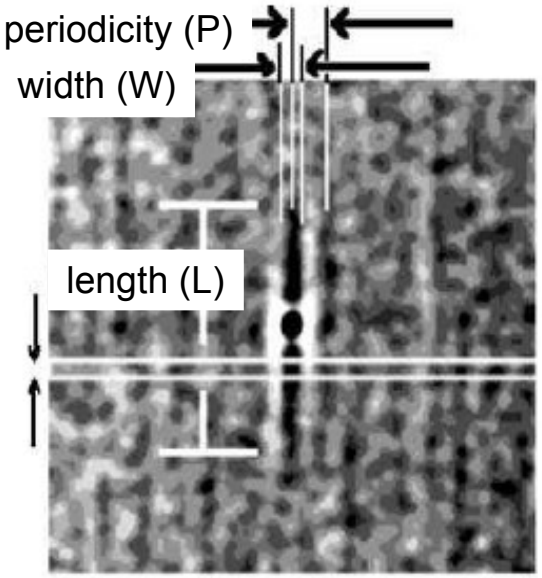

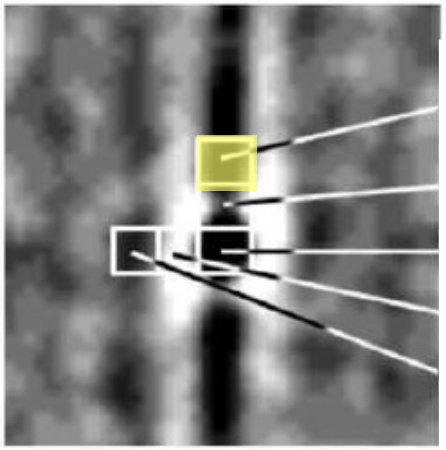

column strength (S)

intra-column depletion origin

inter-column depletion

neighboring column strength (T)

Area TE3 columnar properties
20 female subjects

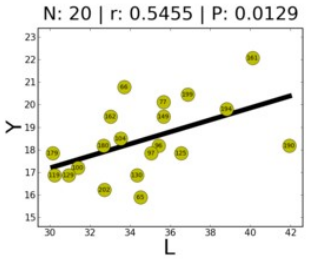

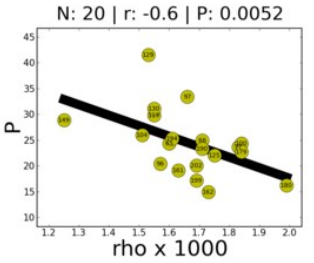

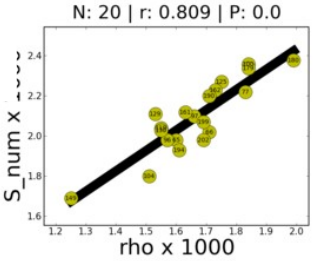

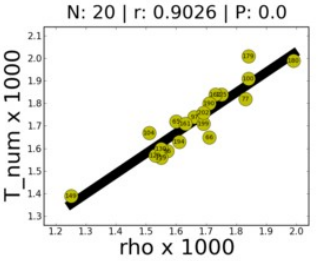

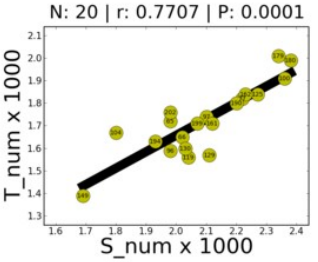

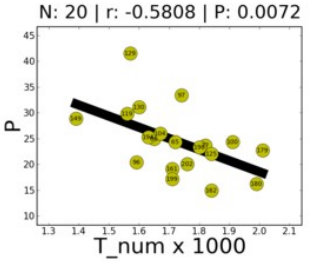

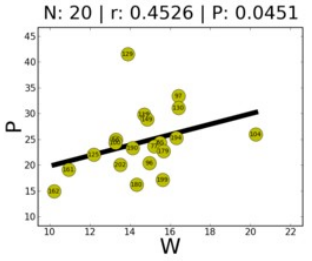

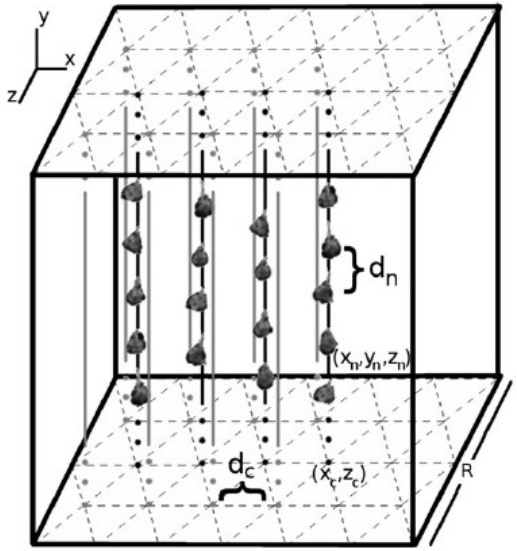

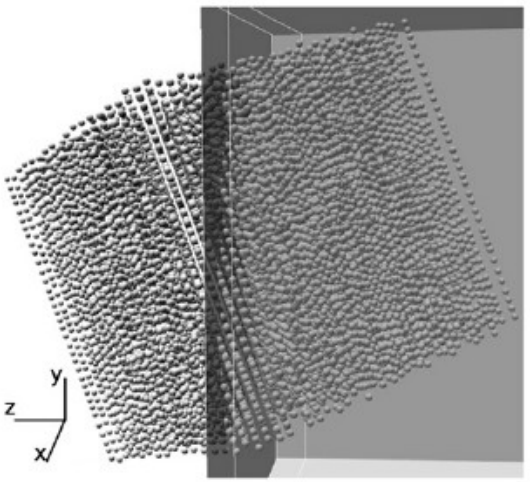

Cruz, Urbanc, Inglis, Rosene, Stanley, NeuroImage 40 (2008)

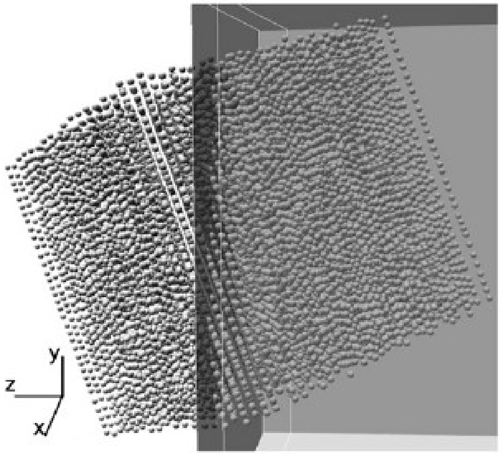

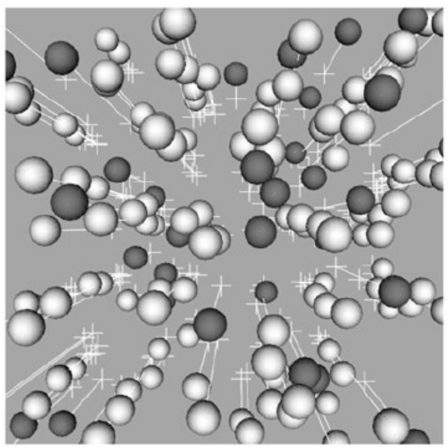

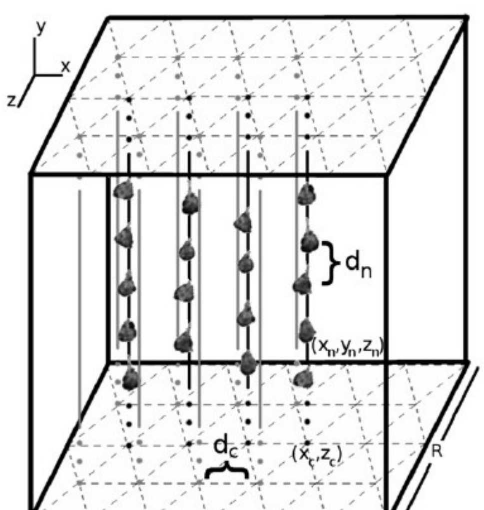

Model A	Model B	Model C	Model D	Experiment
no angle variance no interstitials no col. variance	angle variance no interstitials no col. variance	angle variance interstitials no col. variance	angle variance interstitials col. variance	

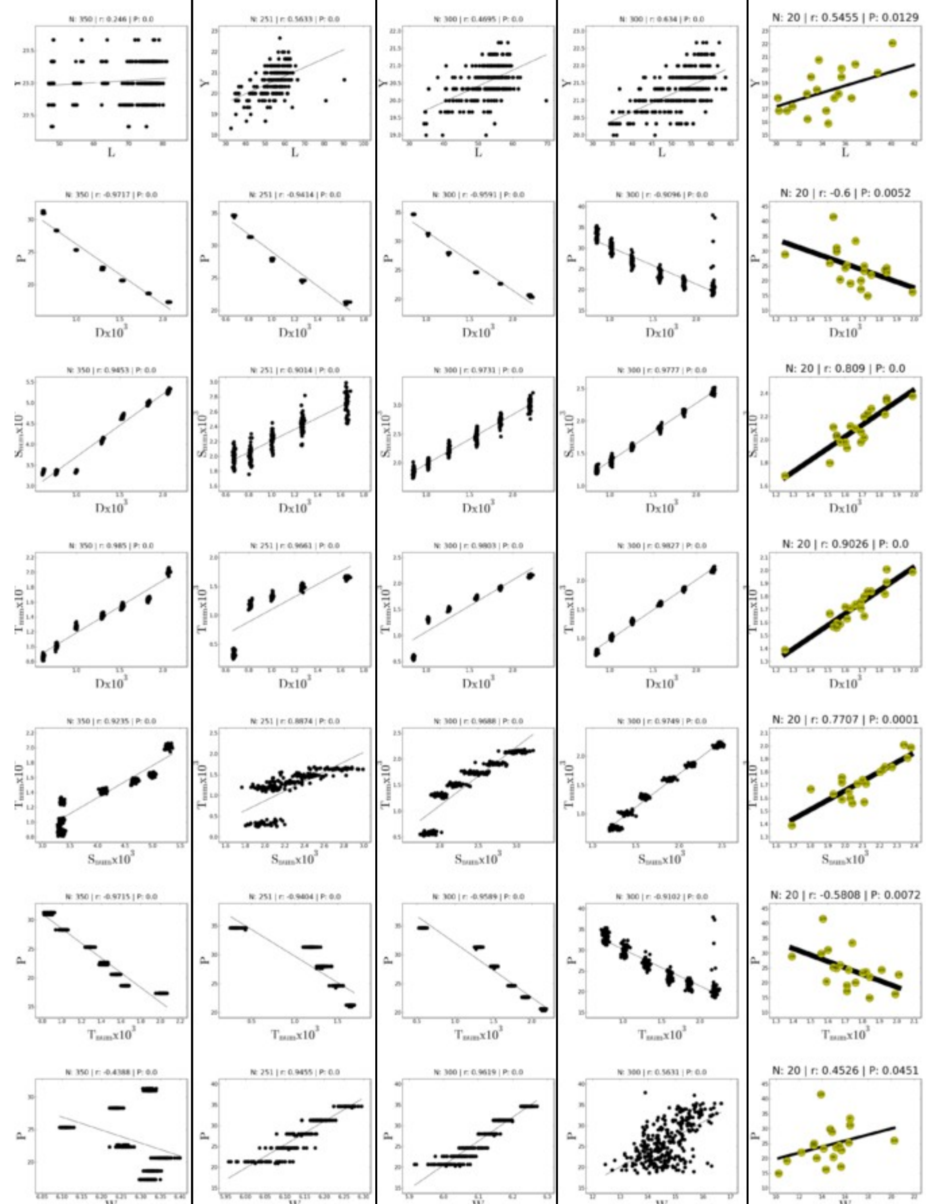

Results – rat cortex

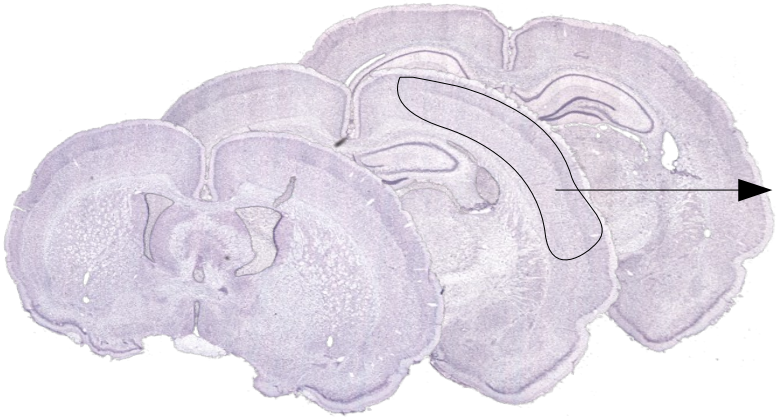

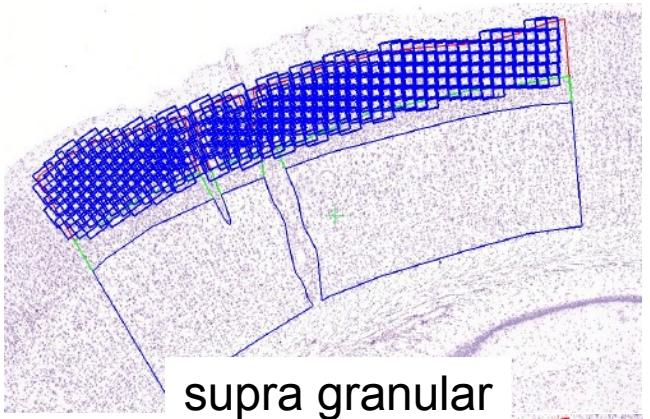

supra granular

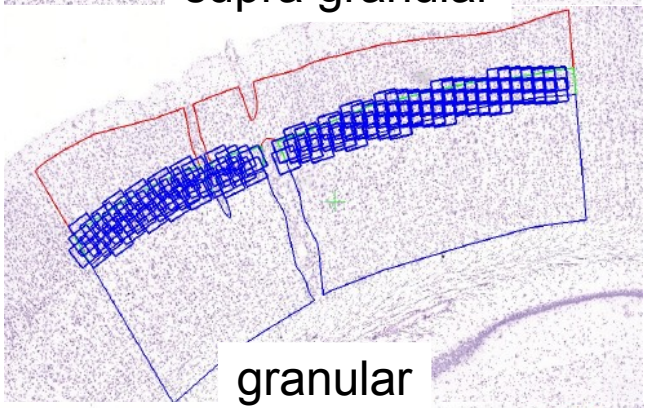

granular

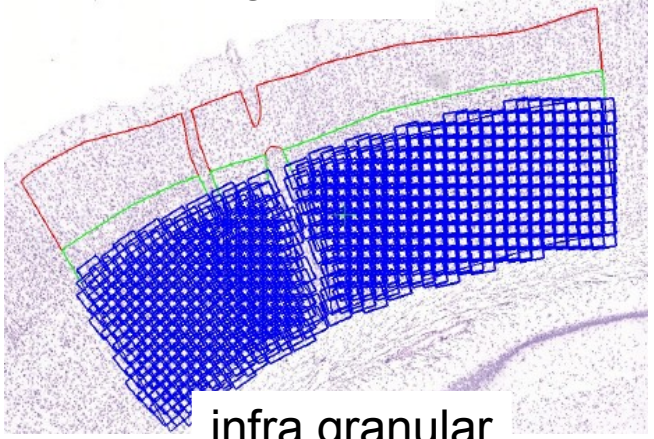

infra granular

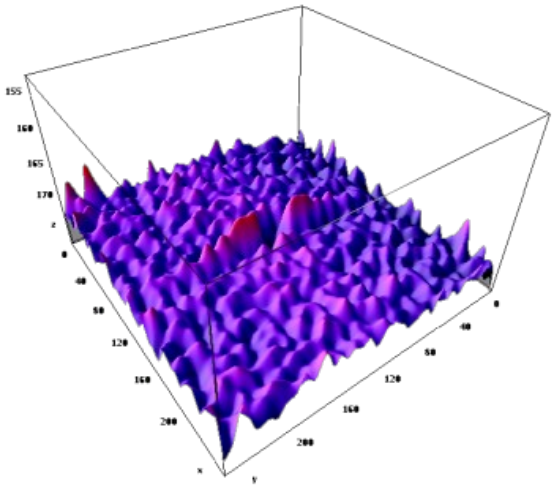

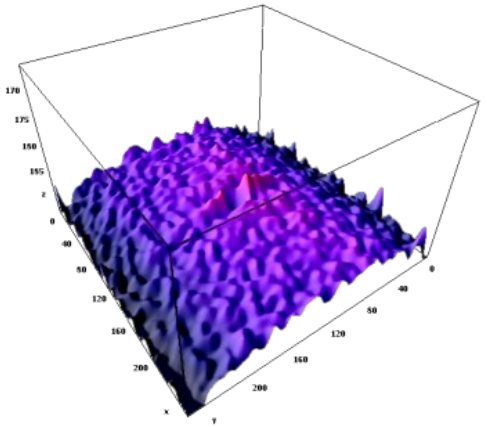

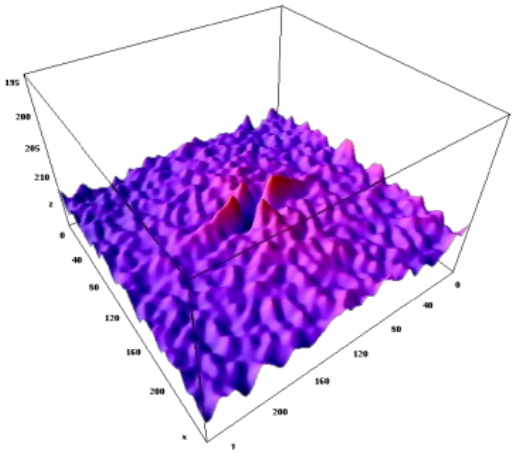

$$N = \frac{1}{\rho e^2 a}$$

ρ = density of cells
(0.002 cells/micron^2)

e = desired error
(**10%/5%/1%**)

a = area of measurement
100 microns^2

***N* = 500/2000/50000 cells per measurement**

Results – rat cortex

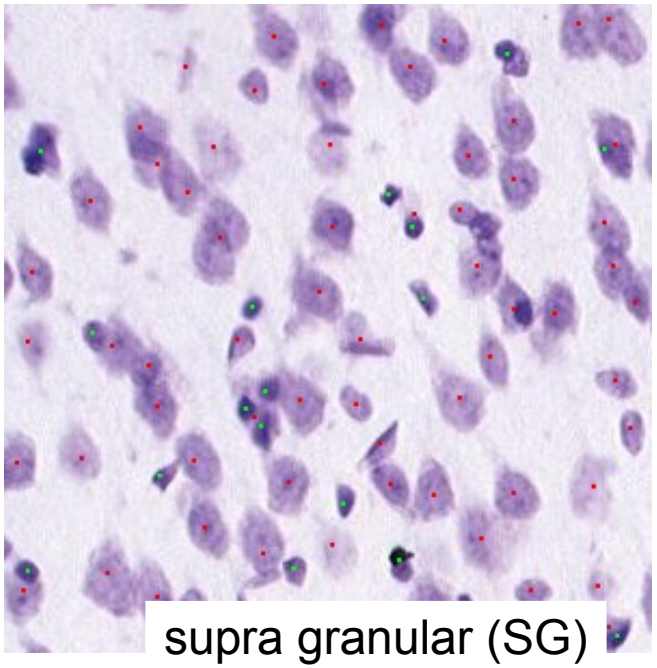
supra granular (SG)

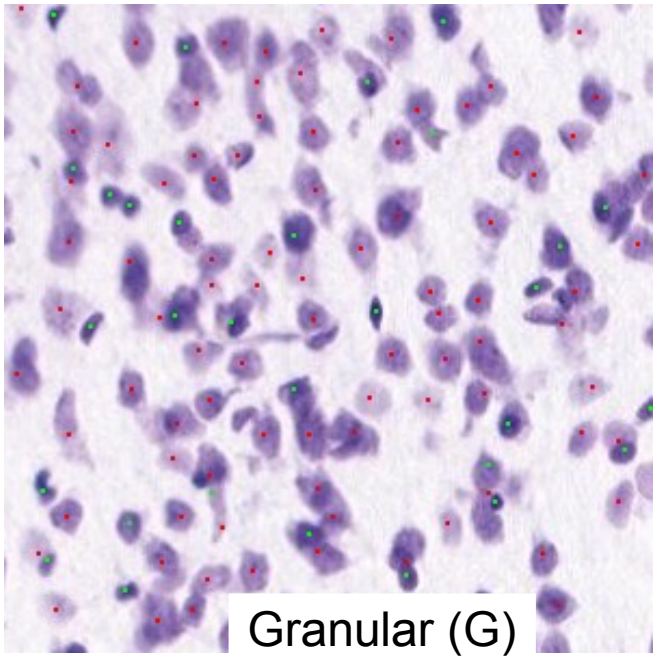
Granular (G)

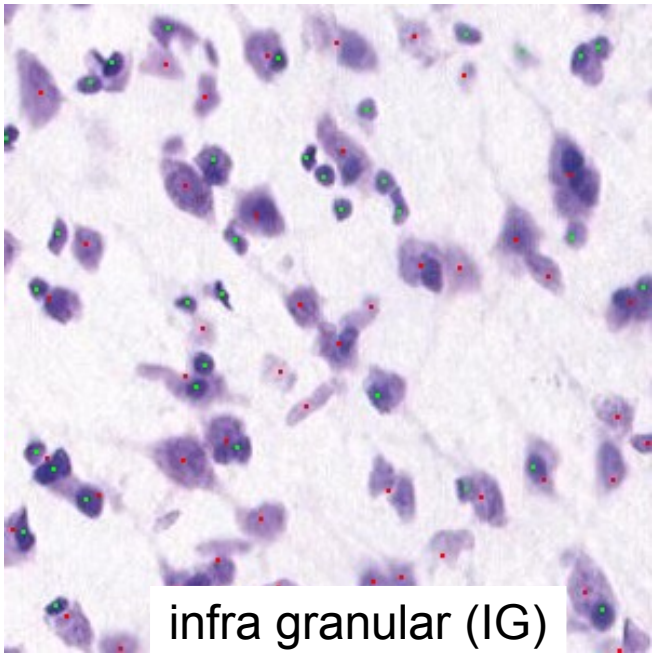
infra granular (IG)

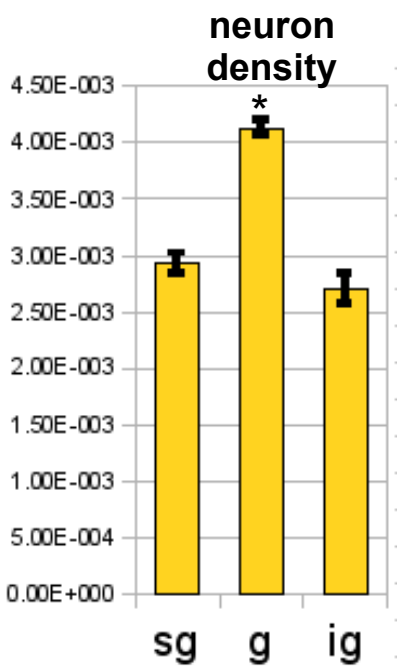

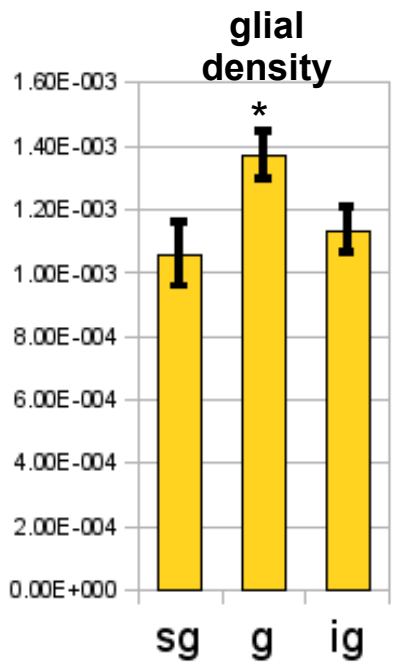

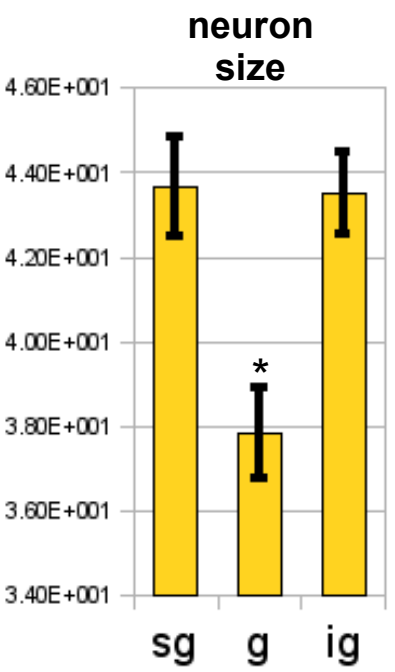

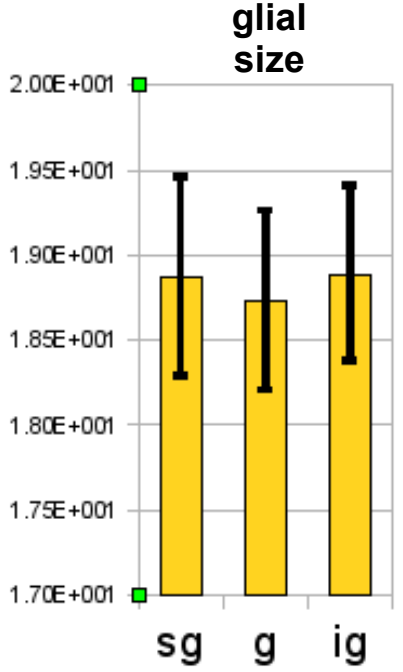

Results – rat cortex

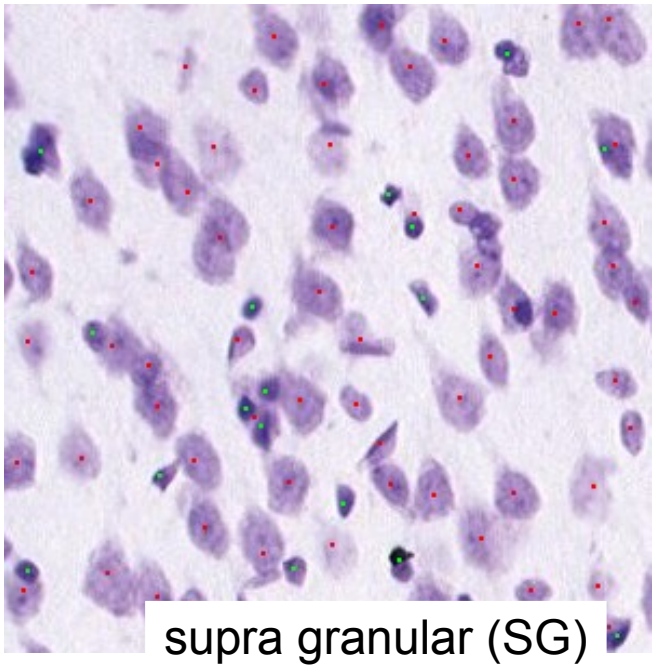
supra granular (SG)

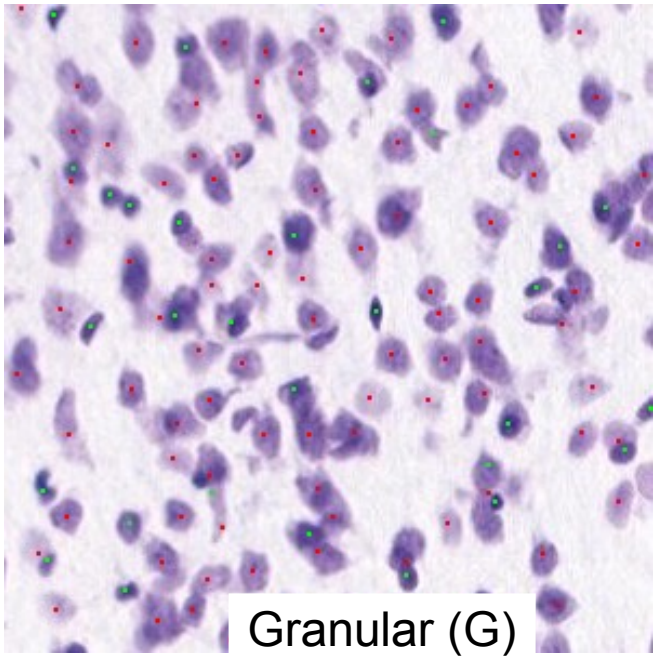
Granular (G)

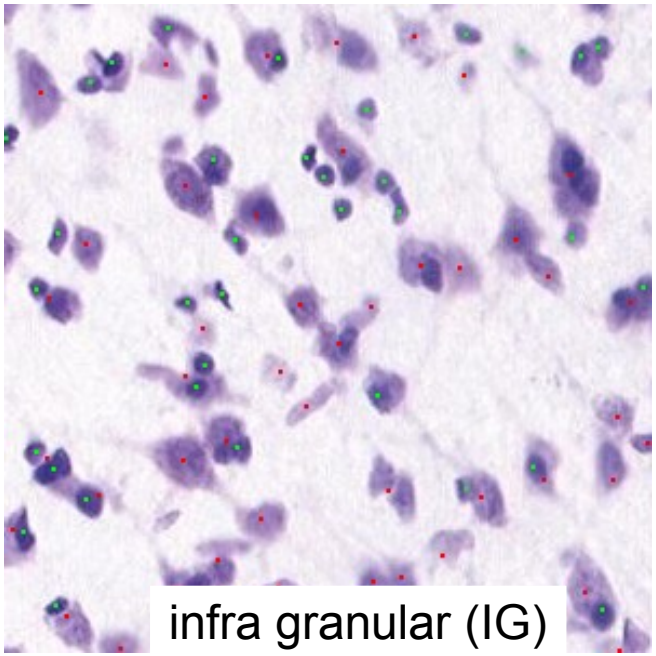
infra granular (IG)

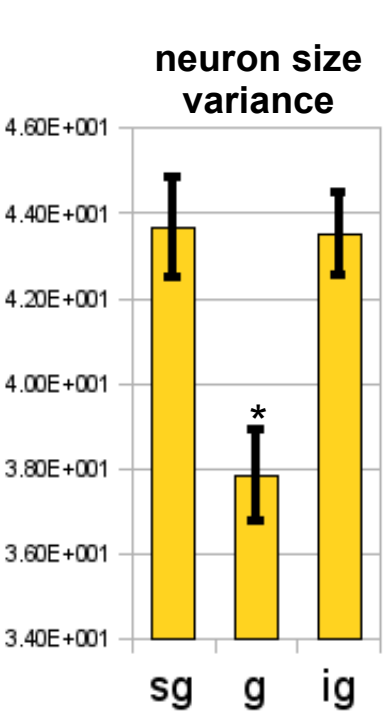

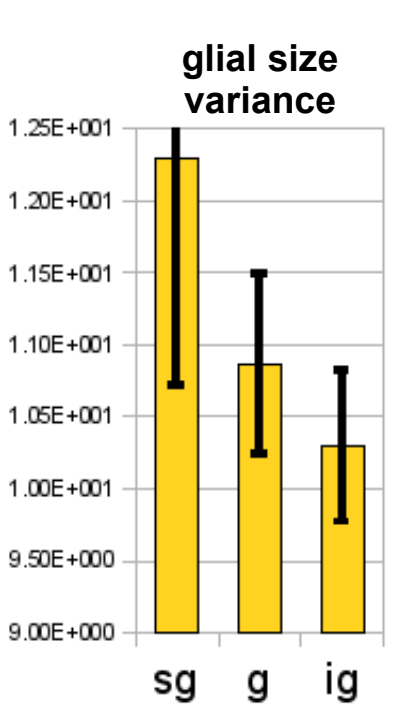

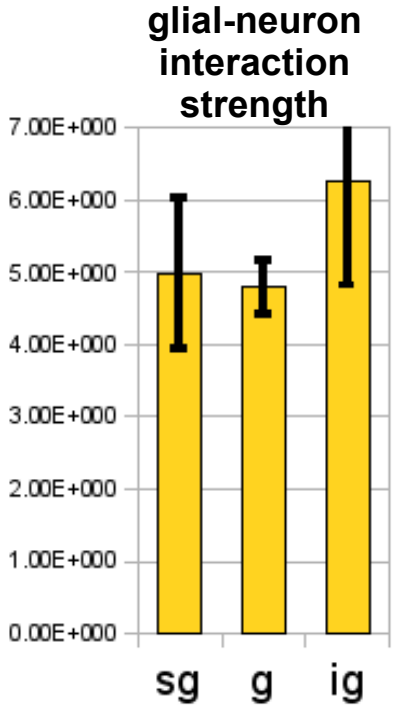

Results – rat cortex

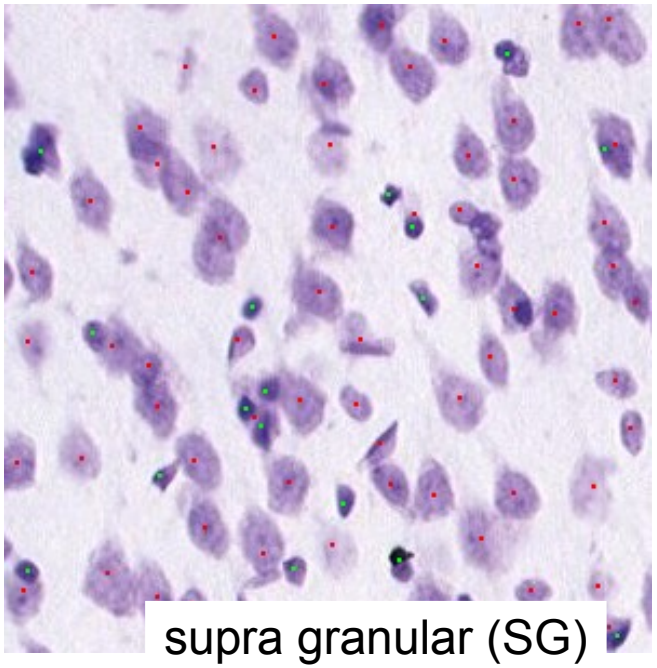

supra granular (SG)

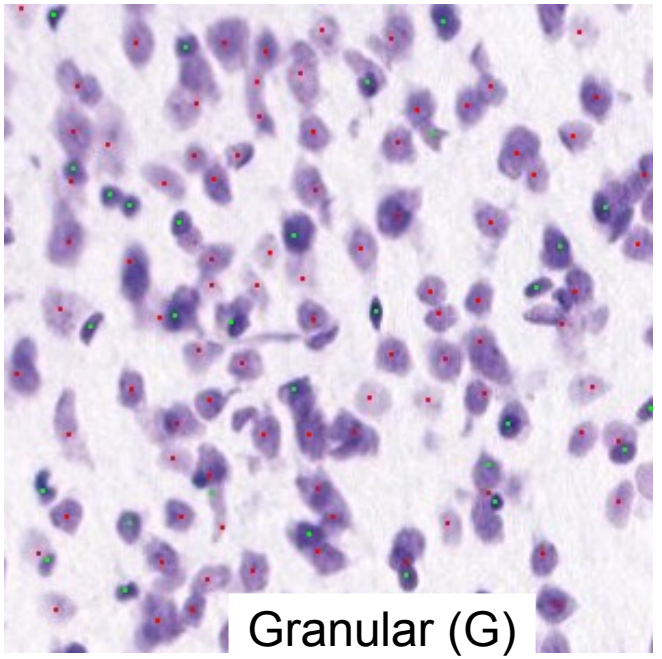

Granular (G)

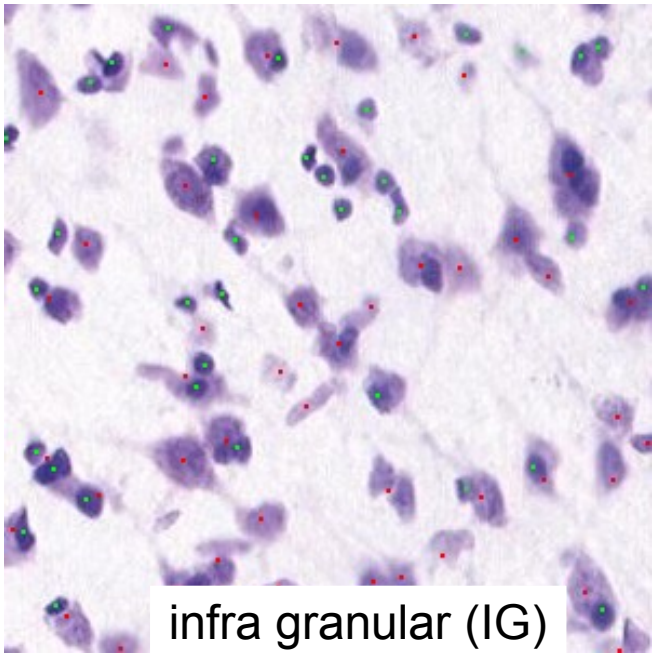

infra granular (IG)

microcolumn strength (S)

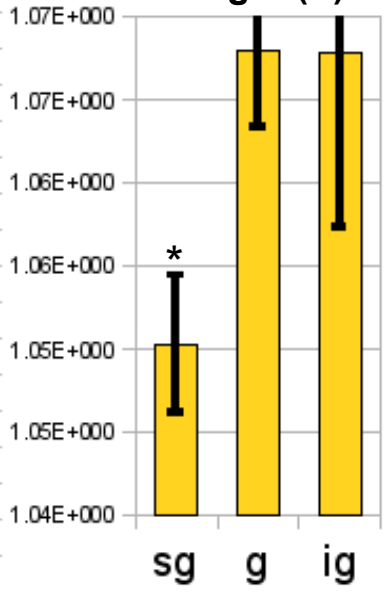

adjacent column strength (T)

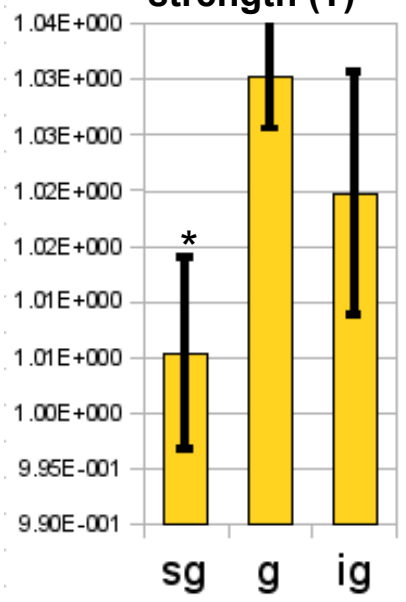

microcolumn width (W)

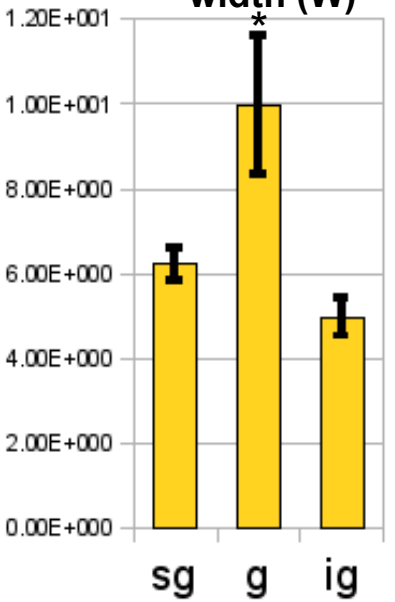

microcolumn length (L)

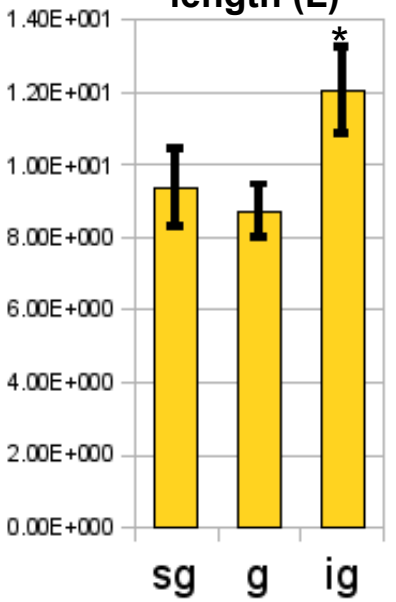

distance to first neuron in column (Y)

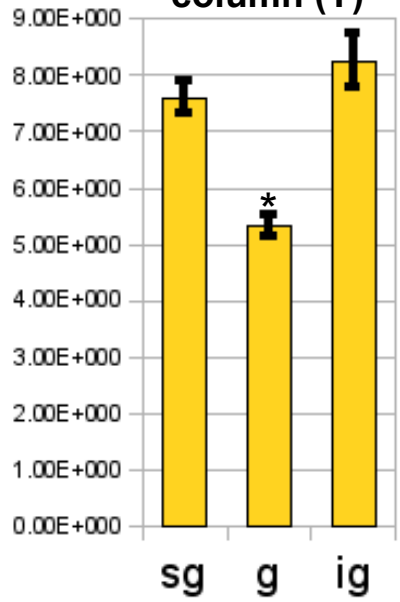

Future Work

Future studies

Investigate mechanisms behind spatial changes due to aging.
- extracellular matrix outside of cell bodies
- changes in dentritic structure
- changes in glial structure

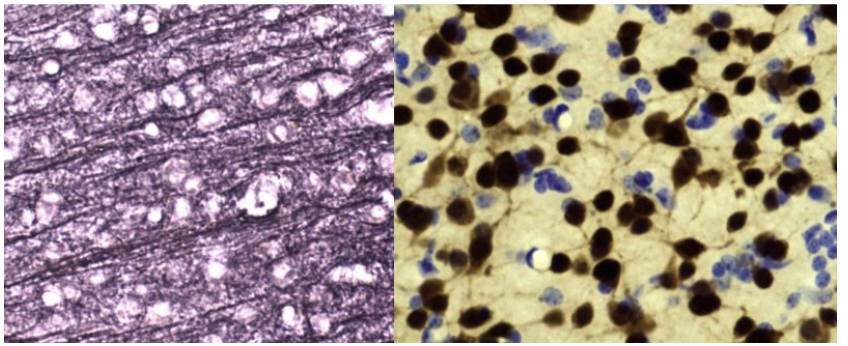

Measure spatial properties of cells through entire monkey and rat cortex in young healthy subjects and in aging studies.

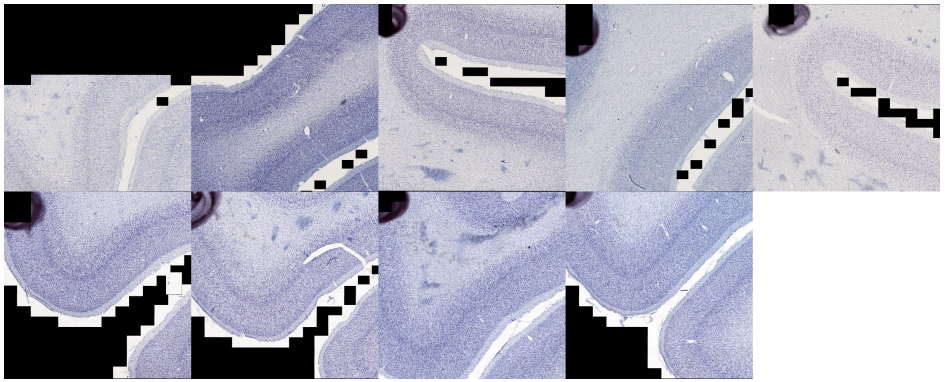

Investigate neural network models using statistical rules learned from spatial arrangement properties of inhibitory, excitatory neurons, and glia.

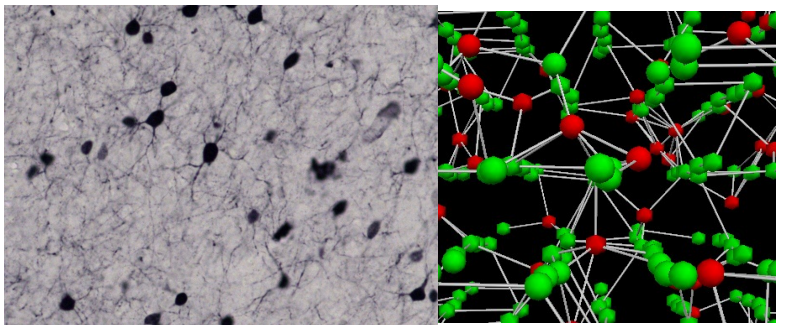

Conclusions

• Some aberrations in the cortex structure are visually apparent, some are not, and some cannot be observed using sampling theory (stereology). Such aberrations still correspond to meaningful changes in brain function. *It is possible that there are many such aberrations or patterns that are unknown.*

• We develop a method that acquires and analyzes the entire cortex at cellular resolution.
- Allows for exploration of unknown and un-hypothesized relationships of quantitative measurements within the brain (more data driven exploration).
- Can (potentially) reduce the amount of tissue and subjects tested.

• Using concepts from statistical physics, we create measurement tools that analyze tissue patterns which may exist right above biological noise.
- Allows for more understanding of the role of tissue structure on function of the cortex in any neuroanatomical study.
- Allows for more data driven research.

Thank you

Extra Slides

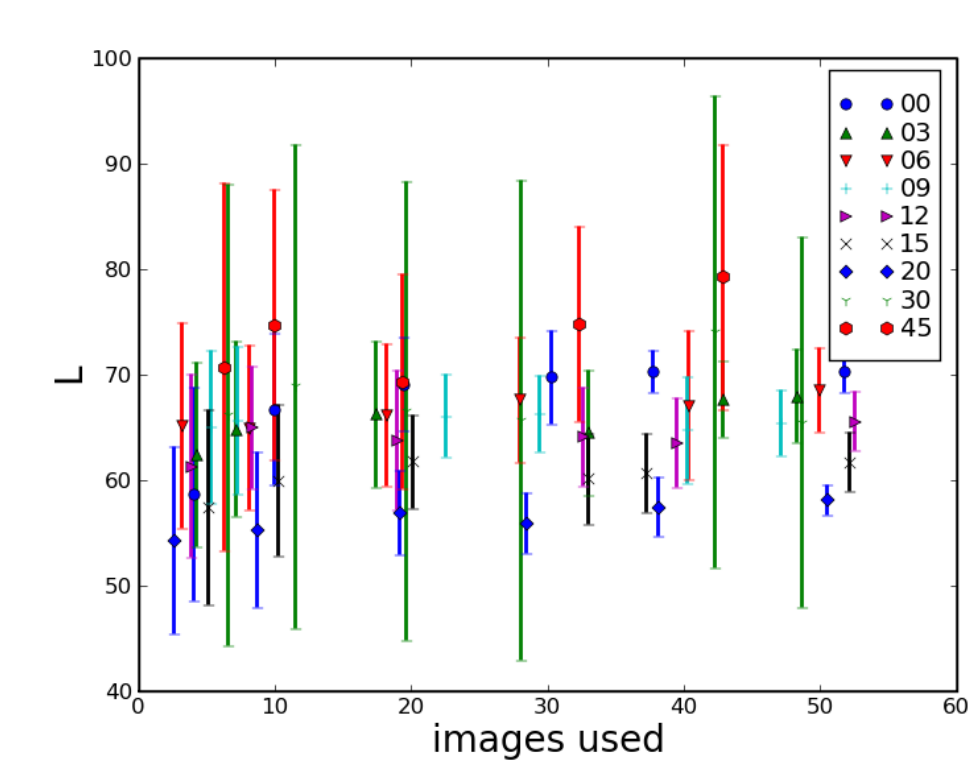
L
images used
00
03
06
09
12
15
20
30
45

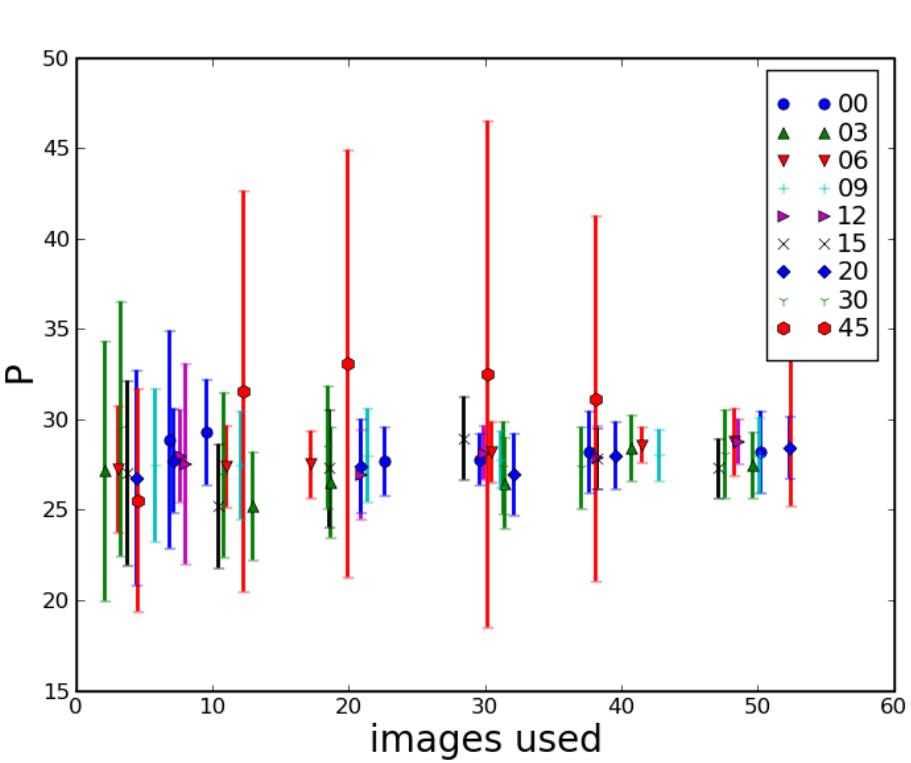
P
images used
00
03
06
09
12
15
20
30
45

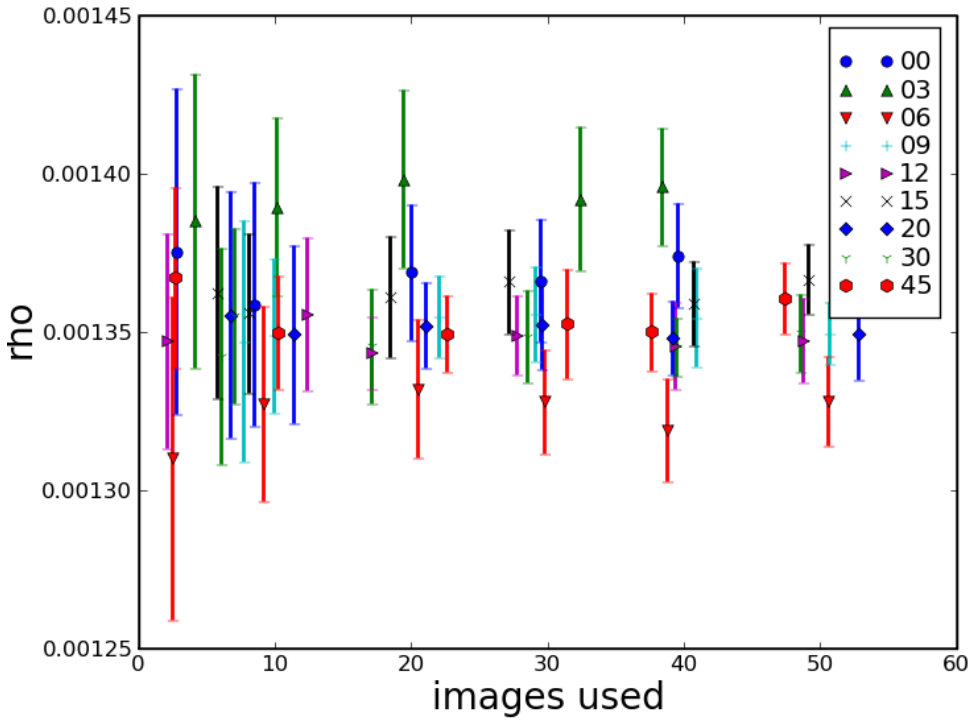
rho
images used
00
03
06
09
12
15
20
30
45

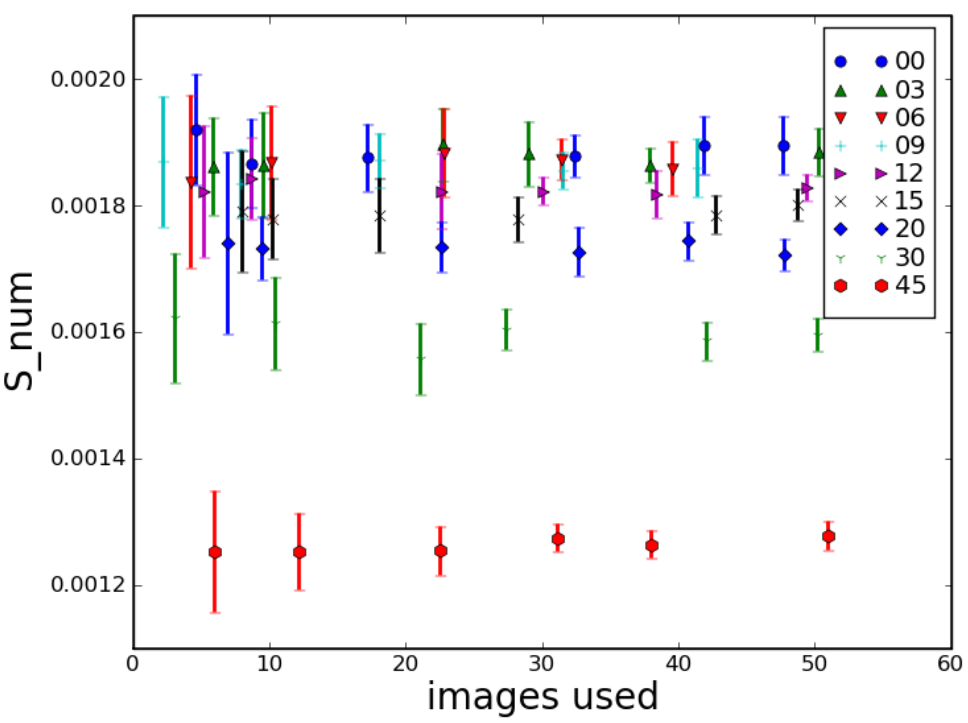
S_num
images used
00
03
06
09
12
15
20
30
45

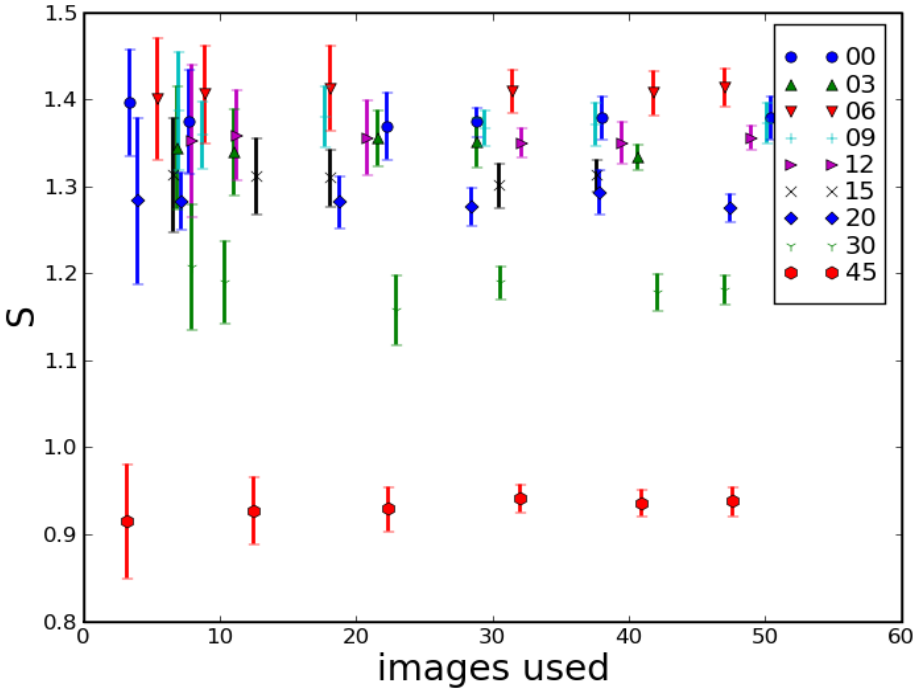
S
images used
00
03
06
09
12
15
20
30
45

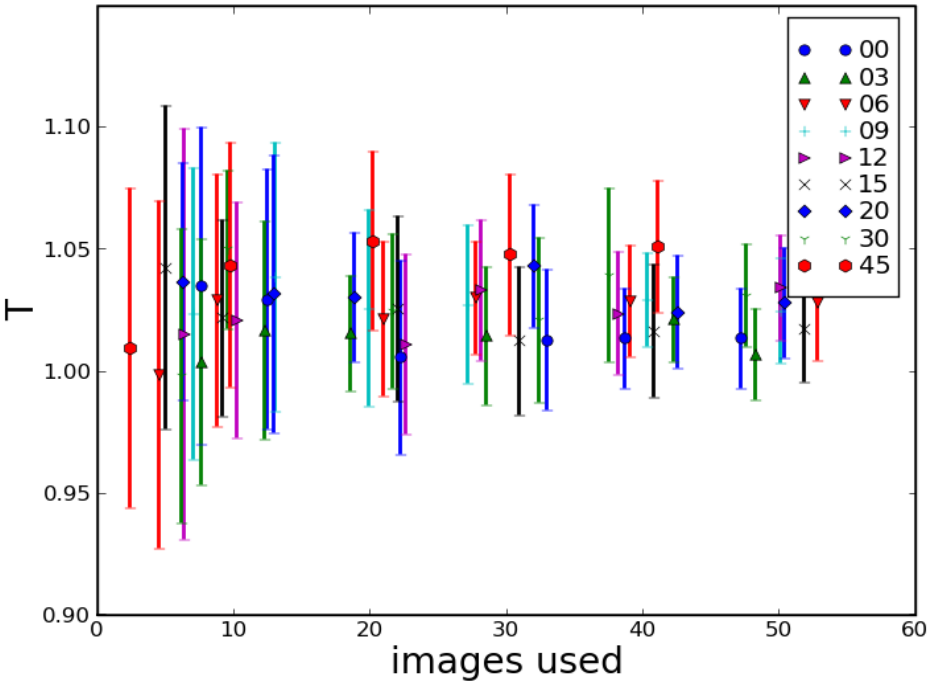
T
images used
00
03
06
09
12
15
20
30
45

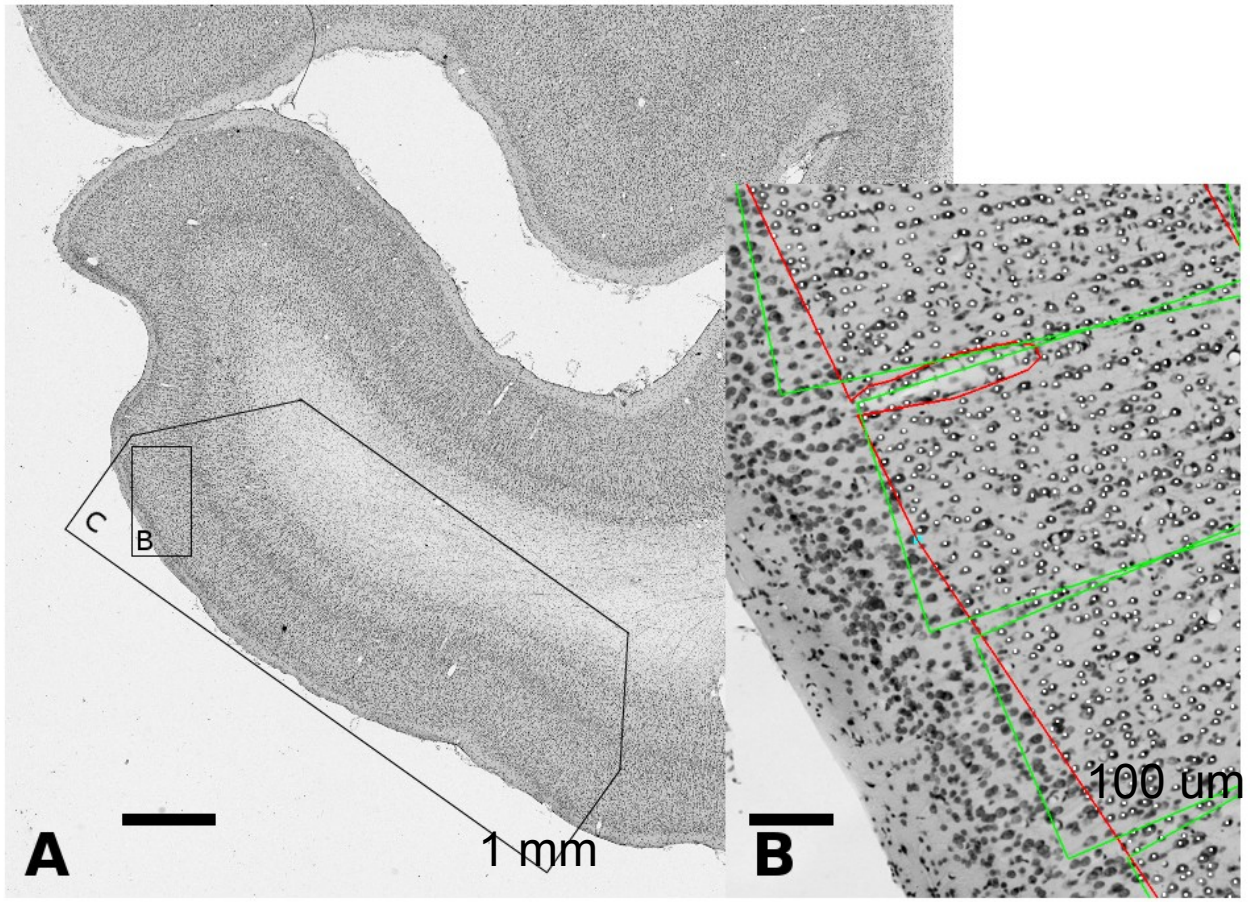

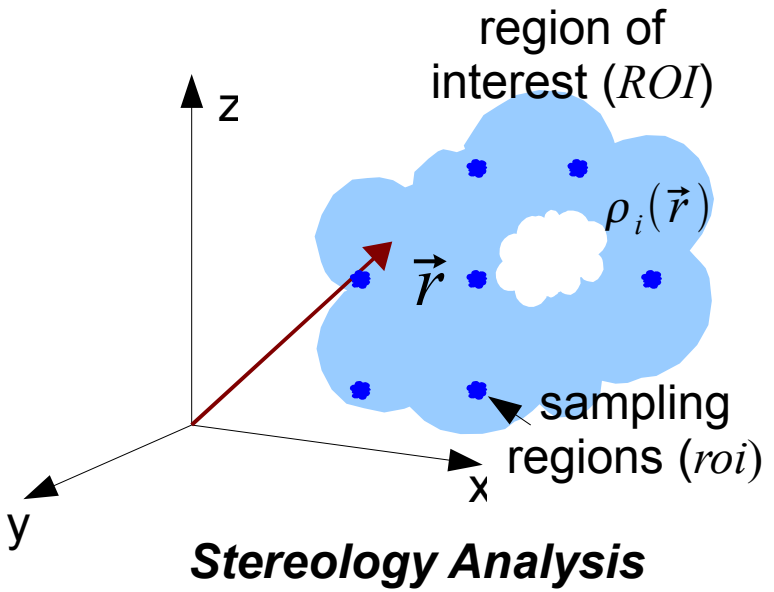

Stereology Analysis

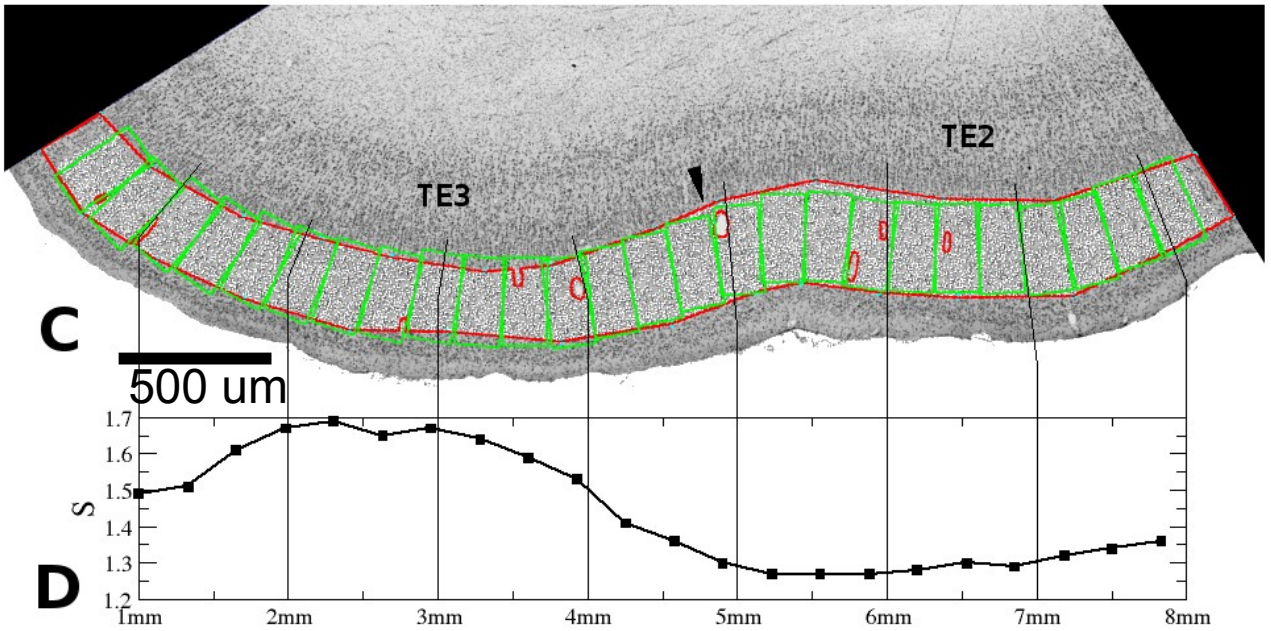

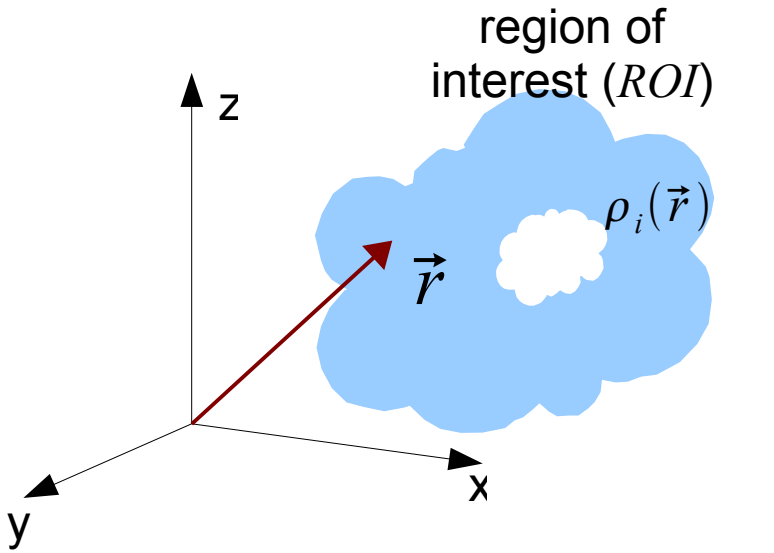

Correlation Analysis

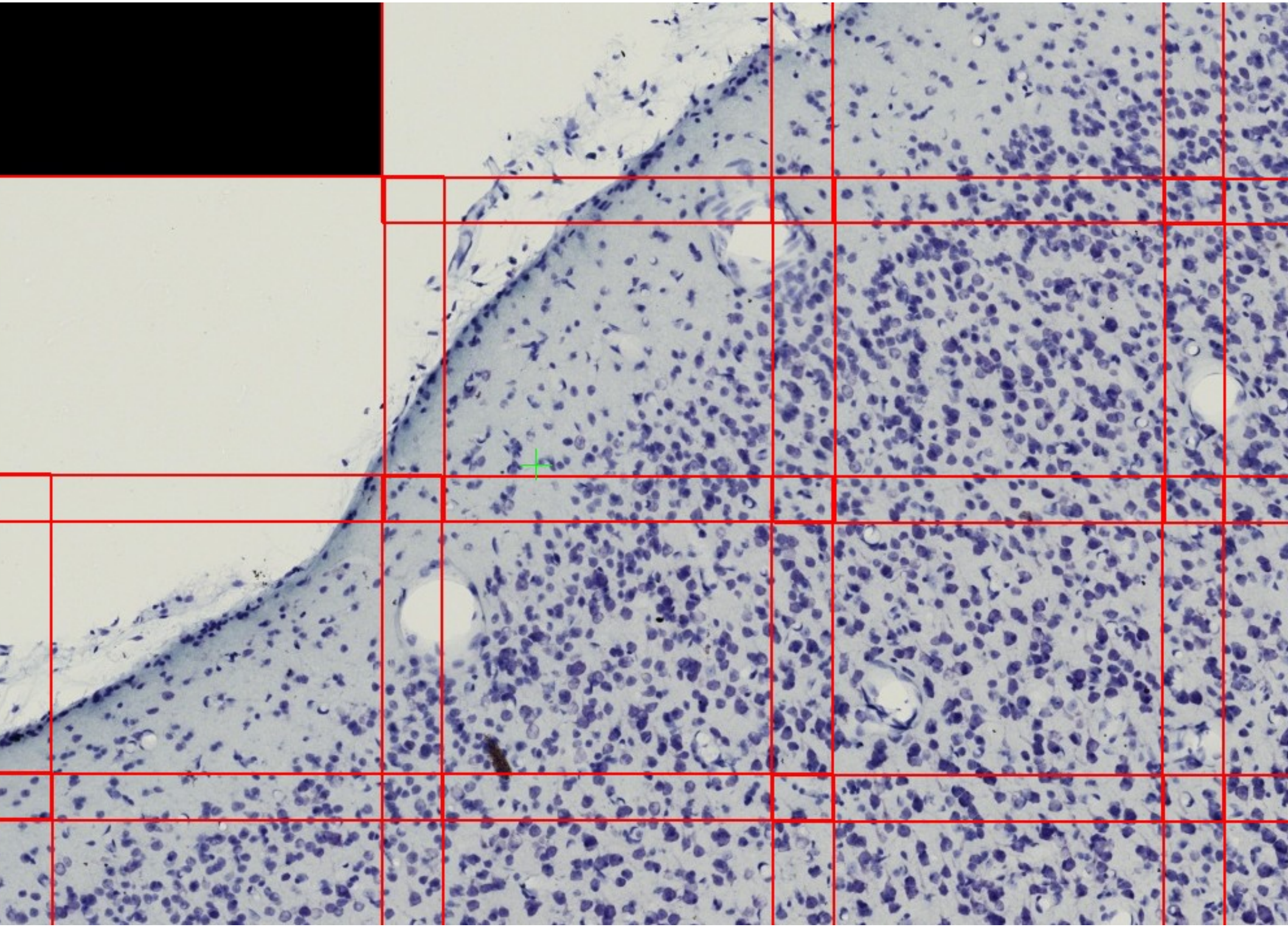

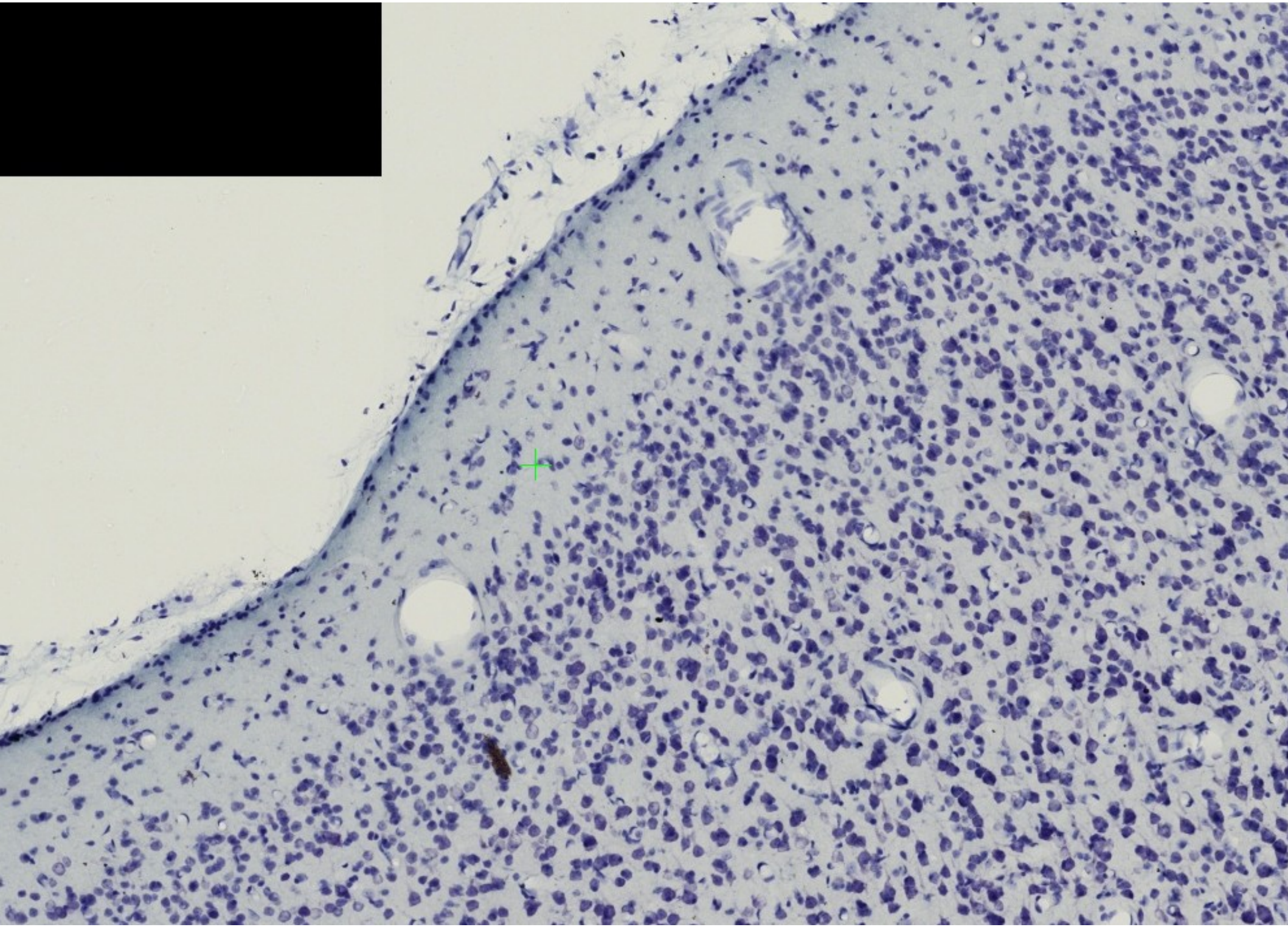

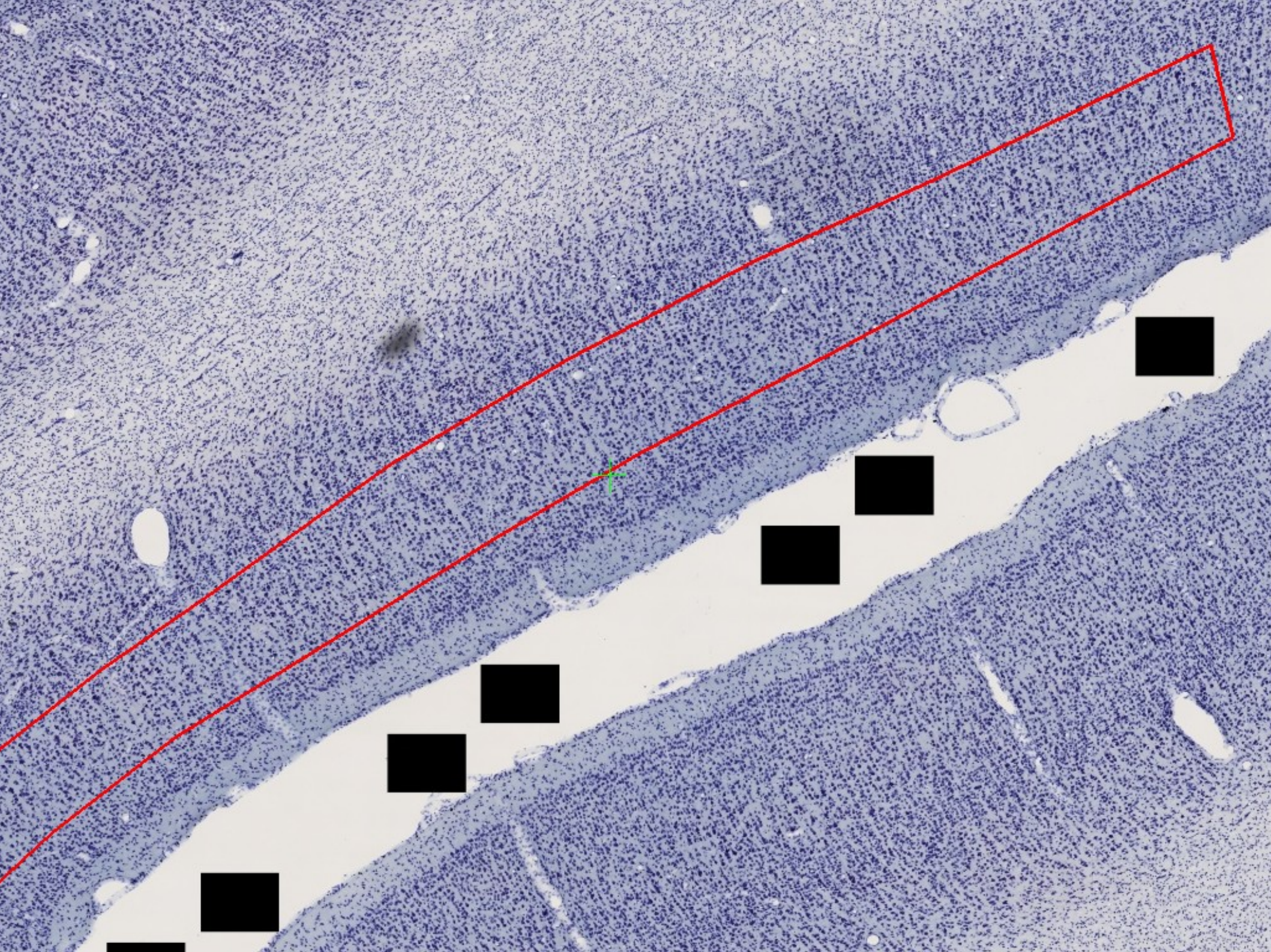

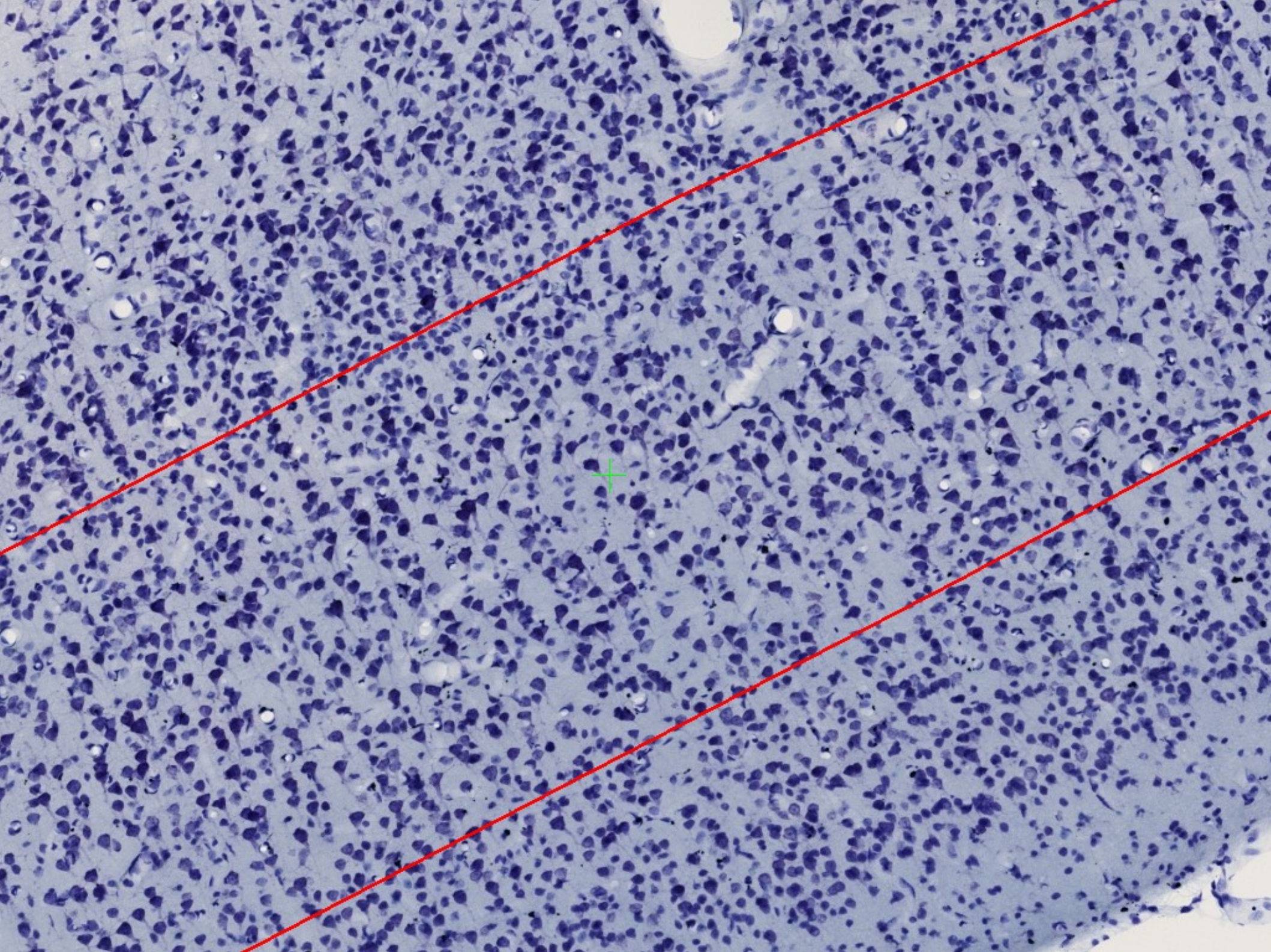

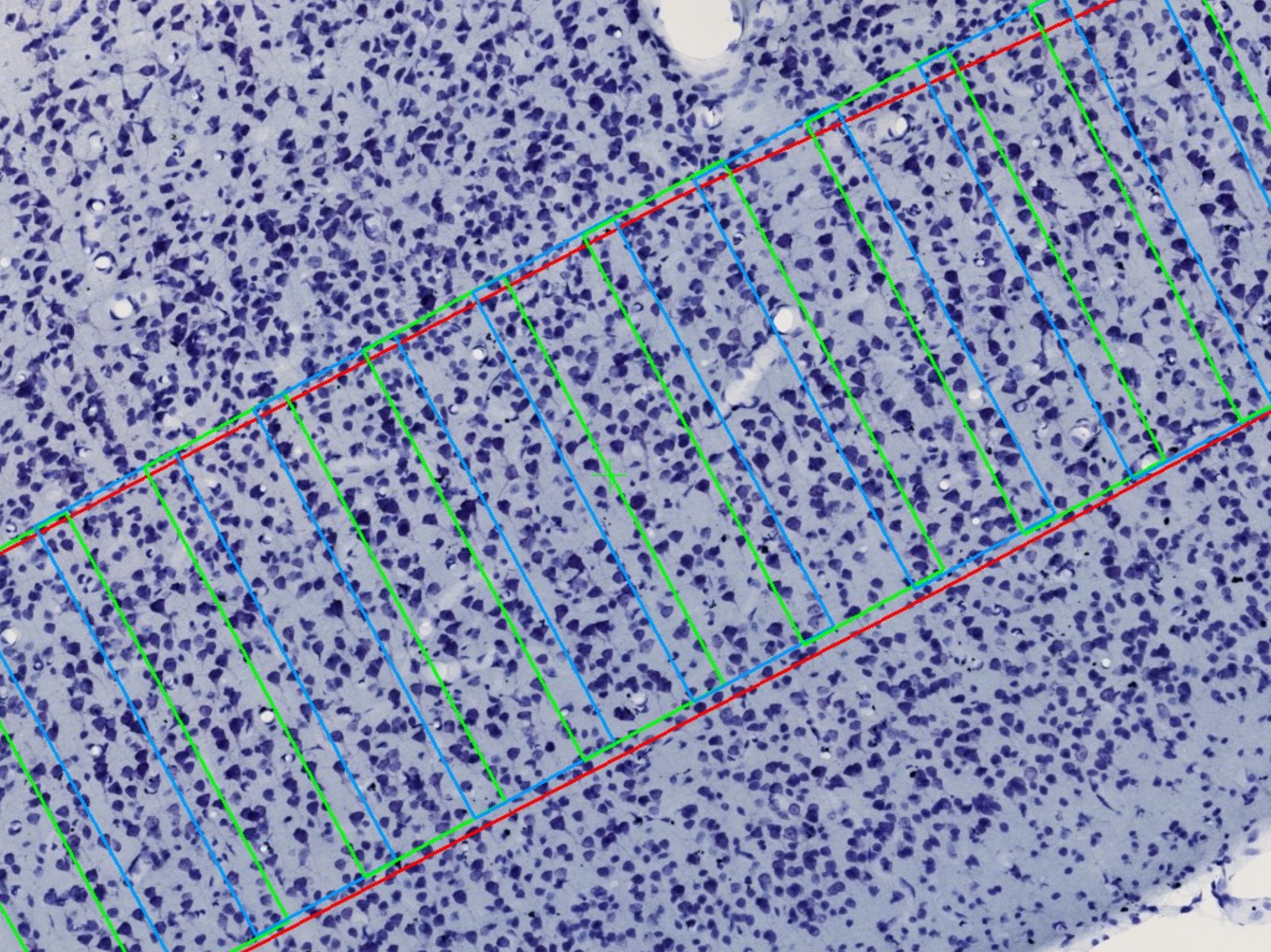

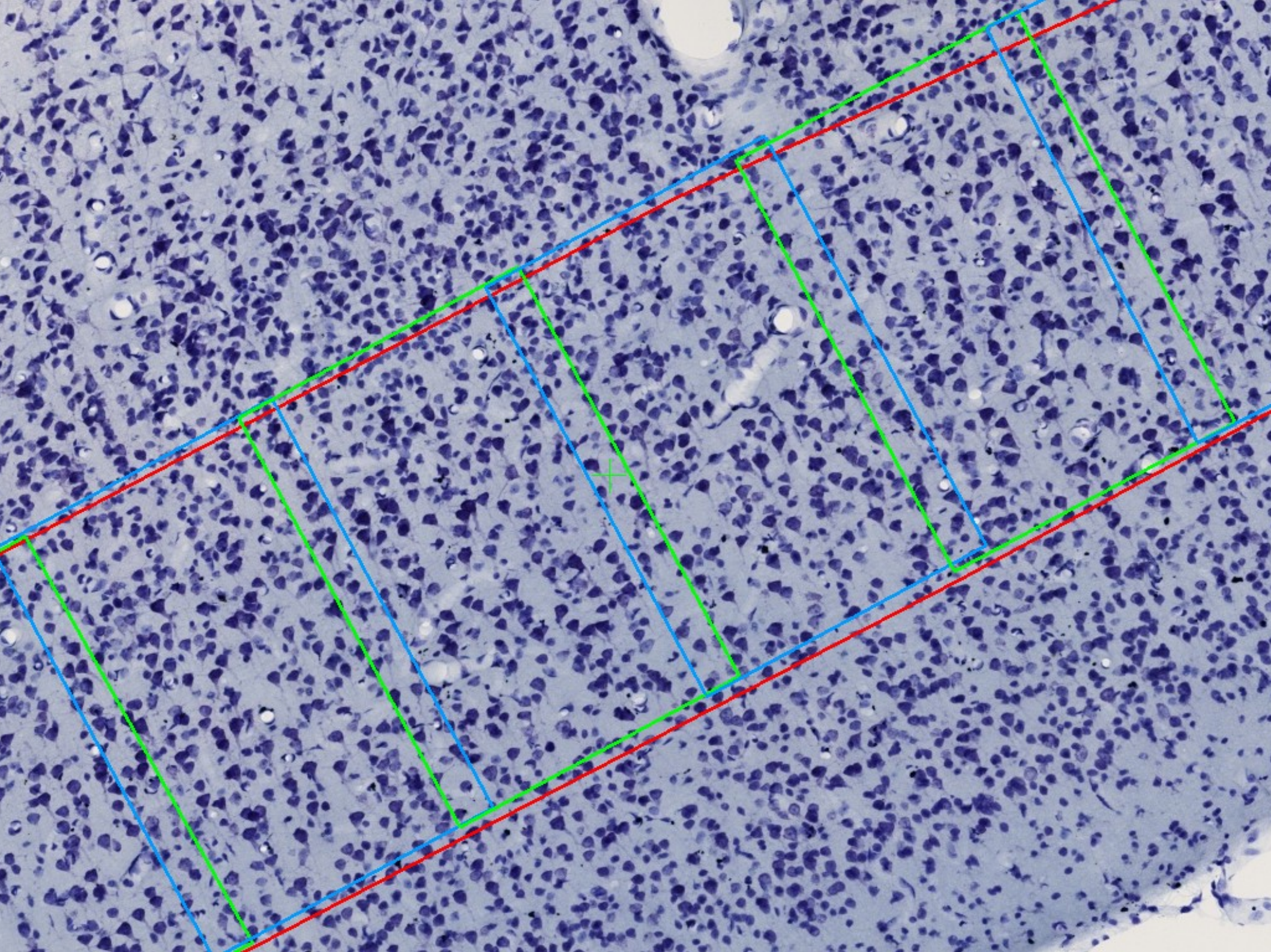

Changes in brain during Normal Aging

Difficult to study due to:
- quantitative information about cognitive status is rarely available
- no clear, drastic changes in anatomy
- no clear delineation of experimental vs control groups

What is known so far:
- Excitatory synapsis are lost in the grey matter
- Fibers of the cells are ???
- Loss of white matter volume, from fibers

Don't see pictures comparing issue because it is hard to see these changes in a single image – changes must be found statistically

Current directions to study: (we find there are changes in microcolumnarity with age. So what can affect that?)
- Cahnges in perineuronal net
- Changes in glial cells
- Changes in dendrites

Step 1: pick method.

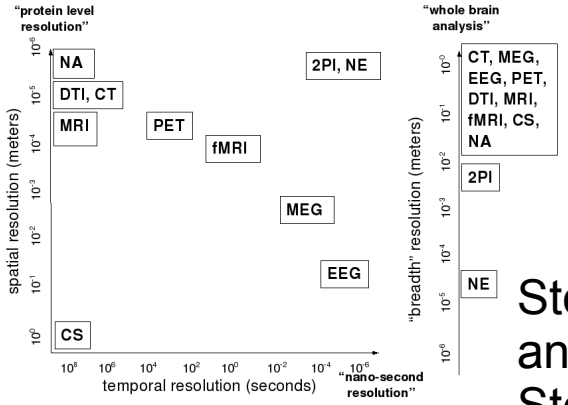

Step 2: select experiment and control based on Step 1.

Step 3: vary experimental group based on Step 2.

give drugs, make lesions, induce thinking, give disease, affect development, let get older, change environment, nurture, teach, allow to sleep, disturb patterns etc.

Step 4: take measurements based on Step 1.